

**Synthesis and Antimicrobial Activity of
Half-Sandwich Ir(III), Rh(III), and Co(III) Complexes**

George William Karpin

Dissertation submitted to the faculty of the Virginia Polytechnic Institute and State University in
partial fulfillment of the requirements for the degree of

Doctor of Philosophy

In

Chemistry

Joseph S. Merola

Joseph O. Falkingham III

Webster Santos

Gary Long

July 26, 2017

Blacksburg, VA

Keywords: antimicrobial, staphylococcus, mycobacteria, ethylenediamine, amino acid; half-sandwich complex; iridium; rhodium; ruthenium

Synthesis and Antimicrobial Activity of Half-Sandwich Ir(III), Rh(III), and Co(III) Complexes

George William Karpin

Abstract

This dissertation describes the synthesis and antimicrobial use of a series of half-sandwich Ir(III), Rh(III), Co(III) amino acid and ethylenediamine complexes. This investigation focuses on the formulation (η^n -arene)M(L)X, (L = ethylenediamine or α -amino carboxylate), (M= Ir, Rh, Ru, Co). Arene, Ligand and metal center variations were designed to tailor antimicrobial activity specific for each organism studied (*Staphylococcus aureus* or Mycobacteria). Each of the D/L-amino acids formed a diasteromeric complex with chiral centers on both the metal center and amino acid ligand. The unique chirality of each center elicits different antimicrobial activity against the Mycobacteria studied. The metal center (M), arene ligand (η^n -arene), and amino acid (aa), were changed independently and studied for the antimicrobial activity. In a similar fashion, each of the complexes modified with ethylenediamine and diamine derivatives were studied for their antimicrobial activity against *S.aureus*. All complexes were synthesized, characterized by nuclear magnetic resonance (NMR), high-resolution mass spectroscopy (HRMS), single-crystal X-ray diffraction, and elemental analysis.

During the course of this work it was found that the amino acid complexes with all metal centers were specific for antimicrobial activity against all types of Mycobacteria, while the diamine derivatives were active against different strains of *S.aureus*. Acitivity was measured to be as low as 2 ug/mL respectively depending on the complex used. A structure activity relationship was developed to determine what combinations of ligand, metal and arene were necessary to achieve the highest antimicrobial activity. The optimal arene R-chain length for Cp^R was determined to be R=hexyl for all complexes studied. The most active amino acidcomplex was determined to be that of L-phenylglycine for Mycobacteria, the cis-1,2-diaminocyclohexane complex is the most

active ligand against *S.aureus*. Each metal center had similar activity levels. Toxicological studies were performed to test their viability to be used in mammalian systems. The complexes with the highest activity were studied against several mammalian cell lines and revealed that mammalian cells were undergoing normal cellular processes at up to 40 times the minimal inhibitory concentration (MIC). A study of the MOA or mechanism of action revealed the ability of the amino acid complexes to affect the peptidyl transferase region on the 23s ribosomal subunit of *M.smegmatis*. This was accomplished by isolating resistant strains of *M.smegmatis* towards the most effective complex ($\text{Cp}^{*\text{hexyl}}\text{Ir(L-phenylglycine)-Cl}$). Cross drug resistance of these mutants was shown with clarithromycin. The DNA of the 23s ribosomal subunit was sequenced revealing a deletion/insertion mutation within domain V (bases 2057-2058).

Synthesis and Antimicrobial Activity of Half-Sandwich Ir(III), Rh(III), and Co(III) Complexes

George William Karpin

General Audience Abstract

This dissertation describes the discovery of laboratory created synthetic organometallic molecules (carbon and metal containing molecules) that exhibit antimicrobial properties. Each of these molecules are specifically designed and tailored to combat several infectious and antibiotic resistant diseases. The different and unique compositions of each of these novel molecules allows for a potentially new class of antibiotics. Each of these organometallic molecules was able to be tailored to combat either *Staphylococcus aureus* or Mycobacteria. Each of these bacteria have significant health risks and are a growing threat to public health. During the course of this work it was found that the molecules containing amino-acids were specific for activity against all types of Mycobacteria studied. The diamine containing molecules were specific for gram positive bacteria (*Staphylococcus aureus*). Activity to confirm this activity was measured by MIC (Minimal inhibitory concentration). This is the amount of the molecule that is needed to stop the growth of the bacteria studied. The complexes with the highest activity were tested for their potential hazardous interactions with mammalian cells. It was revealed that not only do these molecules have activity in combating potentially deadly pathogens but they are not active against several mammalian cell lines. This shows that these can be possible candidates for a new line of antimicrobial drugs.

Acknowledgements

I can not start an acknowledgments section without first recognizing and thanking my mother Phyllis Eaton. If it was not for her I would have never made it through these years to fulfill my dream and achieve my degrees. She had faith in me even when I felt I let her down and continued to support me when I lost faith in myself. It's almost impossible to think I would have made it this far without her. My brother and best friend Andrew, always kept reality in check for me. We battled back and forth as brothers do, but we never lost site of what it really meant to be family. He and I constantly let each other know that our education was a start to something more and it kept us grounded so we did not lose site of the big picture. I would like to thank my committee members and mentors, Prof. Webster Santos, Prof. Gary Long and Prof. Joseph O. Falkingham III. Each of them provided key insight and knowledge critical to my research. Dr. Falkingham's ability to collaborate and knowledge of the drug development process served as the cornerstone for our work in antimicrobial development. I thank Dr. Jerry Via for his support and advice for all things related to research and life. He was able to help me continue my career by offering support and guidance during my tenure. I owe a great deal of gratitude to the research group in our department specifically Dr. Dave Hobart, Dr. David Morris and Dr. Mike Berg who supported and contributed on my projects. The team of graduate and undergraduates over the years who aided me, were also critical to my research: Loren Brown, Chrissy DuChane, Chad Berneir, Chelsea Dollarhite, David DePena, Mai Mgo and Alex Mai. I have to thank my advisor Prof. Joseph S. Merola. Without him I would have never been able to succeed. He saw something in me that I myself did not believe was possible. He supported me through the ups and downs of my career as a student and has influenced me more than I thought was possible. I am lucky to have met him. Finally I would like to dedicate this to my Father, who before his passing, taught me that knowledge and self improvement were the single most important ideals to achieving success. Even though he was not here to see this I believe he knew what I could become.

Table of Contents

1. Introduction.....	1
1.1. Antimicrobial and Toxicological Properties of Transition Metals.....	1
1.2. The Need for New Antimicrobials.....	2
1.3. History of Transition Metals as Therapeutic Agents.....	8
1.4. Microbial Physiology and Drug Interaction.....	11
1.5. Modifying Antimicrobials.....	14
1.6. Project Description.....	18
2. Chapter 2: Anti-staphylococcal Complexes and Activities.....	23
2.1 Introduction.....	23
2.2 Synthesis of the Anti-staphylococcal Complexes.....	24
2.3 Anti-staphylococcal Activities.....	32
2.4 Toxicology.....	39
2.5 Discussion.....	41
2.6 Experimental Section.....	42
3. Mycobacteria and Amino-acid Complexes.....	51
3.1 Introduction.....	51
3.2 Synthesis of Transition metal amino acid complexes.....	52
3.3 Mycobacterial Activity.....	58
3.4 Discussions.....	65
4. Mechanisms of Action.....	70
4.2 Complexes Studied.....	70
4.3 <i>Mycobacterium smegmatis</i> mutant isolation.....	73
4.4 Results and Discussion.....	74

4.5 Conclusions and further work.....	78
5. Conclusions.....	82

Chapter 1: History of Metals In Medicine

1.1: Antimicrobial and Toxicological Properties of Transition Metals

Transition metal complexes play an important role in pharmaceutical chemistry, beginning with the discovery and use of cisplatin as an anticancer drug in 1978.^{1,2} Subsequent studies of transitional metal complexes have been primarily limited to the search for new compounds with anti-cancer activity. However, with very few transition metal pharmaceuticals received FDA approval beyond cisplatin and cisplatin derivatives. More importantly for this discussion, little to no development occurred in the area of antimicrobial activity. This is surprising since, new ways to combat microbial diseases are required to combat the growing number of multidrug resistant bacteria. Metal complexes have been proven as anti-cancer DNA, RNA, and enzyme binding agents. As these are often key targets involved in antimicrobial development⁴, transition metal complexes may have the potential to expand the arsenal of synthetic antimicrobials.³

1.2: The Need for New Antimicrobials

In 2010 the World Health Organization (WHO) reported that antimicrobial resistance is one of the three greatest threats facing humanity today² with 2 billion people worldwide infected by some form of *Mycobacterium tuberculosis*. Spontaneous genetic mutations and selection for antibiotic resistance adds to a growing number of multi drug resistant (MDR) and extensively drug-resistant (XDR) strains of tuberculosis developing each year. XDR strains currently have no known successful treatment.⁸ Due to the slow growth rate of most mycobacteria, treatment for these types of infections can take years to complete.³ The longer patients are prescribed a course of a specific set of antimicrobials, the higher the risk for these drugs to become ineffective. As the number of MDR (Multi-drug Resistant) strains increase, it is almost a certainty that current treatments will be inadequate and ineffective in the near future. In order to combat the growing number of multi-drug resistant strains of bacteria and the threat of an imminent infectious disease

epidemic due to the lack of active antimicrobial agents, the Infectious Diseases Society of America put forth the "10 x '20 Initiative," which aims to develop 10 new antimicrobials by 2020.^{1, 2}

1.3 History of Transition Metals as Therapeutic Agents

1.3.1. Platinum Based Anticancer Compounds

The most widely used therapeutic transition metal complex is cisplatin for the treatment of hard cell malignant tumors. Cisplatin (Figure 1.1)¹ was first discovered by Dr. Barnett Rosenberg at Michigan State⁶ when he used platinum electrodes to generate electric gradients by varying the current and voltage in order to test the effect small electric fields had on the growth of microbial cells. Though cell division and proliferation of the *E.coli* cells was halted, he found that cell growth continued. After growing to abnormally large sizes, the cells could no longer sustain growth or function normally, which led to apoptosis. The seminal discovery of this compound's ability to halt the replication of rapidly dividing cells rendered it important in the treatment of cancer cell lines following FDA approval for pharmaceutical use in 1978. . This experiment led to the discovery of cisplatin. The scientific community began to examine other noble metal complexes that may also have therapeutic properties. The focus of most working in this field was still the development of anti-cancer pharmaceuticals. Other of transition metal complexes were examined for their use as possible anti-cancer drugs. These include but are not limited to metallocene, arene, and carbonyl complexes.⁷

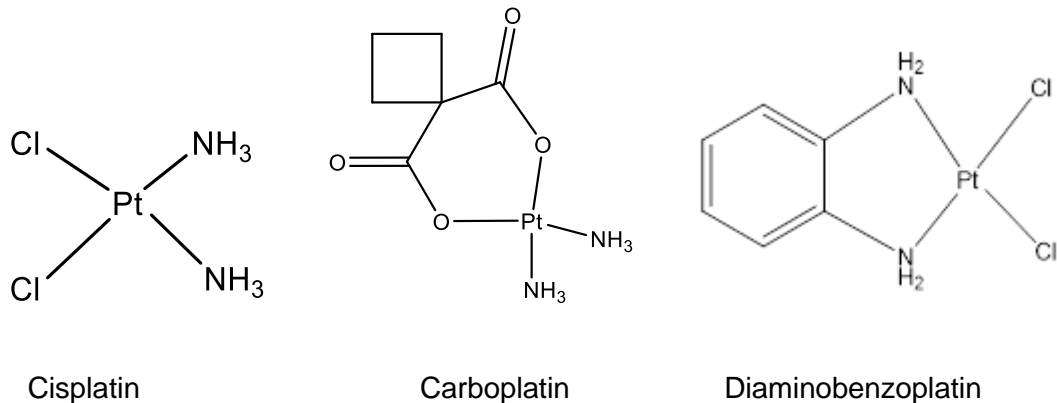


Fig 1.1: Transition metal complexes in medicine currently used to treat hard cell malignant tumors

1.3.2: Platinum and Palladium Antimicrobial Agents

Since the discovery of cisplatin and other platinum based drug derivatives for cancer treatment, there has been little work done to determine what role metal complexes may have as antimicrobial agents. Synthesis of substituted amine complexes with ligand structures similar to cisplatin are usually the focus of research in this area. An example of these complexes that show activity has been reported by Vasic (Figure 1.2)¹⁰. Both minimum inhibitory concentration (MIC) and bactericidal activities of palladium diamine complexes were measured. The longer or more hydrophobic the “R” group the more effective the compound was against the various strains of bacteria. Most notably using the propyl -R group the MIC’s were approximately 125 µg/mL but switching to the n-butyl group lowered the MIC to 31.25 µg/mL for *E. coli*.¹⁰

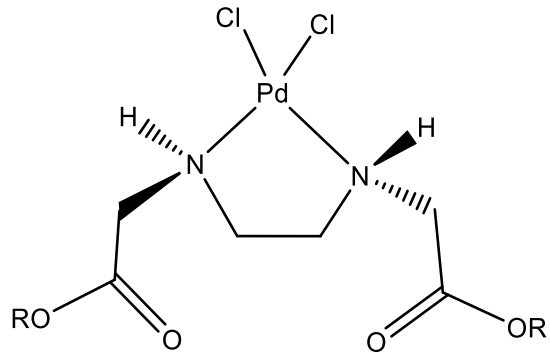


Figure 1.2: Palladium diamine compound scaffold as studied by Vasic.¹⁰

Thiosemicarbazone complexes of platinum show promising antimicrobial activity, particularly against *S.aureus*, with MIC values as low as 1.0 µg/mL. Filousis et al. showed that these complexes show greater potential for their antitumor/anticancer properties (Fig 1.3). One main reason for the lack of interest in the area of transition metals in antimicrobials is the toxicity some of these complexes have been known to exhibit toward mammalian cell. Currently there are no FDA trials for platinum or palladium based antimicrobials. Most of the complexes that contain platinum and palladium have a poor therapeutic to cytotoxic ratio. This ratio, also known as the therapeutic index, is the amount of compound that causes a therapeutic effect compared to the amount that shows toxicity. Often the therapeutic to cytotoxic ratio is similar to the MIC of traditional antimicrobials.

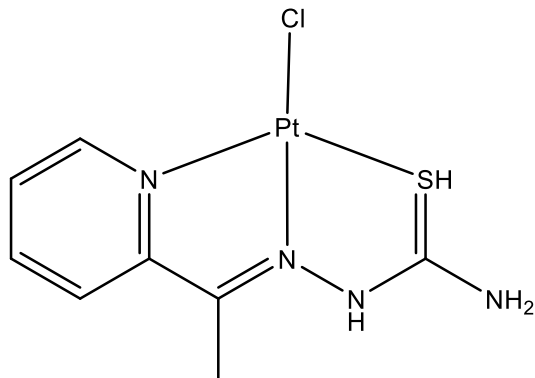


Figure 1.3: Platinum thiosemicarbazone - MIC of 1.0 ug/mL against *S. aureus*

1.3.3 Iridium, Rhodium and Ruthenium Transition Metal Complexes

Some half-sandwich or "piano stool" complexes are being explored for their possible anti-cancer and anti-microbial properties.⁵ The general structure of these compounds is shown below in figure 1.3.3 where X, Y, and Z can be any coordinating atom or ligand. The most significant and extensive work for developing a "half-sandwich" antimicrobial is based on the ability of Ru(II) complexes to combat malaria.¹⁰ Many of these complexes also have shown a favorable therapeutic to cytotoxic ratio for use against hard cell tumors.¹⁰

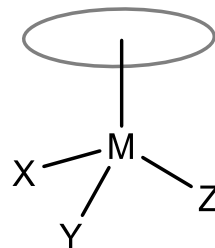


Figure 1.3.3: Basic scaffold structure of the half-sandwich complexes

The Ru(II) complexes focused on the anti-cancer properties of $[(\eta^6\text{-arene})\text{Ru(II)}(\text{en})(\text{Cl})]^+$ (arene = naphthalene or *para*-cymene; en = ethylenediamine) complexes as related to their ability to bind to DNA. Ruthenium complexes have an affinity for binding to the N7 on the guanine residue in all DNA binding studies.^{12,13} Keene et. al, describes dinuclear ruthenium complexes with modified pyridyl ligands that showed strong antimicrobial specificity towards prokaryotic cells,²² with MICs for *S.aureus* and *E.coli* as low as 1 ug/mL. IC₅₀ values for Eukaryotic cells tested were also reported as 78 ug/mL and as high as 400 ug/mL (Figure 1.3.4.) Many complexes show a pattern of increased activity with the increasing hydrocarbon chain separating the two ruthenium centers.

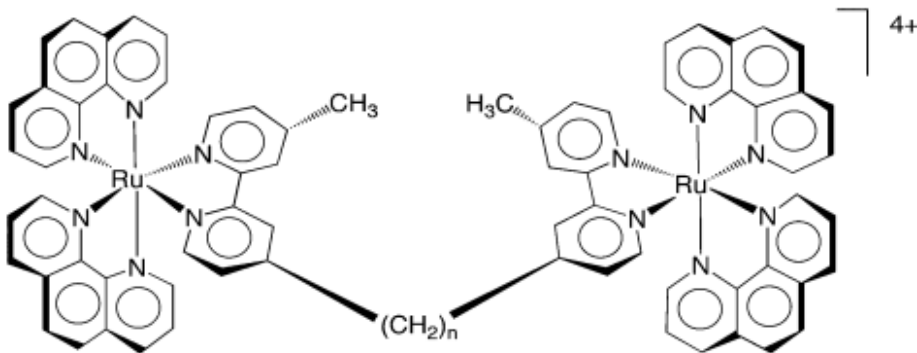


Figure 1.3.4: Binuclear polypyridal complexes, where $(\text{CH}_2)_n = 2, 5, 7, 10, 14$, and 16

It was discovered that when iridium replaced ruthenium in complexes shown in figure 1.3.4, MIC values were greater than 128 $\mu\text{g}/\text{mL}$. The reason for the decrease in activity is not known; however this finding illustrates that not all metal complexes are toxic to all cells, and, consequently, the metal center plays a role in activity.

In one approach to try to combat increased resistance, transition metal complexes have been combined with traditional antimicrobials. When modifying complexes (figure 1.3.4) with different metals, increased antimicrobial activity was observed with modified ruthenium and ferrocene, quinolones and platensimycin (natural product antimicrobial isolated from

streptomycin) as noted by Patra et al.⁴ The DNA of each organism coordinated to the metal centers in non-specific areas. Ferrocene complexes of quinolones bind to the FabF enzyme which prevents fatty acid synthesis that is necessary for cellular development. This is particularly crucial for cell membrane and cell division processes. Platensimycin complexes with Fe, Cr, and Mn were studied using proteomic techniques to follow the protein expression of the fatty acid synthesis in several bacteria. It was determined that several different modifications showed different protein responses causing cell death.⁴ These protein responses were also involved in the inhibition of fatty acid synthesis but in some cases not related to the FabF enzyme. This suggests that more than one enzyme may be inhibited by these complexes.

Ruthenocene and ferrocene trimetallic complexes, as studied by Wenzel, have shown increased antimicrobial activity as compared to amoxicillin and similar penicillin derived drugs²³. Complexes (Fig. 1.3.5) were studied by looking at proteins related to lipid membrane development. Based on the protein expression, the lipid membrane composition was altered in a way that was unsuitable for standard cellular processes to continue. It was also determined that there was metal dependent oxidatative stress related to the complexes with the membrane. In comparison to known antimicrobials, these modified trimetallic systems performed well when used with multidrug resistant strains (Table 1)¹⁵.

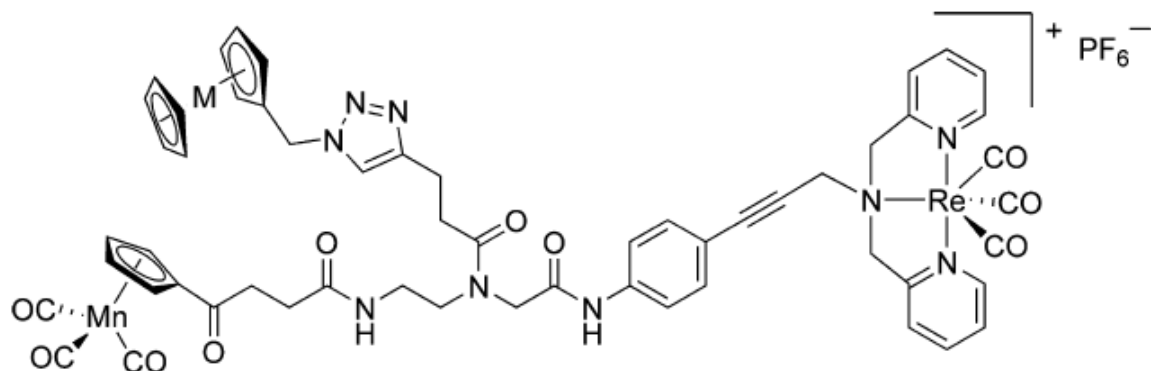


Figure 1.3.5: Trimetallic complexes studied by Wenzel et al, (M is either Fe or Ru).

Table 1: Comparison of trimetallic systems of Ru and Fe with known antimicrobials.²²

	FcPNA		RcPNA		amoxicillin		norfloxacin		vancomycin	
	$\mu\text{g mL}^{-1}$	μM								
<i>B. subtilis</i> (DSM 402)	2	1.4	32	21	3	8.2	1	3.1	0.5	0.3
<i>S. aureus</i> (DSM 20231)	2	1.4	4	2.7	2	5.5	0.5	1.6	0.5	0.3
<i>S. aureus</i> (ATCC43300) (MRSA)	2	1.4	6	4	48	131	0.5	1.6	1	0.7
<i>S. aureus</i> (COL)(MRSA)	2	1.4								
<i>S. aureus</i> (Mu50) (VISA)	6	4								
<i>E. coli</i> (DSM 30083)	nd	nd	nd	nd	64	175	0.5	1.6	96	66
<i>A. baumannii</i> (DSM 30007)	nd	nd	nd	nd	>256	>700	0.75	2.3	64	44

Iridium complexes developed by Sadler have been studied mainly as anti-cancer complexes. These complexes include but are not limited to iridium cyclopentadienyl piano stool variants, with a standard formula of $[(\eta^5\text{-Cp}^*)\text{Ir}(2\text{-phenylpyridine})\text{Cl}]$. The arene ligand and the pyridine ligand were modified at key points to help increase activity (Figure 1.3.6). Measurements of anticancer activity showed that the complexes were more active with an intercalating ligand (i.e. phenyl or biphenyl) attached to the metal center or arene ring. Figure 1.3.6 shows the structure of the different arene ligands coordinated to the complex with the IC₅₀ values against human ovarian cancer cell lines. Sadler discovered that while these complexes had increased activity against cancer cell lines, they also had increased activity against healthy mammalian cells. Complexes lacking the arene component attached to the cyclopentadienyl ring system have substantially higher IC₅₀ activity.²⁸ This shows that the most effective complexes are those containing arene systems attached to the cyclopentadienyl ring.

IC₅₀	0.70 µM	1.0 µM	2.5 µM	1.19 µM
------------------------	----------------	---------------	---------------	----------------

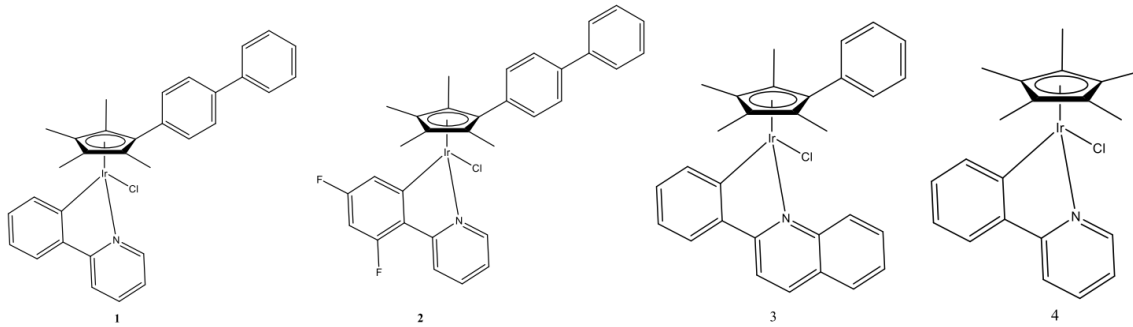


Figure 1.3.6: Iridium arene complexes that inhibit growth of ovarian cancer cells.

1.3.4 Mechanisms of Action for Anti-Cancer Transition Metal Complexes

Malignant cells of all types (i.e. ovarian, testicular, pancreas) share similar characteristics of uncontrolled cellular growth. This suggests the primary mechanism of these complexes is to interfere with cell growth and division based on interactions with DNA. Cisplatin has a specificity for binding to the N7 of guanine residues. Figure 1.6 illustrates the DNA interaction of cisplatin and the N7 guanine residue. Binding to the DNA at this site has been shown to prevent DNA replication and proliferation of the cell lines.⁶ This causes an irreversible reaction in the case of the platinum dichloride derivatives causing the DNA helix to become deformed.

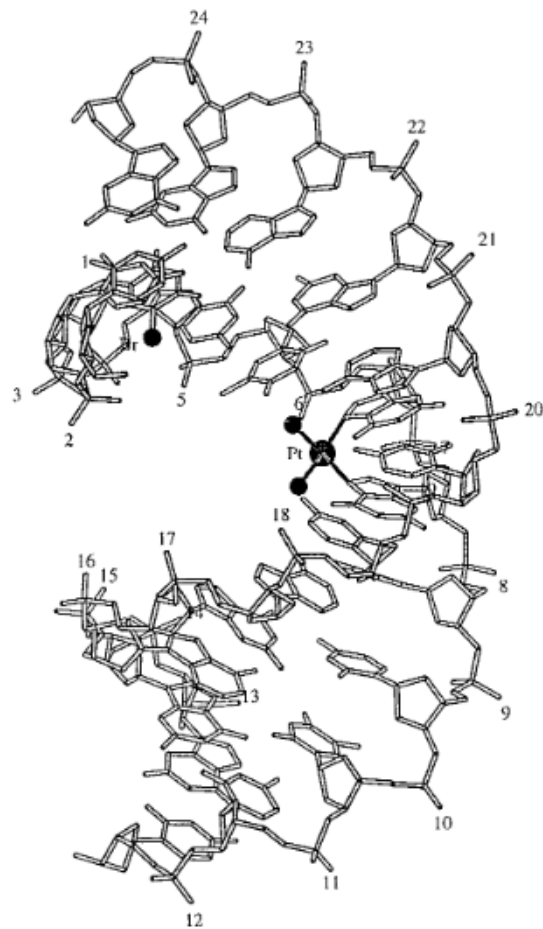


Fig 1.6: Cisplatin binding with the N-7 of guanine in double stranded DNA forms a 45-degree bend in the double helix.²⁶

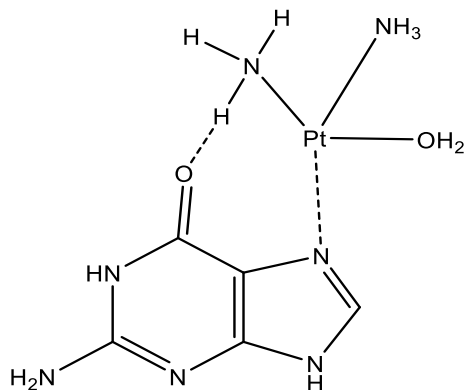
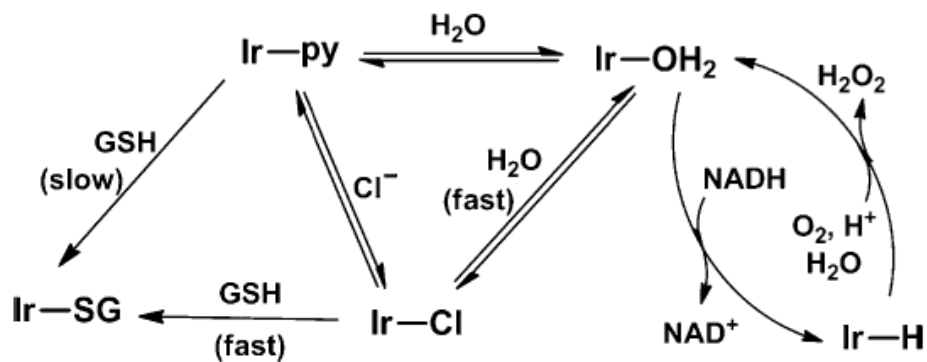


Fig 1.3.7: The interaction between cisplatin and N-7 of guanine

Even though these drugs show promising results against different forms of cancer, most of the transition metal anticancer drugs are toxic to normal healthy cells. This makes these drugs cytotoxic towards the patient. The mode of action is irreversible binding of these complexes to the DNA. Sadler et al. have described a class of iridium complexes with modified Cp-arene ligands that have been shown to produce reactive oxygen species (ROS) in hard cell tumors. The originally proposed mechanism was that intercalation of the arene ligand aids the complex in binding to DNA; however, it was later discovered that oxidation of NADH to NAD⁺ produces radical oxygen species in the form of increased levels of peroxide.²⁹ The creation of reactive oxygen species (Scheme 1.6) shows that there is a mode of action other than DNA binding/intercalation as in cisplatin. Work performed by Sadler shows that transition metal complexes are not unilaterally toxic at the same levels just based on the metal concentration alone.



Scheme 1.6: The proposed reaction pathway of the iridium complexes for the formation of reactive oxygen species (ROS).

1.4: Microbial Physiology and Drug Interaction

It is crucial in the development of any new antimicrobial to understand how transport of the drug into the cell may occur. Microbes have a wide range of unique features. The microbes studied in this review will cover pathogenic gram-positive and gram-negative, as well as mycobacteria. Though the cells of each of these microbes are composed of similar structures, there are key differences that are necessary in understanding how each cell functions. Examining the different molecular makeup and structure of the bacterium studied could help influence the design of small molecules with possible antimicrobial activity. Gram-positive cells have a thick layered cell wall featuring layers of peptidoglycan composed of a polymer of *N*-acetylglucosamine and *N*-acetylmuramic acid. This gives these bacteria a stiff rigid structure. Gram-negative cells have a much larger polysaccharide layer instead of the peptidoglycan layer.

Mycobacteria are acid-fast bacteria. They resist acid based or ethanol based microbial stains. All mycobacteria have a membrane structure containing mycolic acids composed of long chain hydrocarbons. These hydrocarbons are made up of carbon chains around 60-80 carbons

long.⁸ The formation of the long carbon chains requires an immense amount of energy to be exerted for the development of each cell. This causes a waxy outer shell to develop that is rather impervious, making them extremely difficult to penetrate and attack with conventional antibiotics. Unlike traditional gram-positive and negative bacteria, mycobacteria are slow growers due to the need to synthesize the mycolic acids which compose the cells outer membrane.⁸ Figure 1.4.1 shows an example of linkage between mycolic acids to the polysaccharides used in the complex membrane of Mycobacteria. The structure of linkages shown is from *M. smegmatis*.⁹

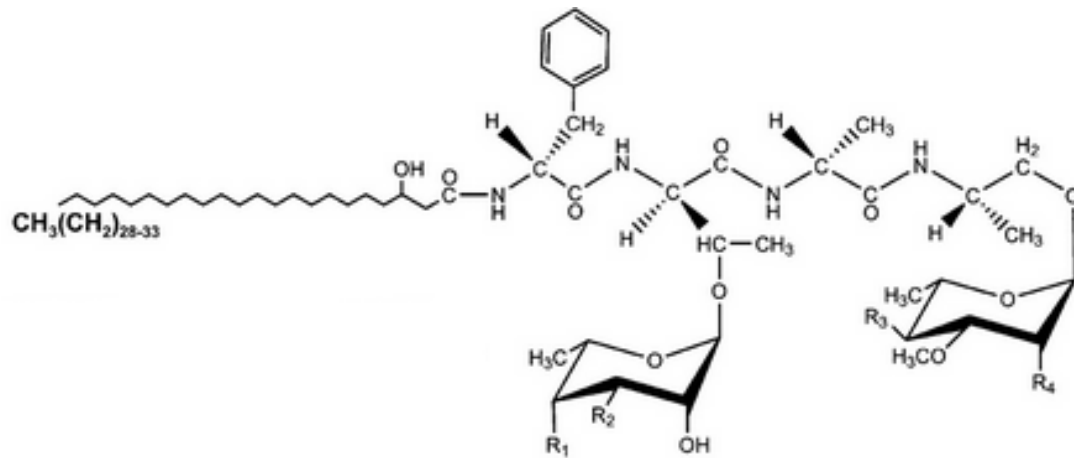


Figure 1.4.1: Generic mycolic acid structure in *M. smegmatis*.⁹

1.5 Modifying Antimicrobials

Modification of current antibiotics has been a common practice to develop a way to combat certain resistances developed by an organism. A series of experiments were performed by modifying Loracarbef (LOR), which is a known β -lactam antibiotic, with several transition metals; zinc, cadmium, nickel, palladium and platinum¹¹. Complexes were analyzed by FT-IR and NMR spectroscopy. Figure 1.5.1 shows the general coordination of the metal between the β -lactam and the carboxylic acid group of LOR¹¹.

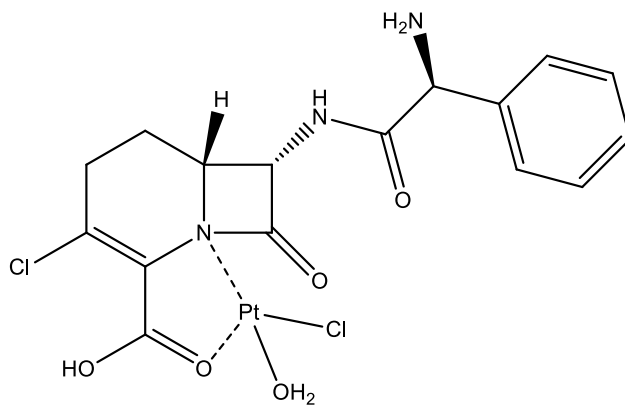


Figure 1.5.1¹¹: Lorcarbef coordinating with platinum

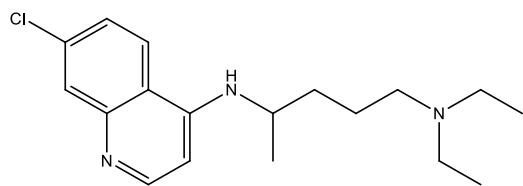
Antimicrobial activity was accurately studied using a disc diffusion technique to measure a zone of inhibition. Sterilized 6mm discs were preloaded with 1200 μg of the coordinated complexes and placed in the center of a growth medium plate inoculated with corresponding bacteria. Each sample was then incubated for 24-48 hrs¹¹. The bacteria tested were *Escherichia coli*, *Klebsiella pneumonia*, *Mycobacterium smegmatis*, *Kluyveromyces fragilis*, and *Saccharomyces cerevisiae*. These tests were also run alongside plates with the free LOR for comparison. The results for each were drastically different. The platinum derivative had activity across all organisms tested in some cases having a greater activity than that of free LOR¹¹. The nickel derivative shows no noticeable antimicrobial activity. While the zone of inhibition can

determine if a compound has antimicrobial properties, an MIC cannot be calculated (Table 1.5.3). This example shows that certain MDR (multi drug resistant) bacteria could become susceptible to a previously used antibiotic with transition metal modification.

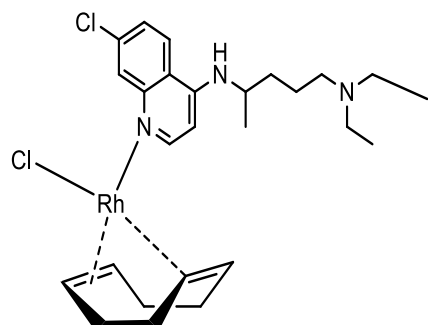
Organism	1	2	3	4	5	6	7	8
LOR	21	19	21	23	20	20	21	7
[Zn(LOR)(H ₂ O)(Cl)] Cl	0	0	0	0	0	0	0	0
[Cd(LOR)(H ₂ O)(Cl)] Cl	0	35	36	24	24	0	30	24
[Ni(LOR)(H ₂ O)(Cl)]Cl	8	0	7	0	0	9	10	0
[Pd(LOR)(H ₂ O)(AcO)] AcO	11	0	0	12	20	16	8	12
[Pt(LOR)(H ₂ O)(Cl)] Cl	10	16	29	12	10	10	18	19

Table 1.5.3 Lorcarbef complexes with multiple metals. Table indicates zone of inhibition in millimeters (larger zone means greater diffusion and activity)¹¹

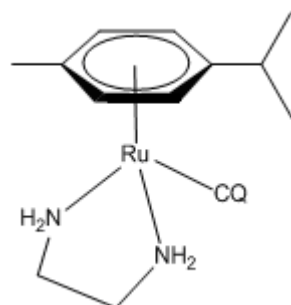
Chloroquine has been used to combat malaria since 1934. It is slowly becoming an ineffective treatment with the rapid spread of multi-drug resistant strains of malaria. Using metals in combination with chloroquine showed increased activity against chloroquine resistant strains, see (Figure 1.5.2)¹⁴. The general metal arene structure $[\text{Ru}(\eta^6\text{-arene})\text{Cl}_2]_2$ can be used as a precursor for a host of substituted metal arene complexes with chloroquine as well as a number of other ligands¹⁵.



Chloroquine (CQ)



Rh(II) complex (1)



Ru(II) complex (2)

Figure 1.5.2 Rh and Ru CQ complexes

Data shows that the CQ binds through the arene (N') nitrogen to the ruthenium metal center¹⁶. Compounds were tested against CQ resistant strains of *Plasmodium falciparum*. For resistant strains of the plasmodium, the CQ Ru(II) complex shows renewed activity¹⁴. This is another example where the modification of current antimicrobials using transition metals can give new life to pharmaceuticals where resistance has rendered them ineffective. Preliminary testing assays were performed using BALB/c mice by Delgado et al¹⁶. The mice were inoculated with *P. berghei* and then received a 4-day treatment of 1 mg/kg with both the Ru(II) and Rh(II) complex. Complex 2 (Figure 1.5.2) shows a 94% reduction in the parasites within the blood of the mice.

while complex 1 shows a 73% reduction after 4 days at 1 mg/kg compared to the control, untreated lab mice. This makes the bound complex more effective than chloroquine alone as a treatment to suppress the parasite¹⁶. Preliminary observations noted no hazardous side effects after a period of 30 days.

1.5.2: Critical remarks on Modified Antibiotics and Metal Complexes

Toxicity test results of several modified antimicrobials showed no lethal effects over a course of 30 days of administration for several compounds¹¹. Modifications of antimicrobial agents by the addition of a transition metal may help alleviate some of the known side effects for some chemical compounds. In cases discussed above, the relative dosage compared to the known control was lower and more effective. This opens the door for many other types of current antimicrobials that can be modified by metal coordination. Modification of other antibiotics that could potentially be used as ligands should be examined. Compounds developed by Zengin demonstrated that hydrophobicity played a key role in the activity of antimicrobial active compounds¹¹. This suggests that the cellular membrane and wall composition are susceptible to certain different configurations of metal coordinated complexes.

The limited body of work that has been reported leaves many unanswered questions as well as possibilities for tailoring organometallic antimicrobials. It has been shown that modification as well as addition to or by the metal complex has positive effects when combined with certain types of antimicrobials. With the rise in multi drug resistant organisms, exploration in this area is necessary to grow the field of antimicrobial discovery. Modifying existing antimicrobials in addition to developing new active organometallic compounds for use as pharmaceuticals could help alleviate the problem of drug resistance and help fulfill the 10x20' initiative proposed by [whoever].

1.6 Project Description

The scope of this work involves the synthesis of a set of transition metal complex antimicrobial agents. Previous work on both iridium and ruthenium arene complexes has shown that the ligands are the key to modifying activity the metal complex exhibits. There are many ligand combinations to be explored, from small synthetic molecules to naturally occurring amino acids and proteins. Naturally occurring compounds, such as amino acids, are an inexpensive diverse group of ligands that can act as bi- or even tri-dentate ligands. These amino acids can provide both hydrophobic and hydrophilic groups. This provides the ability to change the properties of the compound based on the cell's permeability to certain complexes. Using (COD) and amino acid combinations can be traced back to work done by Pannetier in 1975, developing $[\text{Rh}(\text{COD})(\text{aa})]$ complex (Figure 6.1)¹⁸

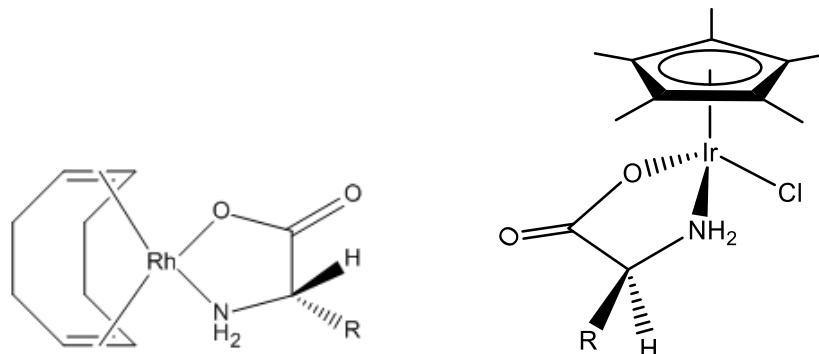
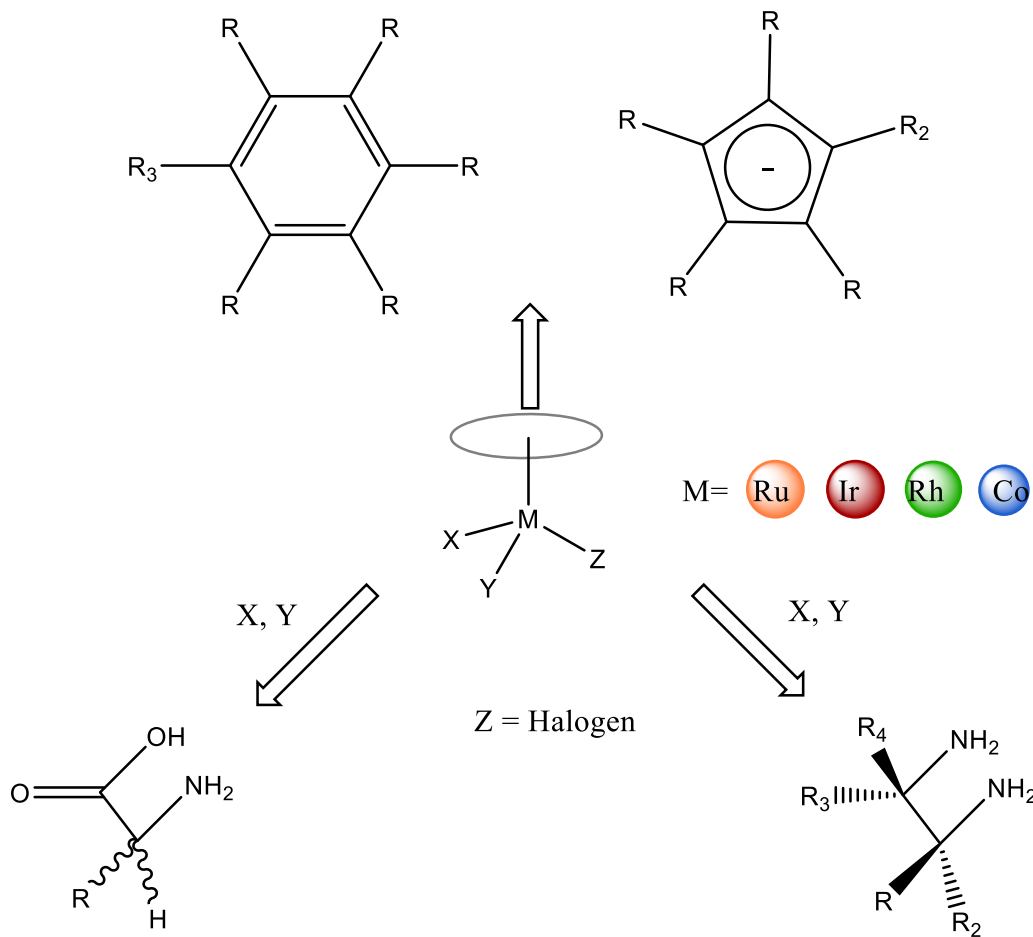


Figure 6.1: Amino acid complexes developed by Panntier(1) and Beck (2).

The Merola group has previously explored half-sandwich complexes with amino acids for asymmetric transfer hydrogenation (ATH).³⁰ Developing several compounds with iridium has also been explored by reaction of $[\text{Ir}(\text{COD})(\text{PMe}_3)_3]\text{Cl}$ with an appropriate bidentate amino acid ligand to form $[\text{Ir}(\text{aa})(\text{H})(\text{PMe}_3)_3]\text{Cl}$ ²⁰ complexes. Work done by Beck²¹ shows the use of amino acids as well to form organometallic bidentate ligands (Figure 6.1).

1.6.1: Design of Tailored Transition Metal Complexes

This investigation focuses on the formulation $(\eta^n\text{-arene})\text{M(L)X}$, where L is a bidentate ligand and X is a halogen, to achieve specific antimicrobial activity. Each subset of ligands and metal centers were changed independently to establish a clear structure activity relationship. The ability to change each part of the complexes independently allows for a systematic approach to tailor new antimicrobials. Along with the different metal centers (Scheme 6.1), a group of biologically active molecules will be explored as the interchangeable ligands (L). After characterization of the synthesized complexes, the initial biological activities will be determined as the MIC (minimal inhibitory concentration) of each complex against a panel of microbes. This ability to change multiple parts of the complex independently can allow the complex to exhibit multiple chemical traits including but not limited to hydrophobic vs. hydrophilic properties.



Scheme 6.1: Modular synthesis of the metallocene complex. The complex is constructed of one π -ligand arene, metal and one bidentate ligand.

As described previously, many pharmaceuticals are only effective in one specific form or size. Using the ligands to dictate the shape of the complex also influences the activity of the complex against a certain set of microbes. Metal charge and oxidation state are also modifications that will be explored. After the design of possible new antimicrobials, their mode of action (MoA) will be investigated to achieve a fundamental understanding of how all the elements of the compound work together and what properties are significant to each of the variable ligand.

References

- (1) Dabrowiak *Metals in Medicine*; J.Wiley and Sons LTD, 2009; Vol. 1.
- (2) Gilbert, D. N.; Guidos, R. J.; Boucher, H. W.; Talbot, G. H.; Spellberg, B.; Edwards, J. E.; Scheld, W. M.; Bradley, J. S.; Bartlett, J. G.; Infect Dis Soc, A. *Clin. Infect. Dis.* **2010**, 50, 1081.
- (3) Ravaglione, M. C.; Smith, I. M. N. *Engl. J. Med.* **2007**, 356, 656.
- (4) In *Multidrug-Resistant Tuberculosis (MDR TB) Fact Sheet*; American Lung Association 2010; Vol. 2011.
- (5) Rice, L. B. *Infect. Control Hosp. Epidemiol.* **2010**, 31, S7.
- (6) Allardyce, C.; Dyson, P.; Simonneaux, G., Ed.; Springer Berlin / Heidelberg: 2006; Vol. 17, p 177.
- (7) Dabrowiak *Metals in Medicine*; J.Wiley and Sons LTD, 2009; Vol. 1.
- (8) Gasser, G.; Ott, I.; Metzler-Nolte, N. *J. Med. Chem.* **2011**, 54, 3.
- (9) Schorey, J. S.; Sweet, L. *Glycobiology* **2008**, 18, 832.
- (10) Vasić, G. P.; Glodjović, V. V.; Radojević, I. D.; Stefanović, O. D.; Čomić, L. R.; Djinović, V. M.; Trifunović, S. R. *Inorganica Chimica Acta* **2010**, 363, 3606.
- (11) Zengin, H.; Dolaz, M.; Golcu, A. *Curr. Anal. Chem.* **2009**, 5, 358.
- (12) Novakova, O.; Kasparkova, J.; Bursova, V.; Hofr, C.; Vojtiskova, M.; Chen, H. M.; Sadler, P. J.; Brabec, V. *Chemistry & Biology* **2005**, 12, 121.
- (13) Beckford, F.; Dourth, D.; Shaloski, M.; Didion, J.; Thessing, J.; Woods, J.; Crowell, V.; Gerasimchuk, N.; Gonzalez-Sarrias, A.; Seeram, N. P. *J. Inorg. Biochem.* **2011**, 105, 1019.
- (14) Rajapakse, C. S. K.; Martinez, A.; Naoulou, B.; Jarzecki, A. A.; Suarez, L.; Deregnaucourt, C.; Sinou, V.; Schrevel, J.; Musi, E.; Ambrosini, G.; Schwartz, G. K.; Sanchez-Delgado, R. A. *Inorganic Chemistry* **2009**, 48, 1122.
- (15) Martinez, A.; Rajapakse, C. S. K.; Naoulou, B.; Kopkalli, Y.; Davenport, L.; Sanchez-Delgado, R. A. *Journal of Biological Inorganic Chemistry* **2008**, 13, 703.
- (16) Sánchez-Delgado, R. A.; Navarro, M.; Pérez, H.; Urbina, J. A. *J. Med. Chem.* **1996**, 39, 1095.
- (17) Navarro, M.; Pekerar, S.; Perez, H. A. *Polyhedron* **2007**, 26, 2420.
- (18) Kabra, V.; Meel, A.; Ojha, S. *Phosphorus, Sulfur & Silicon & the Related Elements* **2007**, 182, 2779.

- (19) Potvin, C.; Davignon, L.; Pannetier, G. *Bulletin De La Societe Chimique De France Partie I-Physicochimie Des Systemes Liquides Electrochimie Catalyse Genie Chimique* 1975, 507.
- (20) Roy, C. P.; Huff, L. A.; Barker, N. A.; Berg, M. A. G.; Merola, J. S. *Journal of Organometallic Chemistry* **2006**, 691, 2270.
- (21) Kramer, R.; Polborn, K.; Wanjek, H.; Zahn, I.; Beck, W. *Chemische Berichte* **1990**, 123, 767.
- (22). Li, F.; Collins, J. G.; Keene, F. R., Ruthenium complexes as antimicrobial agents. *Chemical Society Reviews* **2015**, 44 (8), 2529-2542.
- (23) Pandrala, M.; Li, F.; Feterl, M.; Mulyana, Y.; Warner, J. M.; Wallace, L.; Keene, F. R.; Collins, J. G., Chlorido-containing ruthenium(ii) and iridium(iii) complexes as antimicrobial agents. *Dalton Transactions* **2013**, 42 (13), 4686-4694.
- (24) Li, F.; Harry, E. J.; Bottomley, A. L.; Edstein, M. D.; Birrell, G. W.; Woodward, C. E.; Keene, F. R.; Collins, J. G., Dinuclear ruthenium(ii) antimicrobial agents that selectively target polysomes in vivo. *Chemical Science* **2014**, 5 (2), 685-693.
- (25) Patra, M.; Gasser, G.; Metzler-Nolte, N., Small organometallic compounds as antibacterial agents. *Dalton Transactions* **2012**, 41 (21), 6350-6358.
- (26) Wenzel, M.; Patra, M.; Senges, C. H. R.; Ott, I.; Stepanek, J. J.; Pinto, A.; Prochnow, P.; Vuong, C.; Langlotz, S.; Metzler-Nolte, N.; Bandow, J. E., Analysis of the Mechanism of Action of Potent Antibacterial Hetero-tri-organometallic Compounds: A Structurally New Class of Antibiotics. *ACS Chemical Biology* **2013**, 8 (7), 1442-1450.

Chapter 2: Anti-staphylococcal Complexes and Activities

2.1: INTRODUCTION

Hospital acquired (nosocomial) infections involving *Staphylococcus aureus* and methicillin-resistant *S. aureus* (MRSA) continue to present major challenges in the United States and Europe.¹⁻³ There is also evidence of an alarming increase in *S. aureus* skin infections in children.^{4,5} While both *S. aureus* and MRSA infections occur more frequently amongst persons with weakened defenses against infection in hospitals and healthcare facilities, MRSA infections are also of increasing concern in the community at large.⁶ Many *S. aureus* and MRSA infections are intractable due to antibiotic resistance and the tendency to be localized in high densities, such as in abscesses or biofilms.⁷ Colonization of in-dwelling catheters leads to biofilm formation and results in catheters serving as sources of continual infection in patients.⁷ One strategy to combat these infections is to develop novel and effective anti-infective agents.

This research aims to demonstrate that transition metal complexes comprised of either iridium (Ir), rhodium (Rh), or cobalt (Co) complexed with 1,2-diaminoethanes are active against *S. aureus* and MRSA. Although transition metal compounds have been used for their anti-cancer activity,⁹ there has been little research regarding the use of transition metal complexes as antibiotics¹⁰. Based on encouraging initial results, this work could lead to the identification of new therapeutic targets and development of a new class of urgently needed drugs to address the growing problem of difficult to treat *S. aureus* and MRSA infections.

2.2: Synthesis of Anti-Staphylococcal Complexes

2.2.1: Synthesis of Iridium and Rhodium Complexes

Though the cyclopentadienyl rhodium and iridium amino acid complexes discussed earlier (Section ##) exhibited significant anti-mycobacterial activity,⁸ they did not display any significant anti-staphylococcal activity. A different class of compounds was synthesized by replacing the amino acid ligands with ethylenediamine or 1,2-diaminocyclohexane ligands¹³. That replacement was successful in producing anti-staphylococcal compounds. Investigation of the ethylenediamines revealed that the iridium complex of the known anti-tuberculosis (TB) drug, ethambutol (figure 2.1), which is a substituted diamine, lost its anti-TB activity upon complexation with iridium, but gained modest anti-staphylococcal activity.

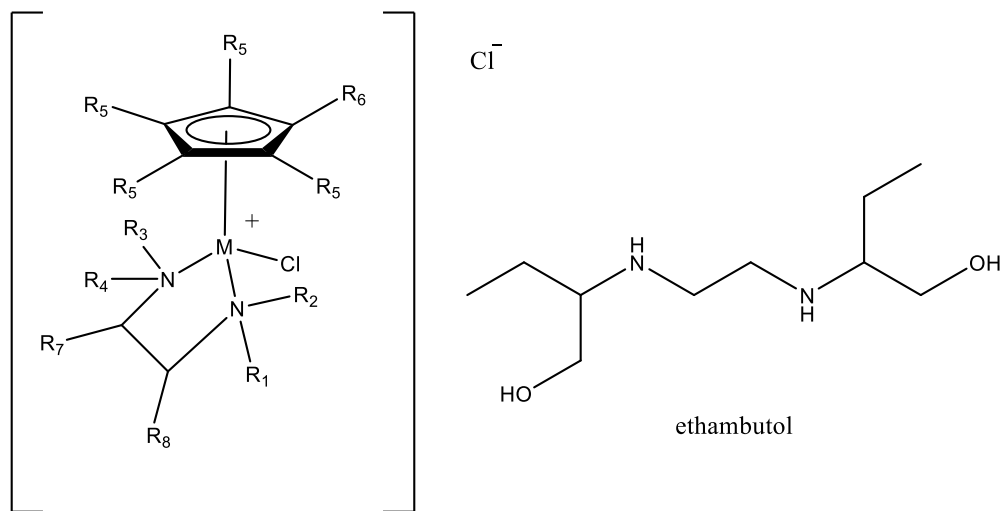


Figure 2.1: General ethylenediamine complex structure (See Table 1). Structure of ethambutol used as anti-TB drug.

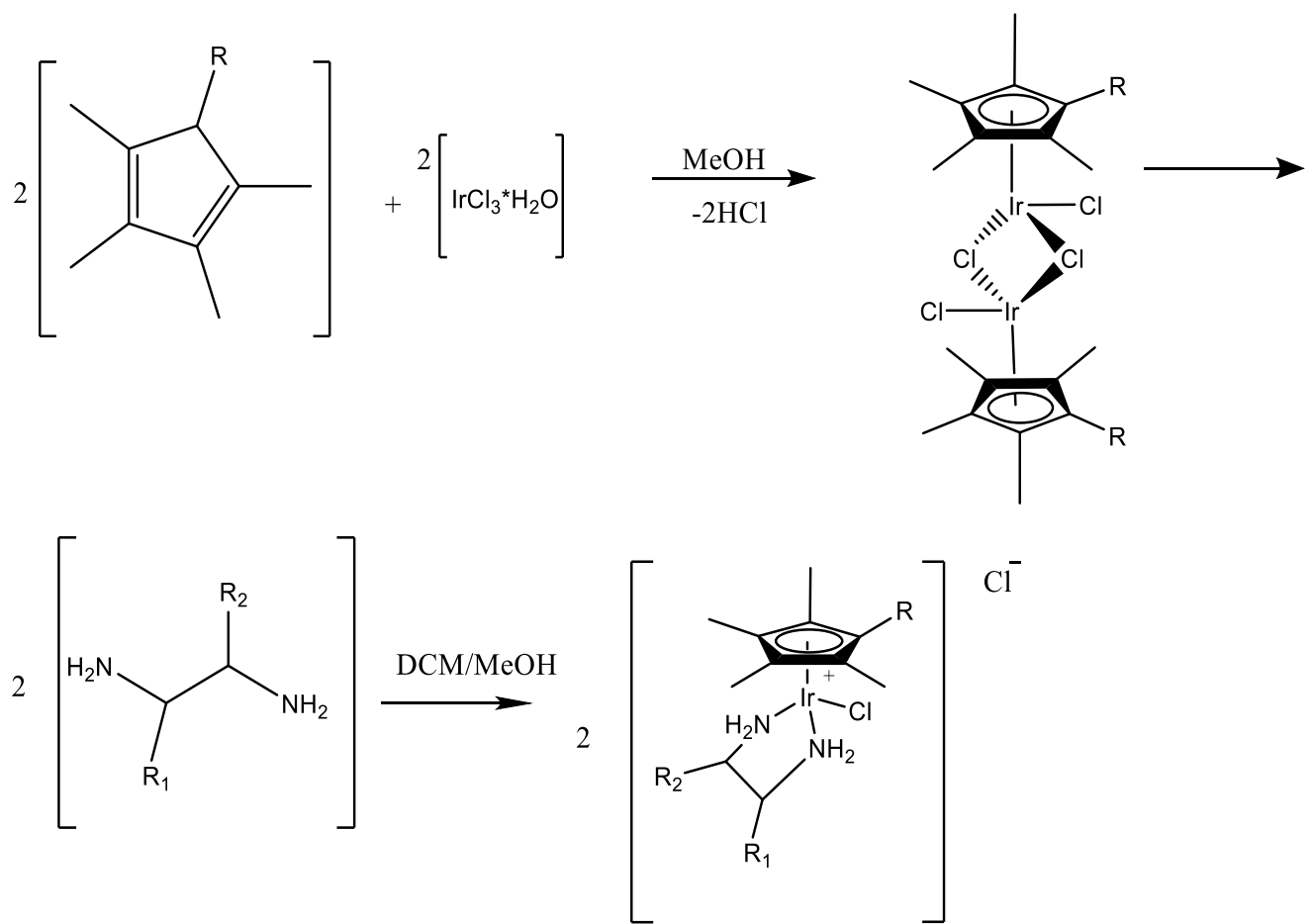
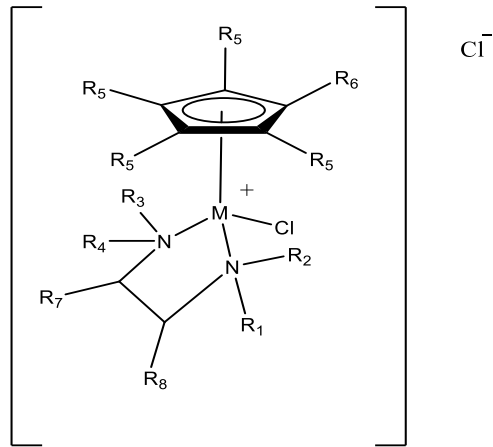


Figure 2.1.2: General synthesis for the ethylenediamine complexes used in these experiments



Compound	R ₁	R ₂	R ₃	R ₄	R ₅	R ₆	X	Metal	Diamine
1-Ir	H	H	H	H	-CH ₃	-(CH ₂) ₇ CH ₃	Cl	Ir	-CH ₂ -CH ₂ -
2-Ir	H	H	H	-C ₁₀ H ₇	-CH ₃	-(CH ₂) ₇ CH ₃	Cl	Ir	-CH ₂ -CH ₂ -
3-Ir	H	H	H	H	-CH ₃	-(CH ₂) ₇ CH ₃	Cl	Ir	Z-cyclohexane
4-Ir	-CH ₃	-CH ₃	-CH ₃	-CH ₃	-CH ₃	-(CH ₂) ₇ CH ₃	Cl	Ir	-CH ₂ -CH ₂ -
5-Ir	-CH ₃	-CH ₃	-CH ₃	H	-CH ₃	-CH ₃	Cl	Ir	CH ₂ -CH ₂ -
6-Ir	H	H	H	C ₇ H ₇	-CH ₃	-(CH ₂) ₇ CH ₃	Cl	Ir	CH ₂ -CH ₂ -
7-Ir	H	H	H	H	-CH ₃	-(CH ₂) ₇ CH ₃	Cl	Ir	E-cyclohexane
9-Ir	H	H	H	H	-CH ₃	-(CH ₂) ₈ CH ₃	Cl	Ir	E-cyclohexane
10-Ir	H	H	H	H	-CH ₃	-(CH ₂) ₁₀ CH ₃	Cl	Ir	E-cyclohexane
11-Rh	H	H	H	H	-CH ₃	-(CH ₂) ₇ CH ₃	Cl	Ir	-CH ₂ -CH ₂ -
12-Rh	H	H	H	-C ₁₀ H ₇	-CH ₃	-(CH ₂) ₇ CH ₃	Cl	Ir	-CH ₂ -CH ₂ -
13-Rh	H	H	H	H	-CH ₃	-(CH ₂) ₇ CH ₃	Cl	Ir	Z-cyclohexane
14-Rh	-CH ₃	-CH ₃	-CH ₃	H	-CH ₃	-CH ₃	Cl	Ir	CH ₂ -CH ₂ -
15-Rh	H	H	H	C ₇ H ₇	-CH ₃	-(CH ₂) ₇ CH ₃	Cl	Ir	CH ₂ -CH ₂ -
10-Co	H	H	H	H	-CH ₃	-CH ₃	I	Co	E-cyclohexane
11-Co	H	H	H	H	-CH ₃	-CH ₃	I	Co	Z-cyclohexane

Table 1: General structure and numbering for rhodium and iridium complexes. The table lists the various diamine ligand substitutions (R₁, R₂, R₃ and R₄), the C₅Me₄R substitution as well as the metal (See figure 2.1.2).

Each of the complexes developed and tested for anti-microbial testing was also tested for solubility and stability in a series of solvents. In each of the solvents tested, the complex remained in solution and was able to be recrystallized. Each complex recrystallized was then characterized via NMR and high resolution mass spectrometry (HRMS). Every complex studied was stable in solution for greater than 3 months. Table 1.1 lists the complexes studied and examined for solubility and stability in water and methanol. As –R sidechain on the cyclopentadienyl ring is increased, there is a loss of solubility. With 9-Ir, which has a dodecyl side chain, the solubility is less than 1mg/mL. This does not affect the MIC values, which are well below 500 µg/mL. Figure 2.1.3 shows a sample NMR spectra of the N-naphthylethylene diamine (9-Ir) complex after recrystallization using a two solvent system. A sample of 9-Ir (30 mg) was dissolved into 10 mL of DCM. Diethyl ether was layered slowly on top of the DCM layer causing a yellow powder to precipitate (9-Ir).

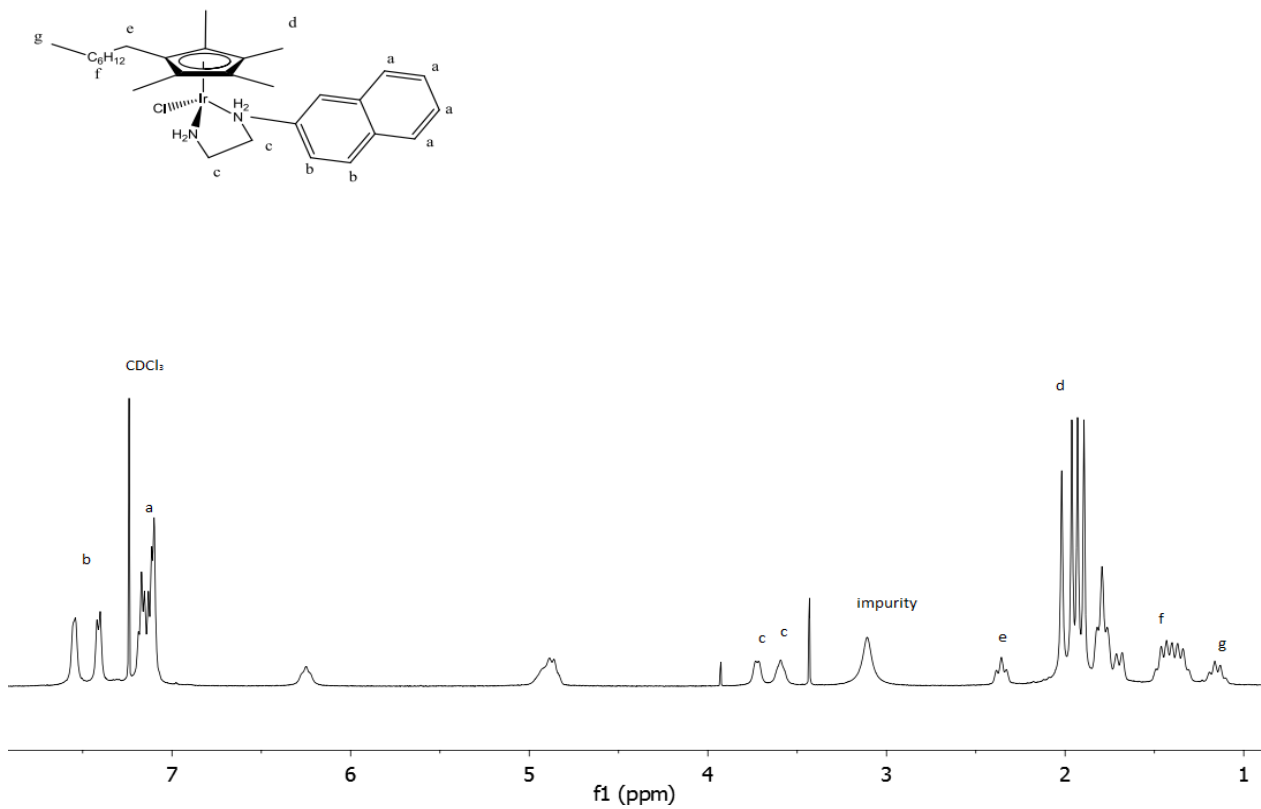


Figure 2.1.3: Naphtyl Iridium octyl complex ^1H NMR after recrystallization

The NMR spectrum is easily defined; chemical shifts and coupling constants are listed in supplemental 1. Even after being open to air and in solution for several months these complexes do not oxidize or degrade into another iridium byproduct.

Complex	Solvent System	Concentration
1-Ir	Water	15 mg/mL
1-Ir	MeOH	>15 mg/mL
3-Ir	Water	>15 mg/mL
9-Ir	Water	0.5 mg/mL
9-Ir	MeOH	~15 mg/mL

Table 1.1: Complexes studied for solubility and stability

2.2.2: Synthesis of Ruthenium Complexes.

With a successful history of ruthenium complexes in anti-cancer trials and development through FDA trials, complexes with ruthenium as a metal seemed likely candidates for antimicrobial studies. Ruthenium complexes (Figure 2.2.1) were synthesized and characterized using the same techniques as their iridium and rhodium counterparts. These complexes of the Ir/Rh piano stool complexes exhibit similar solubility and NMR properties (Supplemental 1). Table 2.2 lists the ruthenium complexes used for anti-microbial testing.

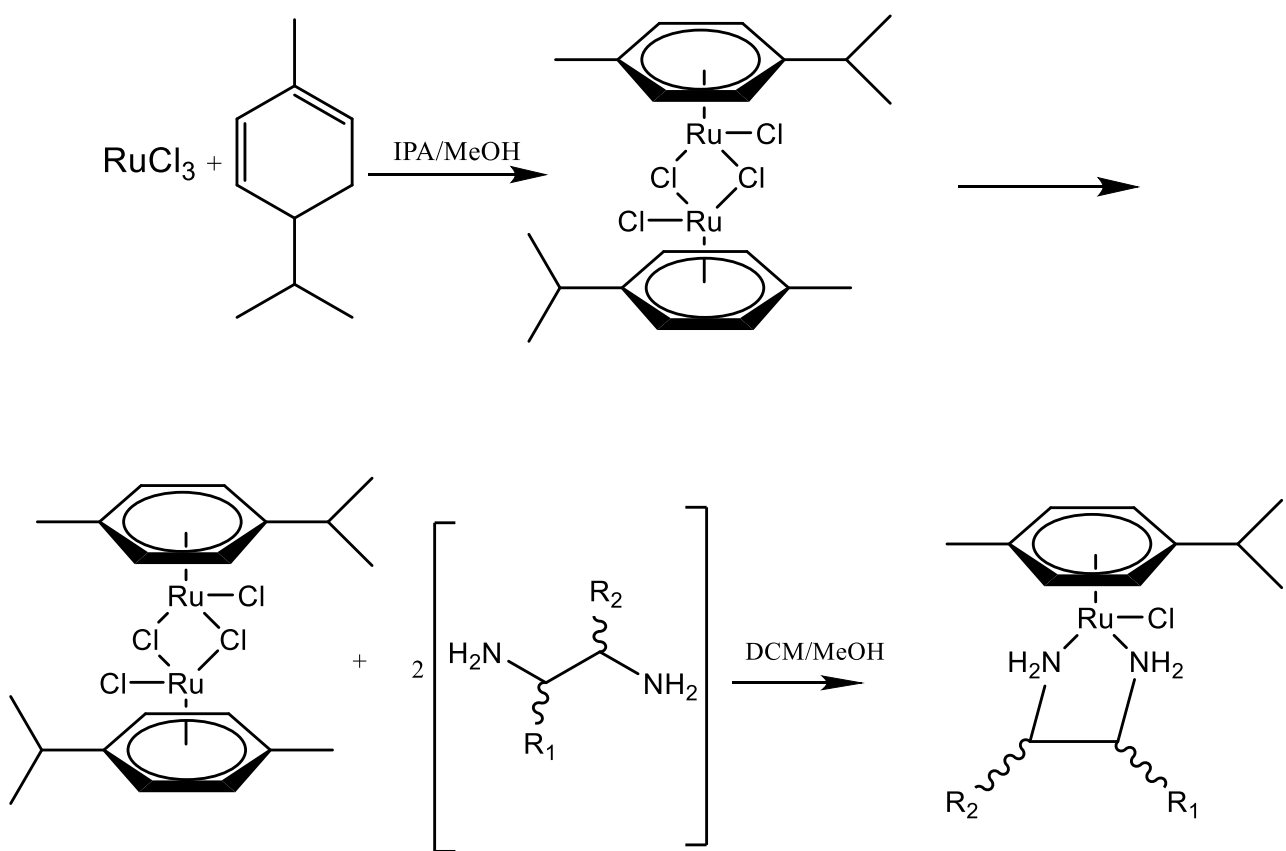
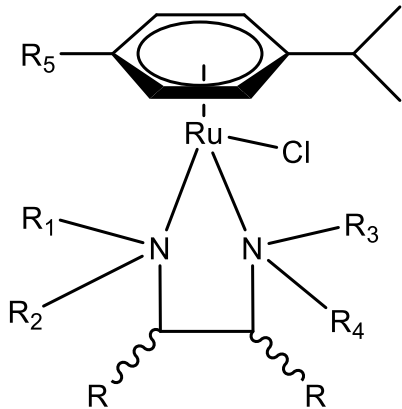


Figure 2.2.1: Reaction scheme of Ruthenium complexes using generic ethylenediamine ligands



Compound	R ₁	R ₂	R ₃	R ₄	R ₅	X	Metal	Diamine Backbones
1-Ru	H	H	H	H	-CH ₃	Cl	Ru	-CH ₂ -CH ₂ -
2-Ru	H	H	H	-C ₁₀ H ₇ (naphthylene)	-CH ₃	Cl	Ru	-CH ₂ -CH ₂ -
3-Ru	H	H	H	H	-CH ₃	Cl	Ru	Z-cyclohexane
4-Ru	-CH ₃	-CH ₃	-CH ₃	-CH ₃	-CH ₃	Cl	Ru	-CH ₂ -CH ₂ -
5-Ru	-CH ₃	-CH ₃	-CH ₃	H	-CH ₃	Cl	Ru	CH ₂ -CH ₂ -

Table 2.2: Ruthenium (p-cymene) complexes used for antimicrobial testing. All complexes were analyzed and confirmed by NMR and Mass Spec.

2.2.3: Synthesis of Cobalt Complexes.

To reduce the cost of transition metal antimicrobials as well as to use a more earth-abundant alternative, we felt it prudent to explore the syntheses of the first row congener of iridium: cobalt. The same synthetic pathway successful for iridium (Figure 2.3) was not available for cobalt, so a new synthesis was used based on cyclopentadienyl cobalt dicarbonyl [CpCo(CO)₂] and pentamethylcyclopentadienylcobalt dicarbonyl [Cp*Co(CO)₂] compounds as the starting

material. Based on this synthesis scheme in figure 2.3 the new cobalt complexes were formed. Each cobalt complex was analyzed following the same techniques as the Ir/Rh analogues. For spectral analysis and data see materials section 1.

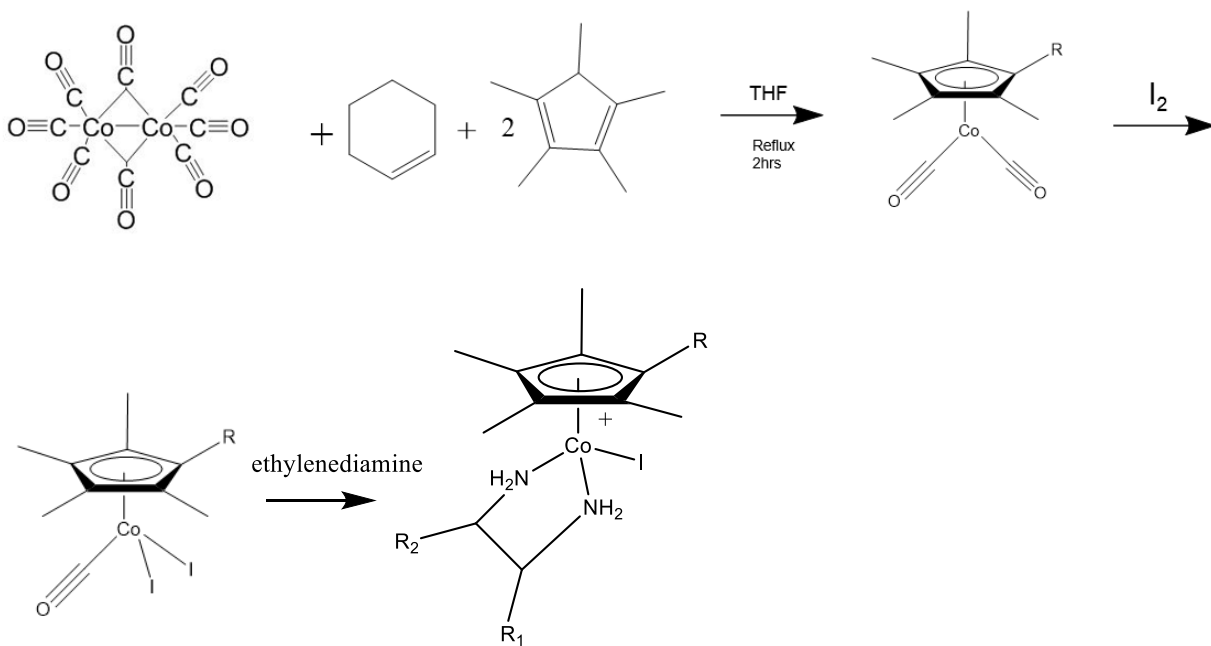


Figure 2.3: Outline of the synthesis of cobalt-containing TTMCS with ethylenediamine as the ligand. The procedure is the same for all diamines that include cobalt as the metal

2.3: Anti-staphylococcal Activities.

Ethylenediamine complexes using Cp^{*R} and cis-1,2-diaminocyclohexane (3-Ir) had potent antibiotic activity against *S. aureus* and the recent clinical isolates of MRSA. MICs of 4-8 mg/L against both *S. aureus* and the MRSA strains were observed (Table 2). Further, the MBCs (bactericidal concentration) for 3-Ir were almost the same as the MICs, demonstrating its bactericidal activity (Table 2). The two Ir-ethylenediamine compounds lacking the cyclic based backbone, 2-Ir and 6-Ir, exhibited weak anti-staphylococcal activity (Table 2). The two cobalt-based cyclopentadienyl diamines (10-Co and 11-Co) lacked anti-staphylococcal activity (Table

1). However, it should be pointed out that those two compounds lacked the octyl group, as did the inactive Ir-compound 5-Ir (Table 1). The data in Table 1 not only demonstrates that these first generation of TMCs exhibit potent activity against both *S. aureus* and MRSA (e.g., iridium ethylenediamine complex 3-Ir), but also provides preliminary insight into the antibiotic structure-activity relationships (SARs) for these complexes. The SAR analysis is possible due to the large number of complexes synthesized.

Table 2:

Minimal Inhibitory Concentration, MIC (mg/L) (Minimal Bactericidal Concentration, MBC, mg/L)

Compound	<i>S.aureus</i>	<i>S. aureus</i>	MRSA						
	29213	6538	Patient	43300	523000	53016	36361	34864	34380
1-Ir	250 (250)	250 (250)	250 (250)	250 (250)	250 (250)	250 (250)	250 (250)	250 (250)	250 (250)
2-Ir	62.5	62.5	62.5	32(32)	62.5	62.5	62.5	62.5	62.5
3-Ir	4 (8)	4 (8)	8 (8)	8 (8)	8 (8)	4 (16)	8 (8)	8 (16)	8 (8)
4-Ir	250 (250)	250 (250)	250 (250)	250 (250)	250 (250)	250 (250)	250 (250)	250 (250)	250 (250)
5-Ir	> 250	> 250	> 250	> 250	> 250	> 250	> 250	> 250	> 250
6-Ir	32	32	32	62.5	32	ND	ND	ND	32
7-Ir	16(16)	16(16)	32	32	32	32	32	32	32
8-Ir	4 (4)	4(4)	4(4)	4(8)	4(8))	4(8)	4(8)	4(8)	4(8)
9-Ir	16(32)	16(32)	8(16)	8(16)	8(16)	8(16)	8(16)	8(16)	8(16)
10-Ir	250 (250)	250 (250)	250 (250)	250 (250)	250 (250)	250 (250)	250 (250)	250 (250)	250
11-Rh	16(32)	16(32)	8(16)	8(16)	8(16)	8(16)	8(16)	8(16)	8(16)
12-Rh	62.5	62.5	62.5	32(32)	62.5	62.5	62.5	62.5	62.5
13-Rh	4 (4)	4(4)	4(4)	4(8)	4(8)	4(8)	4(8)	4(8)	4(8)

14-Rh	16(16)	16(16)	32	32	32	32	32	32	32	32
15-Rh	250 (250)	250 (250)	250 (250)	250 (250)	250 (250)	250 (250)	250 (250)	250 (250)	250 (250)	250 (250)
1-Ru	62.5	62.5	62.5	32	62.5	62.5	62.5	62.5	62.5	62.5
2-Ru	62.5	62.5	62.5	32	62.5	62.5	62.5	62.5	62.5	62.5
3-Ru	16(16)	16(16)	32	32	32	32	32	32	32	32
4-Ru	250 (250)	250 (250)	250 (250)	250 (250)	250 (250)	250 (250)	250 (250)	250 (250)	250 (250)	250 (250)
5-Ru	250 (250)	250 (250)	250 (250)	250 (250)	250 (250)	250 (250)	250 (250)	250 (250)	250 (250)	250 (250)
10-Co	> 250	> 250	> 250	> 250	> 250	> 250	> 250	> 250	> 250	> 250
11-Co	> 250	> 250	> 250	> 250	> 250	> 250	> 250	> 250	> 250	> 250
Vancomycin	2 (2)	1 (1)	0.5 (1)	1 (1)	1 (1)	1 (1)	1 (2)	1 (2)	1 (1)	1 (1)

Table 2. MICs/MBCs of transition metal ethylenediamine complexes against *S. aureus* and MRSA isolates.

2.3.1 Structure Activity Relationships:

Substitutions to the amino groups with either four (4-Ir) or three (5-Ir) methyl groups on the nitrogen atoms leads to a loss of activity (Table 2). We conclude that the hydrogen bond contributions of the NH-functionalities on opposite sides of the diamine core are important for activity. Several observations support the conclusion that the active species in these experiments is the organometallic complex and not the metal-free ligand. Comparison of complex 1-Ir, which incorporates ethylene-diamine as the organic ligand, and the free ligand, supports this finding. Ethylenediamine (EDA) alone exhibits no anti-staphylococcal activity (data not shown), so the observed activity against the staphylococci for compounds incorporating this ligand is almost certainly due to the complex. These observations lead us to conclude that these TMCs are robust and do not dissociate under conditions of the assay to yield a common iridium or rhodium species that would account for activity. Complexes 2-Ir and 3-Ir show that increased hydrophobicity of the diamine ligand is associated with enhanced anti-staphylococcal activity compared to the parent ethylenediamine complex 1-Ir (Table 1).

This data concludes that each individual piece of the “piano-stool complex” plays a crucial role to the activity against a given set of microbes. We can confirm that while the metal center plays a role in the activity it is the combination of all the “pieces” that give these compounds their antimicrobial activity. If the complexes were falling apart in solution or in the cellular matrix the activity would be similar for every complex. This is made evident with the decrease of the effectiveness of the ethambutol complex. In an in vitro study against a panel of mycobacteria, the ethambutol complex was noted to have little to activity. If this is the case, it must be concluded

that the complexes are remaining intact. This further proves that it is the whole complex and not an individual piece interacting with microbes.

2.3.2 Cis vs Trans Diaminocyclohexane Iridium / Rhodium Complexes:

Changing the stereochemistry of the ligand diaminocyclohexane from *R,S* to *S,S* resulted in a drastic change in MIC activity. The MIC for the *trans* counterpart was drastically increase to 125 ug/mL as compared with the *cis* diamine. The ^1H and ^{13}C NMR spectra of the isomers were identical. The two complexes were recrystallized and then submitted for X-ray crystallography. Figure 2.3.1 shows the crystal structure for both cis and trans complexes with IrCp^*Cl . Based on the X-ray crystal structure, the cis complex has formed bent/chair structure makes access to one of the sides of the iridium more favorable. This may allude to a possible reason *cis* is more active. If the chloride ligand is easily exchanged at the iridium metal center, the compound may have more space/access to interact with other parts of the cellular machinery. In many pharmaceuticals one isomer over another can prove to be either non-effective or in many cases toxic. This 3D structure may hint at what components of a TTMC are necessary for an active complex.

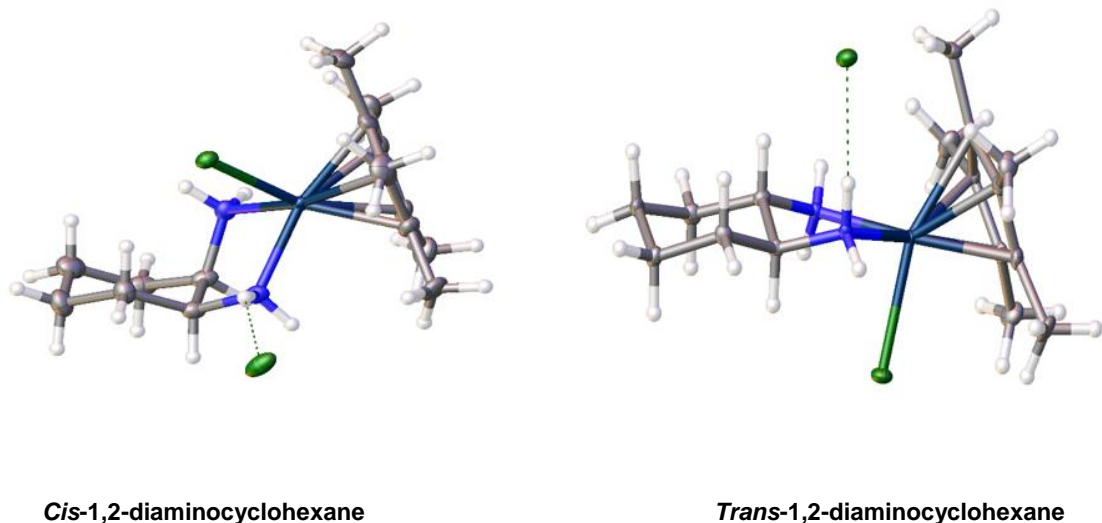


Figure 2.3.1: Cis vs Trans-1,2-diaminocyclohexane. Distinct structural differences concerning the stereochemistry in the ligands create three dimensionally different complexes.

For the following time kill studies the *S. aureus* strains were acquired from **American Type Culture Collection** (ATCC). These are laboratory tested and typed strains to ensure their purity. Survival of *S. aureus* strain ATCC 6358 and MRSA strain 34380 when exposed to 8 mg **3-Ir**/L (i.e., MIC/MBC) after 1, 2, 3, and 6 h exposure at 37° C were measured in two independent experiments (Figure 1). **3-Ir** killed both the antibiotic-susceptible *S. aureus* and the methicillin-resistant *S. aureus* strains (Figure 2).

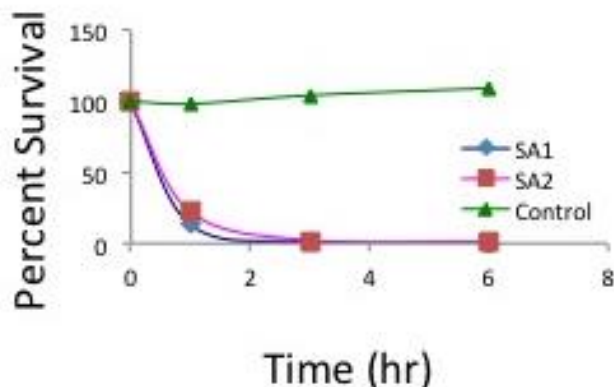


Figure 2.4: Killing *S. aureus* strain ATCC 6358 with 3-Ir.

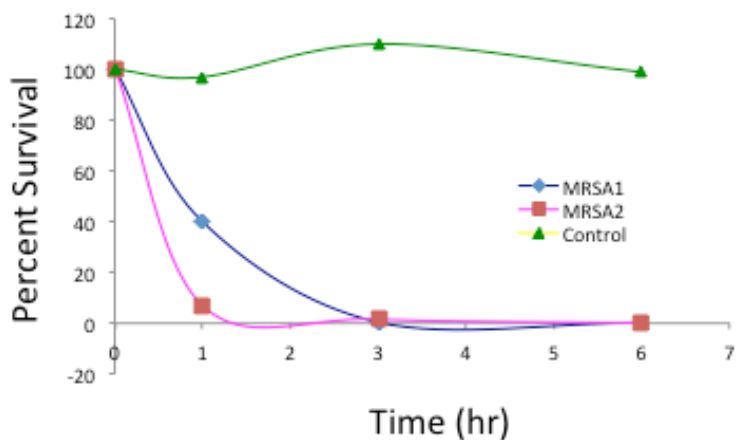


Figure 2.5: Killing of MRSA strain 34380 with 3-Ir.

The data shows that after 1 hour the complex has the ability to kill 80% of all the cells in the culture. The ability for the complex to cause such rapid cell death suggests that the mechanism must be affecting a critical piece of the cellular machinery.

2.4: Toxicology

Hemolytic activities.

In order to better gauge the viability of these new types of antimicrobials, hemolysis data is necessary. The TMCs with strong antibiotic activity (**1-Ir**, **2-Ir**, **3-Ir**) did not demonstrate hemolytic activity (< 10% hemolysis of sheep red blood cells at >145 mg/L) compared to vancomycin. Complexes using the dodecyl (9-Ir) and tetradecyl sidechains on the Cp ring exhibited some hemolytic activity ~125 mg/L. This shows that there is a difference in membrane interaction between the sidechains and the cell membranes themselves.

Chemical Toxicology:

To determine if the ethylenediamine complexes were specific for other microbes and not all cell types, the complexes were screened against a series of other microorganisms as well as mammalian cells. The complexes were selected to test toxicology of mammalian cells based on their activity against the previously tested *S. aureus* cell lines. Only active complexes were selected. The BacTiter-Glo™ Microbial Cell Viability Assay was used to determine ATP levels produced by the cell culture over a period of 6hrs. The protocol by Promega is listed in supplemental 1. Figures 2.4.1 and 2.4.2 show the levels of ATP produced over 6 hours. These levels are compared to a control, where there was no complex administered. Figure 2.4.1 shows similar ATP levels as the control until a concentration of 250 µg/mL or greater. While being able to produce ATP and spend energy, the human embryonic kidney (HEK) cells were able to carry out all necessary cellular process.

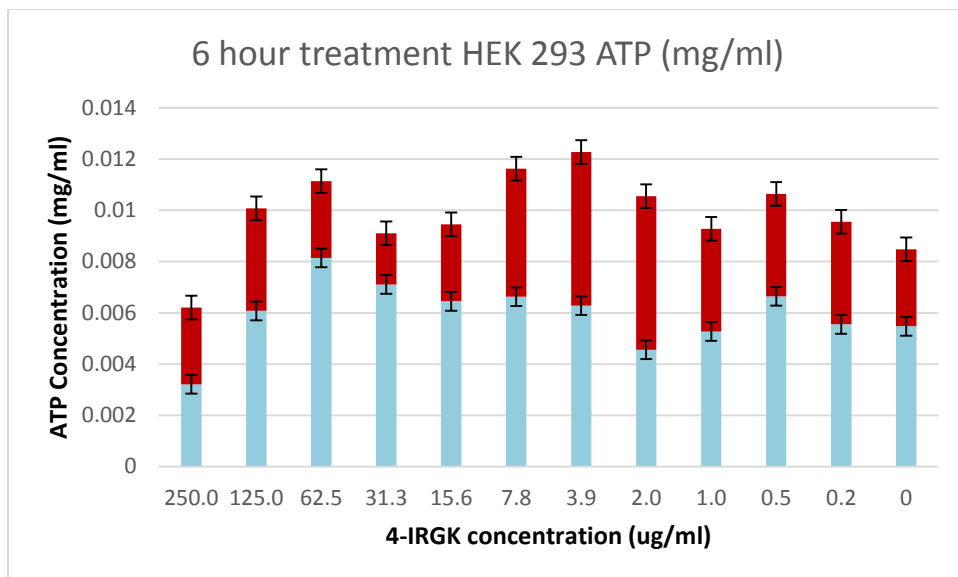


Figure 2.4.1: ATP level concentrations of human embryonic kidney in µg/mL. Each sample was monitored for 6hrs and compared to control at 0 µg/mL.

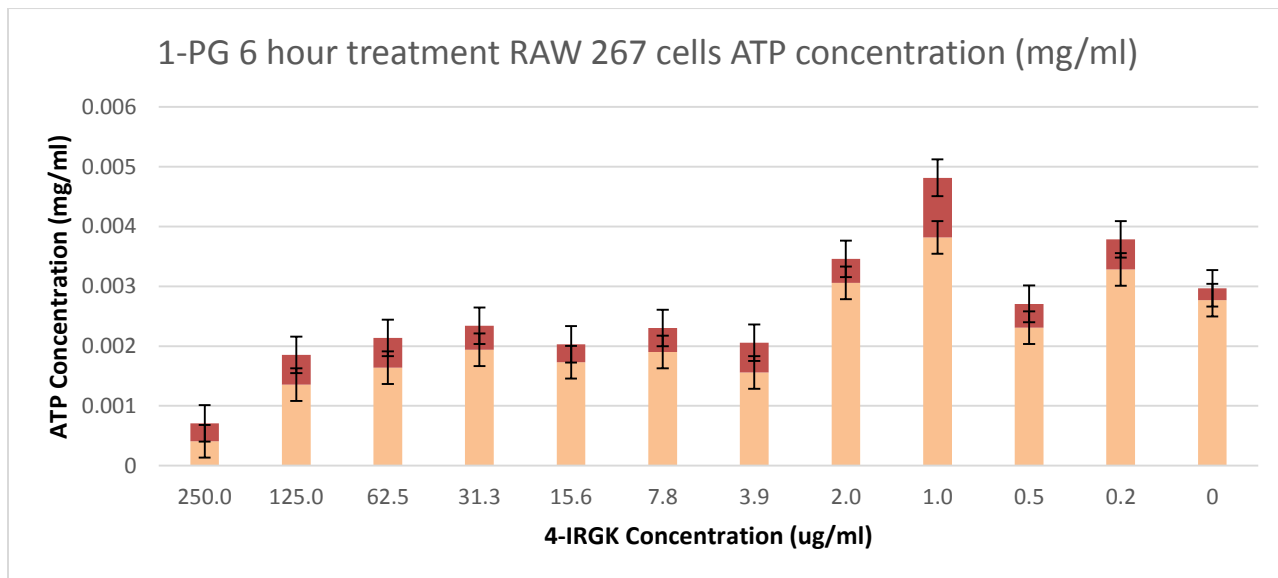


Figure 2.4.2: Murine Macrophages (RAW) were measured for ATP levels in µg/mL. Cellular ATP levels were nominal up until 125 µg/mL.

While the cobalt complexes discussed above were not tested, the iridium complexes that showed significant activity against *S. aureus* and MRSA strains showed no evidence of toxicity against

Vero cell line ATCC CCL-81 (ref. 29) at the highest concentrations tested of 500 µg mL⁻¹. In addition, compound 4-Ir was tested for toxicity in mice and it was determined that no detrimental toxicological effects were present at doses of 5 mg kg⁻¹²⁹.

2.5 Conclusion:

The transition metal complexes described here show specific activity against *S. aureus* strains and lack activity against other microorganisms (i.e., *Escherichia coli*, *Mycobacterium smegmatis*, *Candida albicans*, and *Aspergillus niger*). In addition, the specificity of the complexes that show activity indicates that there are specific structure/activity relationships that must be met. This is most dramatically noted in the high activity observed for complexes of the *cis* isomer of 1,2-diaminocyclohexane (4-Ir and 15-Co) and the total lack of activity of the complexes made with the *trans* isomer of 1,2- diaminocyclohexane (7-Ir and 16-Co). The combination of high and specific activity for certain complexes, the low cytotoxicity as tested with Vero, HEK, and RAW cell lines and the low hemolytic activity all suggest that this transition metal platform may prove to be useful in overcoming antibiotic resistance in *S. aureus*.

EXPERIMENTAL SECTION

Chemistry.

The ability to create these complexes with a straightforward two-step synthesis for the iridium variants (**Scheme 1**) provides a great advantage over many typical elaborate synthetic techniques used to create many drugs on the market today. The general synthesis and structure of the iridium chloro-bridged dimers may be found here¹²⁻¹³. The synthesis of the cobalt-complexes required a different pathway (**Scheme 2**) using either cyclopentadienylcobaltdicarbonyl [$\text{CpCo}(\text{CO})_2$] or pentamethylcyclopentadienylcobaltdicarbonyl [$\text{CpCo}(\text{CO})_2$] following the procedure of Koelle et al¹⁴. Full details of the cobalt complexes will be the subject of a forthcoming paper. Exemplars for both iridium and cobalt compounds can be found in the supplementary information.

General Procedure.

A round bottom flask was charged with appropriate amounts of the respective $[\text{IrCp}^{\text{xR}}\text{Cl}_2]_2$ in methylene chloride with magnetic stirring. After 10 minutes the ethylenediamine was added in a 2.1 molar excess drop wise to the stirring solution. After the addition of the ethylenediamine the solution was allowed react for an additional 30 minutes. The complexes were recrystallized with dichloromethane and ether or hexanes and collected on a fine fritted filter as yellow crystalline powders. ^1H NMR and ^{13}C NMR spectra were collected on a Varian MR-400 NMR spectrometer. High resolution mass spectrometry data was collected on Agilent 6220 Accurate Mass TOF LC-MS. Elemental analyses were performed by Atlantic Microlabs, Norcross, GA.

Materials.

Unless otherwise stated, synthetic work was carried out in air with untreated solvents. Commercially available reagents were obtained from the following sources: *cis*-1,2-diaminocyclohexane, N-benzylethylenediamine, N,N,N,N-tetramethylethylenediamine, N-(1-naphthyl)ethylenediamine and reagent grade solvents were purchased from Sigma-Aldrich, St. Louis, MO 63103. Deuterated solvents for NMR spectroscopy were obtained from Cambridge Isotope Laboratories. $[(\eta^5\text{-C}_5\text{Me}_5)\text{IrCl}_2]_2$, $[(\eta^5\text{-C}_5\text{Me}_4\text{C}_8\text{H}_{17})\text{IrCl}_2]_2$ and $\text{CoCp}(\text{CO})\text{I}_2$.

Synthesis of $[(\eta^5\text{-C}_5\text{Me}_5)\text{Ir}(\text{ethylenediamine})\text{Cl}]^+(\text{Cl}^-)$ Following the general procedure: 100 mg (0.125 mmol) of $[\text{IrCp}^*\text{Cl}_2]_2$ was combined with 15.9 mg of ethylenediamine in methylene chloride. The product was then recrystallized from methylene chloride. Yield: 91.7 mg (86.4%) HRMS/ESI+ (*m/z*): Calcd for $\text{C}_{12}\text{H}_{23}\text{N}_2[\text{Ir}]^+\text{Cl}$ 423.1257 Found 423.1265 Anal calc. $\text{C}_{12}\text{H}_{23}\text{Cl}_2\text{N}_2\text{Ir}$ C: 31.44 H: 5.06; Found C: 31.65 H: 5.10 ^1H NMR (400 MHz, Chloroform-*d*) δ 6.81 (br s, 2H), 5.74 (br s, 2H), 3.27 (m, 2H), 3.07 (d, 2H) 1.89 (dd, 15H, 5CpMe) ^{13}C NMR (101 MHz, Chloroform-*d*) δ 93.2 (CpC) 92.8 (CpC) 92.2 (CpC), 54.1 (CH₂)

Synthesis of $[(\eta^5\text{-C}_5\text{Me}_5)\text{Ir}(\text{cis}-1,2\text{-diaminocyclohexane})\text{Cl}]^+(\text{Cl}^-)$ Following the general procedure: 87.1 mg of $[\text{IrCp}^*\text{Cl}_2]_2$ was combined with 26.2 mg of *cis*-1,2-diaminocyclohexane. After recrystallization the product was recovered. Yield: 100.7 mg (96.4%). HRMS/ESI+ (*m/z*): Calcd for $\text{C}_{16}\text{H}_{29}\text{N}_2[\text{Ir}]^+\text{Cl}$ 477.1747; Found 477.1752. Anal calc. $\text{C}_{16}\text{H}_{28}\text{Cl}_2\text{N}_2\text{Ir} \cdot (\text{H}_2\text{O})$ C: 36.19 H: 5.71; Found C 35.83 H: 5.73 ^1H NMR (400 MHz, Chloroform-*d*) δ 5.72 (s, 2H, NH₂) 3.27 (m, 1H, CH), 3.09 (m, 1H, CH), 2.34 – 2.14 (m, 2H), 2.08 (d, *J* = 12.6 Hz, 2H), 1.91 (d, 15H CpMe), 1.65 (q, *J* = 12.9 Hz, 2H CH₂), 1.43 (q, *J* = 12.9 Hz, 2H) 1.26 (m, 2H), 1.22 (m, 2H, CH₂). ^{13}C NMR (101 MHz, Chloroform-*d*) δ 93.53 (CpC), 92.25(CpC), 84.75(CpC), 84.04(CpC), 34.9, 32.05, 31.72, 28.14, 26.93, 21.41, 10.44, 9.74.

Synthesis of $[(\eta^5\text{-C}_4\text{Me}_4\text{C}_8\text{H}_{17})\text{Ir}(\text{cis-1,2-diaminocyclohexane})\text{Cl}]^+(\text{Cl}^-)$ Following the general procedure: 50.0 mg of $[\text{IrCp}^{*(\text{octyl})}\text{Cl}_2]_2$ was combined with 24.3 mg of *cis*-1,2-diaminocyclohexane. After recrystallization the product was recovered as a yellow powder. Yield: 53.1 mg (98.5%). HRMS/ESI+ (*m/z*): Calcd for $\text{C}_{23}\text{H}_{43}\text{N}_2[{}^{193}\text{Ir}]\text{Cl}$ 575.2751; Found 575.2764 Anal calc. $\text{C}_{23}\text{H}_{43}\text{Cl}_2\text{N}_2\text{Ir}$ C: 45.23 H: 7.10; Found C: 45.19 H: 7.15 ^1H NMR (400 MHz, Chloroform-*d*) δ 3.38 (2, H), 3.10 (m, 2H), 2.24 (t, *J* = 8.0 Hz, 4H), 2.08 (m, 2H), 1.84(s, CpMe), 1.81 (s, CpMe), 1.78 (s, CpMe), 1.76 (s, CpMe) 1.64 (t, *J* = 8.0 Hz, 2H, CH_2), 1.43 (p, *J* = 8.1 Hz, 4H), 1.32 (m, 4H, 2 CH_2), 1.16 (m, 4H. 0.86 (t, 3H, CH_3) ^{13}C NMR (101 MHz, Chloroform-*d*) δ 88.2 (CpC) 86.2 (CpC) 86.1 (CpC), 51.39 (CH) 49.34 (CH), 31.88(CH_2), 31.87(CH_2), 30.59(CH_2), 29.69 (CH_2), 29.50(CH_2), 29.28(CH_2), 29.07(CH_2), 27.61(CH_2), 26.44 (CH_2), 26.22(CH_2), 25.17 (CH_2), 24.12 (CH_2), 15.25 (CH_3).

Synthesis of $[(\eta^5\text{-C}_5\text{Me}_4\text{C}_8\text{H}_{17})\text{Ir}(\text{N-(1-naphthyl)ethylenediamine})\text{Cl}]^+(\text{Cl}^-)$ Following general procedure: 50 mg of $[\text{IrCp}^{*(\text{octyl})}\text{Cl}_2]_2$ was combined in methylene chloride with 32.1 mg of N-(1-naphthyl)ethylenediamine dissolved in 10 mL of methanol. After recrystallization the product was recovered as a yellow powder. Yield: 40.6mg (67%). HRMS/ESI+ (*m/z*): Calcd for $\text{C}_{29}\text{H}_{43}\text{N}_2[{}^{193}\text{Ir}]$ 647.2321 Found 647.2394 Anal calc. $\text{C}_{29}\text{H}_{43}\text{Cl}_2\text{N}_2\text{Ir}$ C: 49.71 H: 6.46 Found C: 48.86 H: 5.96 ^1H NMR (400 MHz, Chloroform-*d*) δ 7.55 (d, *J*=6.9 Hz, 1H, ArH), 7.41 (d, *J* = 6.9 Hz, 1H, ArH), 7.14 (m, 4H, ArH), 4.88 (m, 2H), 3.72 (d, *J* =7.5 Hz, 1H), 3.60 (d, *J* =7.5 Hz, 1H), 3.11 (s, 2H), 2.36 (t, *J*=11.5 Hz, 2H), 2.02 (s, 3H, CpMe), 1.99 (s, 3H, CpMe) 1.93 (s, 3H, CpMe), 1.89 (s, 3H, CpMe), 1.79 (t, *J*=12.6, 2H, CH_2), 1.72 (d, 1H, CH) 1.52 – 1.28 (m, 4H), 1.16 (m, *J* = 11.5 Hz, 3H, CH_3). ^{13}C NMR (101 MHz, Chloroform-*d*) δ 129.9 (aryl), 127.9 (aryl), 127.8 (aryl) 86.2 (CpC) 86.1 (CpC), 60.39 (CH₂) 58.2 (CH₂), 31.88(CH₂), 31.87(CH₂), 30.59(CH₂), 35.69 (CH₂), 32.50(CH₂), 27.28(CH₂), 26.07(CH₂), 27.55(CH₂), 22.30 (CH₂), 14.15 (CH₃).

Synthesis of [(η 5-C₅Me₅)Ir(1S, 2S)-1,2-Bis(4-fluorophenyl)ethylenediamineCl]+(Cl-)

) Following the general procedure 2.2: 50 mg of [IrCp*Cl₂]₂ was combined with 42.3 mg of (1S, 2S)-1, 2-Bis(4-fluorophenyl)ethylenediamine dihydrochloride in a 50/50 mix of methylene chloride and methanol. 15 mg of sodium bicarbonate was added to the solution mixture. After recrystallization the product was recovered as a yellow powder. Yield: 67.5 mg (88%) HRMS/ESI+ (m/z): Calcd for C₂₄H₂₉N₂F₂[193Ir]Cl 611.1622; Found 611.1636. 1H NMR (400 MHz, DMSO-d6) 7.29 (dd, J = 8.5, 5.5 Hz, 2H), 7.22 (dd, J = 8.5, 5.5 Hz, 2H), 7.10 – 7.02 (m, 4H), 6.81 (m, 1H), 6.24 – 6.12 (m, 1H, NH), 5.58 (m, 1H, NH), 4.61 (t, J = 11.5 Hz, 1H), 4.40 (t, J = 11.5, 1H), 1.72 (s, 15H, CpMe). 13C NMR (101 MHz, DMSO-d6) 144.8 (aryl), 135.1 (aryl), 132.5 (aryl), 129.7 (aryl), 85.8 (CpC), 26.7 (CH), 8.95 (CpMe).

Synthesis of [(η 5-C₄Me₄C₅H₁₃)Ir(cis-1,2-diaminocyclohexane)Cl]+(Cl-)Following the general procedure 2.2: 50 mg of [IrCp*^{hexyl}Cl₂]₂ was combined with 15.9 mg of cis-1,2-diaminocyclohexane. After recrystallization the product was recovered. Yield: 52.0 mg (85%). HRMS/ESI+ (m/z): Calcd for C₂₁H₃₉N₂[193Ir]Cl Calc 547.2509; Found 547.2541
1H NMR (400 MHz, Chloroform-d) δ 6.51 (s, 1H, NH), 5.71 (s, 1H, NH), 4.03 (m, 1H, CH), 3.31 (m, 1H, CH), 2.24 (t, J = 8.5, 2H), 1.89 – 1.81 (d, J = 8.5, 15H, CpMe), 1.78 (m, 4H), 1.47 – 1.34 (m, 4H), 1.34 – 1.12 (m, 2H), 0.92 – 0.76 (m, 3H, CH₃). 13C NMR (101 MHz, Chloroform-d) δ 87.41 (CpC) 86.14 (CpC), 47.6 (CH) 46.31 (CH), 35.55 (CH₂), 32.64(CH₂), 29.69 (CH₂), 29.50 (CH₂), 27.61(CH₂), 26.44 (CH₂), 26.22, 24.12 (CH₂), 12.45 (CH₃), 10.4 (CpMe).

Synthesis of [(η 5-C₄Me₄C₁₂H₂₅)Ir(cis-1,2-diaminocyclohexane)Cl]+(Cl-)Following the general procedure 2.2: 50 mg of [IrCp*^{dodecyl}Cl₂]₂ was combined with 12.0 mg of cis-1,2-diaminocyclohexane. After recrystallization the product was recovered. Yield: 39.2 mg (67%).

HRMS/ESI+ (m/z): Calcd for C₂₇H₅₁N₂[193Ir]Cl Calc 631.3448 ; Found 631.3475 1H NMR (400 MHz, Chloroform-d) δ 5.69 (s, 1H, NH), 4.24 (s, 1H, NH), 3.24 (m, 1H, CH), 3.05 (m, 1H, CH), 2.39 – 2.19 (bm, 6H), 1.85 (s, 15H, CpMe), 1.71 – 1.62 (m, 4H), 1.61 – 1.52 (m, 4H), 1.51–1.45 (m, 4H), 1.40 (m, 6H), 1.35–1.15 (m, 10H), 0.84 (m, 3H, CH₃).

Synthesis of [(η⁵-C₅Me₄C₈H₁₇)Ir(1S,2S)-1,2-Bis(4-fluorophenyl)ethylenediamineCl][Cl]. Following the general procedure 2.2: 50 mg of [IrCp^{*}Cl₂]₂ was combined with 42.3 mg of (1S,2S)-1,2-Bis(4-fluorophenyl)ethylenediamine dihydrochloride in a 50/50 mix of methylene chloride and methanol. 15 mg of sodium bicarbonate was added to the solution mixture. After recrystallization the product was recovered as a yellow powder. Yield 67.6 mg (88%). HRMS/ESI+ (m/z): Calcd for C₂₅H₃₂N₂F₂[193Ir]Cl 611.17; Found 611.9852 Anal calc. C: Calc 44.51 H: 4.58 Found C: 44.58 H: 4.67 ¹H NMR (400 MHz, DMSO-d₆) 7.29 (dd, J = 8.5, 5.5 Hz, 2H), 7.22 (dd, J = 8.5, 5.5 Hz, 2H), 7.10 – 7.02 (m, 4H), 6.81 (m, 1H), 6.24 – 6.12 (m, 1H, NH), 5.58 (m, 1H, NH), 4.61 (t, J = 11.5 Hz, 1H), 4.40 (t, J = 11.5, 1H), 1.72 (s, 15H, CpMe)¹³C NMR (101 MHz, DMSO-d₆) 144.8 (aryl-F), 135.1 (aryl), 132.5 (aryl), 129.7 (aryl), 85.8 (CpC), 26.7 (CH), 8.95 (CpMe).

Synthesis of [(η⁵-C₄Me₄C₆H₁₃)Ir(cis-1,2-diaminocyclohexane)Cl][Cl]

Following the general procedure 2.2: 50 mg of [IrCp^{*hexyl}Cl₂]₂ was combined with 15.9 mg of *cis*-1,2-diaminocyclohexane. After recrystallization the product was recovered. Yield 45.4 mg (89%). HRMS/ESI+ (**m/z**): Calcd for C₁₆H₂₉N₂[¹⁹³Ir]Cl Calc 477.09; Found 478.1652. Anal Calc: C: 40.28 H: 6.13 Found C: 38.32 H: 6.96 ¹H NMR (400 MHz, Chloroform-d) δ 6.51 (s, 1H, NH), 5.71 (s, 1H, NH), 4.03 (m, 1H, CH), 3.31 (m, 1H, CH), 2.24 (t, J = 8.5, 2H), 1.89 – 1.81 (d, J = 8.5 15H, CpMe), 1.78 (m, 4H), 1.47 – 1.34 (m, 4H), 1.34 – 1.12 (m, 2H), 0.92 – 0.76 (m, 3H, CH₃) ¹³C NMR (101 MHz, Chloroform-d) δ 87.41 (CpC) 86.14 (CpC), 47.6 (CH) 46.3 (CH), 35.55(CH₂),

32.64(CH₂), 29.69 (CH₂), 29.50(CH₂), 27.61(CH₂), 26.44 (CH₂), 26.22, 24.12 (CH₂), 12.45 (CH₃), 10.4 (CpMe)

Synthesis of $[(\eta^5\text{-C}_5\text{Me}_4\text{C}_8\text{H}_{17})\text{Ir}(1S,2S)\text{-1,2-Bis(4-methoxyphenyl)ethylenediamine}]\text{[Cl]}$

Following the general procedure 2.2: 50 mg of [IrCp*Cl₂]₂ was combined with 46.2 mg of (1S, 2S)-1,2-Bis(4-methoxyphenyl)ethylenediamine dihydrochloride in a 50/50 mix of methylene chloride and methanol. 17 mg of sodium bicarbonate was added to the solution mixture. After recrystallization the product was recovered as a yellow powder. Yield 48.3 mg (62%).

HRMS/ESI+ (*m/z*): Calcd for C₂₆H₃₅N₂O₂[193Ir]Cl calc: 635.2008 Found: 635.2005 ¹H NMR (400 MHz, Chloroform-d) δ 7.49 (d, J = 8.5 Hz, 1H), 7.38 (d, J = 8.5 Hz, 1H), 6.71 (d, J = 8.6 Hz, 1H), 6.62 (d, J = 8.6 Hz, 1H), 4.79 (m, 1H, NH), 3.67 (m, 2H), 3.55 (m, 2H), 2.01 (s, 2H), 1.88 (s, 15H, CpMe), 1.59 (s, 6H, 2CH₃). ¹³C NMR (101 MHz, Chloroform-d) δ 159.56 (aryl), 130.24 (aryl), 129.78 (aryl), 129.60 (aryl), 114.32 (aryl), 114.16 (aryl), 86.68 (CpC), 77.19 (CpC), 63.27 (CH), 55.11 (CH), 54.99 (CH), 9.52 (CpMe), 9.31 (CpMe)

Synthesis of $[(\eta^5\text{-C}_5\text{H}_5)\text{Co}(\text{cis-1,2-diaminocyclohexane})\text{I}]^+(\text{I}^-)$ Cobalt procedure is modified from the general procedure: 100 mg of CoCp(CO)I₂ was dissolved in methylene chloride and allowed to stir for 10 minutes capped under nitrogen. 2.1 molar equivalence of *cis*-1,2-diaminocyclohexane was added dropwise via syringe to the solution and allowed to stir for 20 minutes under nitrogen. The solution immediately bubbles and eludes CO gas from the reaction. The solution turns a clear red-brown color. The solvent and excess *cis*-1,2-diaminocyclohexane was removed using a rotary evaporator. A dark red-brown powder was formed. The powder was then dissolved in deionized water and filtered on a fine frit to remove undesired products. The filtrate was collected and the water was removed and 76 mg of product was collected. **HRMS/ESI+ (*m/z*):** Calcd for C₁₁H₁₉N₂[Co]I 365.0033; Found 364.9924. ¹H NMR (400 MHz, methanol-d4) δ

4.8 (s, H, Cp), 3.29 (m, 2H, 2CH), 1.79 (m, 4H, 2CH₂), 1.35 (m, 4H, 2CH₂), 1.6 (m, 4H), 1.35 (m, 4H, 2CH₂),

Staphylococcal strains and measurement of MIC and MBC. *Staphylococcus aureus* strains ATCC 6358 and ATCC 29213 were obtained from the American Type Culture Collection (ATCC), the unrelated methicillin-resistant *S. aureus* strain 43330 was obtained from Danville Community Hospital, and the recent patient isolates of MRSA (523000, 522870, 34864, 36361, 53016, and 34380) were obtained from Georgetown University Medical Center.¹⁵ MICs were measured by broth microdilution of fresh overnight cultures according to the Clinical and Laboratory Standards Institute (CCLI) guidelines with cation-adjusted Mueller-Hinton broth and an inoculum of 10⁵ CFU/mL.¹¹ Stocks of the compounds were dissolved in Mueller-Hinton broth. The MIC (mg/L) was defined as the lowest concentration of compound completely inhibiting the appearance of turbidity by eye and confirmed by absorbance 540 nm. The MBC (mg/L) was defined as the lowest concentration of compound reducing the colony count by 99.9 % of the colony count in the initial, compound-free, inoculated well after 24 hr incubation. All results represent the average of three independent measurements.

References

- (1) Klevens, R. M.; Morrison, M. A.; Nadle. J. et al. Invasive methicillin-resistant *Staphylococcus aureus* infections in the United States. *J. Am. Med. Assoc.* **2007**, *298*, 1763–1771.
- (2) De Kraker, M. E. A.; Davey, P. G.; Grundmann, H. et al. Mortality and hospital stay associated with resistant *Staphylococcus aureus* and *Escherichia coli* bacteremia: estimating the burden of antibiotic resistance in Europe. *PLoS Medicine* **2011**, *8*, e1001104.
- (3) Hadler, J. L.; Petit, S.; Mandour, M.; Cartter, M. L. Trends in invasive infection with methicillin-resistant *Staphylococcus aureus*, Connecticut, USA, 2001-2010. *Emerg. Infect. Dis.* **2012**, *18*, 917-924.
- (4) Nasseri, I.; Jerris, R. C.; Sobol, S. E. Nationwide trends in pediatric *Staphylococcus aureus* head and neck infections. *Arch. Otolaryn. Head Neck Surg.* **2009**, *135*, 14-16.
- (5) Saxena, S.; Thompson, P.; Birger, R.; Bottle, A.; Spyridis, N.; Wong, I.; Johnson, A. P.; Gilbert, R.; Sharland, M. et al. Increasing skin infections and *Staphylococcus aureus* complication in children, England, 1997-2006. *Emerg. Infect. Dis.* **2010**, *16*, 530-533.
- (6) Kouyos, R.; Klein, E; Grenfell, B. Hospital-community interactions foster coexistence between methicillin-resistant strains of *Staphylococcus aureus*. *PLoS Pathogens* **2013**, *9*, e1003134.
- (7) Balaban, N.; Cirioni, O.; Giacometti, A. et al. Treatment of *Staphylococcus aureus* biofilm infection by the quorum-sensing inhibitor RIP. *Antimicrob. Agents Chemother.* **2007**, *51*, 2226-2229.
- (8) Karpin, G.; Merola, J. S.; Falkinham, J. O. III. Transition metal- α -amino acid complexes with antibiotic activity against *Mycobacterium* spp. *Antimicrob. Agents Chemother.* **2013**, *57*, 3434-3436.
- (9) Dabrowiak, J. C. 2009. Metals in Medicine. J. Wiley and Sons, Ltd. New York
- (10) Ben Hadda, T.; Akkurt, M.; Filali Baba, M. et al. Anti-tubercular activity of Ruthenium (II) complexes with polypyridines. *J. Enzy. Inhib. Med. Chem.* **2009**, *24*, 457-463.
- (11) Maisuria B. B.; Actis, M. L.; Hardrict, S. N. et al. Comparing micellar, hemolytic, and antibacterial properties of di- and tricarboxyl dendritic amphiphiles. *Bioorg. Med. Chem.* **2011**, *19*, 2918-2926.
- (12) Morris, D.M.; McGeagh, M.; DePena, D.; Merola, J.S. Extending the Range of Pentasubstituted Cyclopentadienyl Compounds: the Synthesis of a Series of Tetramethyl(alkyl or aryl)Cyclopentadienes, their Iridium Complexes and Their Catalytic Activity for Asymmetric Transfer Hydrogenation, *Polyhedron*, accepted for publication.
- (13) Merola, J. S.; Morris, D.; De Weerd, N. Di- μ 2-chlorido-bis-[chlorido(η (5)-2,3,4,5-tetra-methyl-1-propyl-cyclo-penta-dien-yl)iridium(III)]. *Acta Cryst. Sect. E, Struct. Rep. Online* **2013**, *69*:m176.

(14) Koelle, U.; Fuss, B.; Belting, M.; Raabe, E. Pentamethylcyclopentadienyl transition metal complexes. 9. Reactions and solid-state and solution behavior of dinuclear cobalt(II) complexes $[C_5Me_5Co(\mu\text{-}X)]_2$

(15) Clinical and Laboratory Standards Institute. 2012. Methods for dilution, antimicrobial susceptibility tests for bacteria that grow aerobically, 9th ed. Approved standard M07-A7. Clinical and Laboratory Standards Institute, Wayne, PA.

Chapter 3: Mycobacteria and Amino-Acid Complexes

3.1: Introduction

A number of species of the environmental nontuberculous mycobacteria (NTM) are opportunistic human pathogens¹. There is considerable accumulated evidence that the prevalence and incidence of nontuberculous mycobacterial infection are increasing⁽²⁻⁷⁾. The major NTM representatives include the slowly growing *Mycobacterium avium*, *Mycobacterium intracellulare*, *Mycobacterium kansasii*, *Mycobacterium xenopi*, *Mycobacterium malmoense*¹ and the rapidly growing *Mycobacterium abscessus*, *Mycobacterium chelonae*, and *Mycobacterium fortuitum*⁽⁸⁾. *M. avium* and *M. abscessus* are emerging pathogens of individuals with cystic fibrosis^(9, 10). A number of species cause dermal and subcutaneous infections in humans and animals, including *Mycobacterium marinum*^(11, 12), *Mycobacterium ulcerans*^(13, 14) and *Mycobacterium haemophilum*⁽¹⁵⁾. Because of the paucity of effective anti-mycobacterial antibiotics and relative antibiotic-resistance of the mycobacteria, treatment of these infections is problematic. Thus, there continues to be a need for both systemic and topical anti-mycobacterial agents.

Transition metals, in combination with a variety of ligands, have been shown to exhibit cytotoxic or antibiotic activity⁽¹⁶⁾. The transition metals, primarily ruthenium⁽¹⁷⁾ and platinum⁽¹⁸⁾ have been linked with a variety of ligands to yield complexes with varying degrees of cytotoxic or antibiotic activity. To date there has been no significant systematic study designed to elucidate the role of the transition metal (e.g., rhodium, iridium, and ruthenium) or ligand on antibiotic activity. With the onset of multi-drug resistant strains of many types of pathogenic bacteria (e.g., *Mycobacterium tuberculosis* and methicillin-resistant *Staphylococcus aureus*, MRSA) the field of transition metal drug exploration has been of growing interest. Antimicrobial activities of ruthenium(II) complexes have been shown to combat these bacteria and offer a new field of study in antimicrobial activity⁽¹⁹⁾.

In an effort to move towards identifying novel anti-mycobacterial compounds, we report the MICs, MBCs, hemolytic, and cytotoxic activities of a group of 41 transition metal-amino acid complexes against strains of *M. abscessus*, *M. avium*, *M. intracellulare*, *M. chelonae*, *M. marinum*, *M. bovis* BCG, and *Mycobacterium smegmatis*. These results will be used to guide the synthesis and tailor the design of more effective transition metal-amino acid complexes for chemotherapy of nontuberculous mycobacterial infections.

3.2: Synthesis of Transition metal- α -amino acid complexes.

Chemical Synthesis

For the iridium and rhodium complexes, the majority tested here have been previously characterized by David Morris and J.S. Merola et al. Figure 3.1 shows the overall synthesis for the amino acid Cp*-R complexes. Several novel amino acid complexes were synthesized building on previous work by Morris et. al. These complexes were previously described as being transfer hydrogenation catalysts. With these complexes that used the use of naturally occurring biological ligands (amino acids), their use in a biological system was explored. Upon review of the literature, similar complexes were explored for anti-cancer activity as well as comparison towards healthy mammalian cells.⁽¹⁸⁾

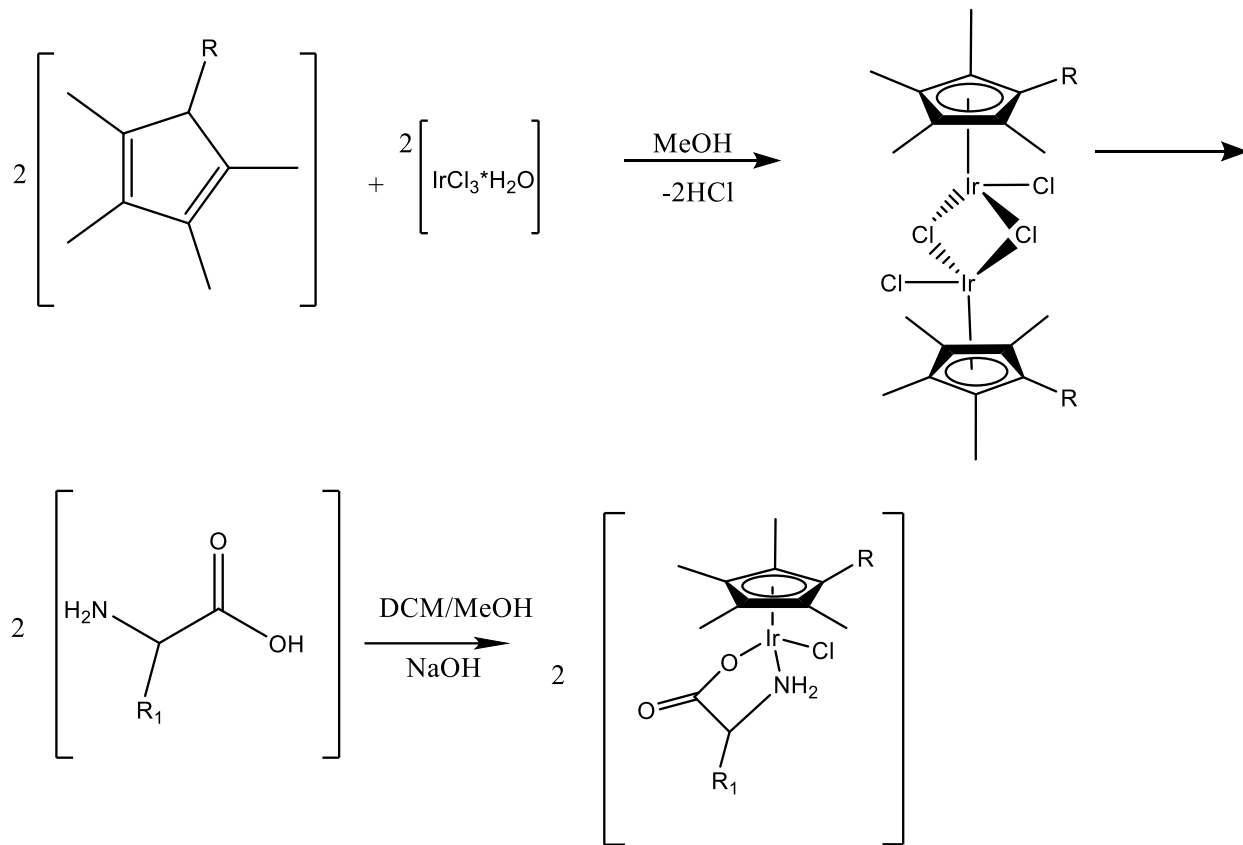


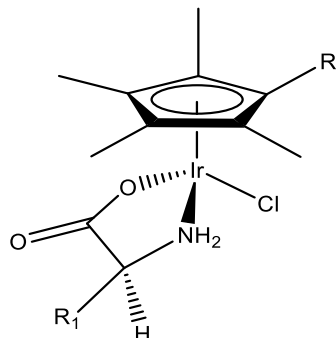
Figure 3.1: Synthesis of iridium transition metal complexes for use as anti-mycobacterial drugs. R₁ refers to any side chain both synthetic or from naturally occurring amino acids. Iridium can be replaced by rhodium via the same methods. – R refers to a number of organic groups.

Each of the complexes developed and tested for anti-microbial testing were also tested for solubility and stability in a series of solvents. In each of the solvents tested, the complex remained in solution and was able to be recrystallized. Each complex recrystallized was then studied via NMR and Hi-res Mass Spectrometry. Every complex studied was stable in solution for greater than 3 months. Table 3.1 lists the complexes studied and examined for solubility and stability in water and methanol. As –R sidechain on the cyclopentadienyl ring is increased, there is a loss of solubility in polar aprotic solvents. With 9-Ir which makes use of a dodecyl side chain, the solubility is less than 1mg/mL. This does not affect the MIC values, which are well below 0.5

mg/mL. A sample of 1-PG (30 mg) was dissolved into 10 mL of DCM. Diethyl ether was layered slowly on top of the DCM layer causing a yellow powder to precipitate (1-PG). This was to ensure a pure sample for testing.

Complex	Solvent System	Concentration
1-PG	Water	15 mg/mL
1-PG	MeOH	>15 mg/mL
1-Pro	Water	>15 mg/mL
2-Pro	Water	0.5 mg/mL
2-PG	MeOH	~15 mg/mL

Table 3.1: Complexes studied for solubility and stability



Compound	R ₁	R ₆	X	Metal
1-(L-PG)*	H	-(CH ₂) ₇ CH ₃ (octyl)	Cl	Ir
2-(L-PG)*	H	-(CH ₂) ₇ CH ₃ (octyl)	Cl	Ir
1 (L-phe)	H	-(CH ₂) ₇ CH ₃	Cl	Ir
1 (L-pro)	-CH ₃	-CH ₃	Cl	Ir
1 (D-val)	-CH ₃	-CH ₃	Cl	Ir
1 (D-pro)	H	-CH ₃	Cl	Ir
1 (L-leu)	H	-CH ₃	Cl	Ir
1 (L-iso)	H	-CH ₃	Cl	Ir
1 (L-hyp)	H	-CH ₃	Cl	Ir

1 (gly)	H	--(CH ₂) ₇ CH ₃	Cl	Ir
2 (L-ser)	H	-CH ₃	Cl	Rh
2 (L-PG)*	H	-CH ₃	Cl	Rh
2 (D-val)	-CH ₃	-CH ₃	Cl	Rh
2 (D-pro)	H	-(CH ₂) ₇ CH ₃ (octyl)	Cl	Rh
5-(L-PG)*	H	-CH ₃	I	Co
5-(L-pro)	H	-CH ₃	I	Co

Table 3.2: General structure and numbering for rhodium and iridium complexes. The table lists the various amino acid ligand substitutions, the C₅Me₄R substitution as well as the metal. *PG = phenylglycine

3.2.2: Synthesis of Cobalt Complexes.

As with the anti-staphylococcal complexes a search to reduce the cost of transition metal antimicrobials as well as to use a more earth-abundant alternative, cobalt was considered as an alternative metal center. The same synthetic pathway successful for iridium (Figure 3.3) was not available for cobalt, so a new synthesis based on cyclopentadienyl cobalt dicarbonyl [CpCo(CO)₂] and pentamethylcyclopentadienylcobalt dicarbonyl [Cp*Co(CO)₂] compounds as the starting material. As with the previously mentioned iridium complexes, the same group of amino acids was used as ligands for creating the Cp* cobalt complexes. Each cobalt complex was analyzed following the same techniques as the Ir/Rh analogues. Solubility was once again explored for use in biological systems.

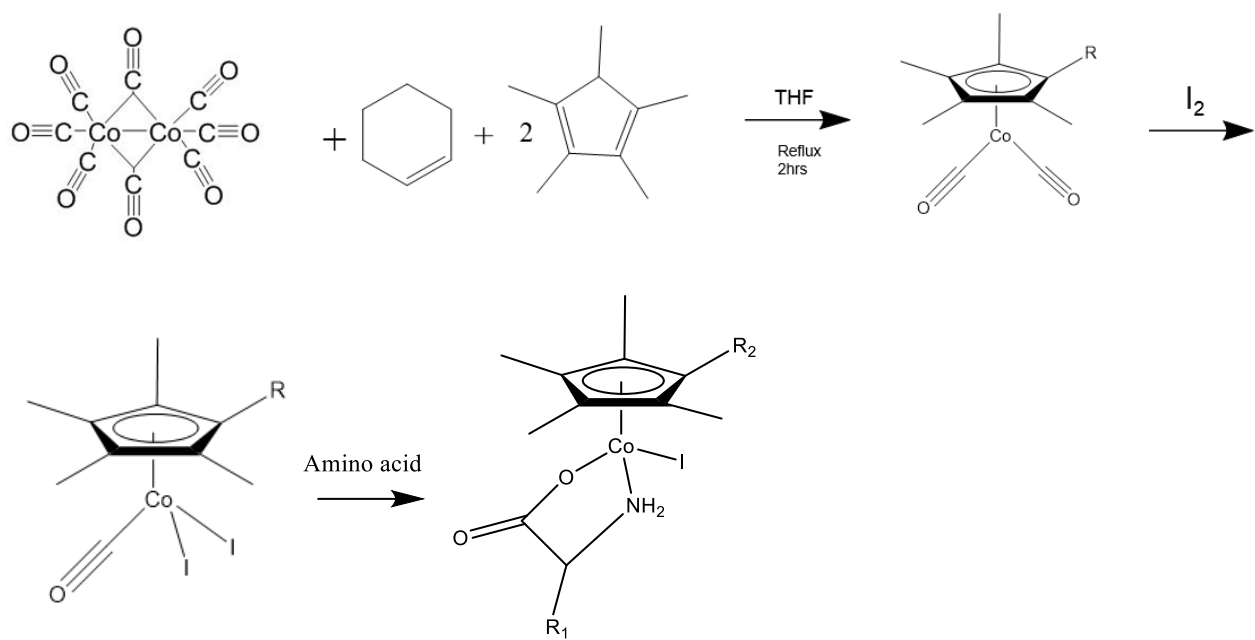


Figure 3.2: Outline of the synthesis of cobalt-containing amino acid complexes. The procedure is the same for all amino acids that include cobalt as the metal

Here figure 3.3 shows the structure and HNMR for the complex 1-PG. For all other spectral analysis and characterization, data see materials section 1.

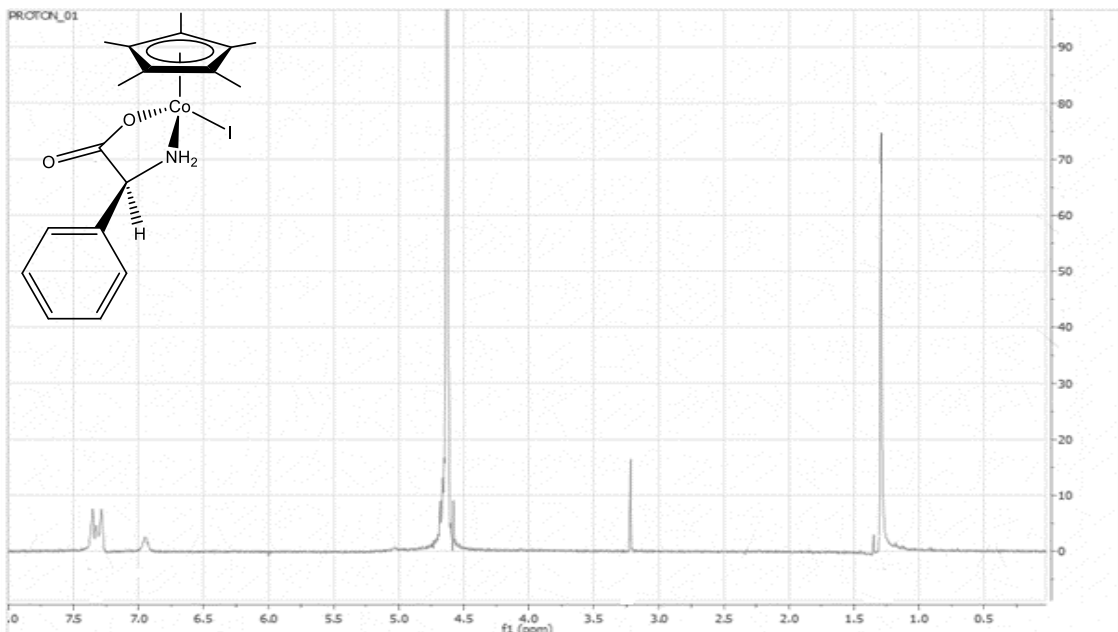


Figure 3.3: Cobalt complex (1-PG) ^1H NMR after recrystallization

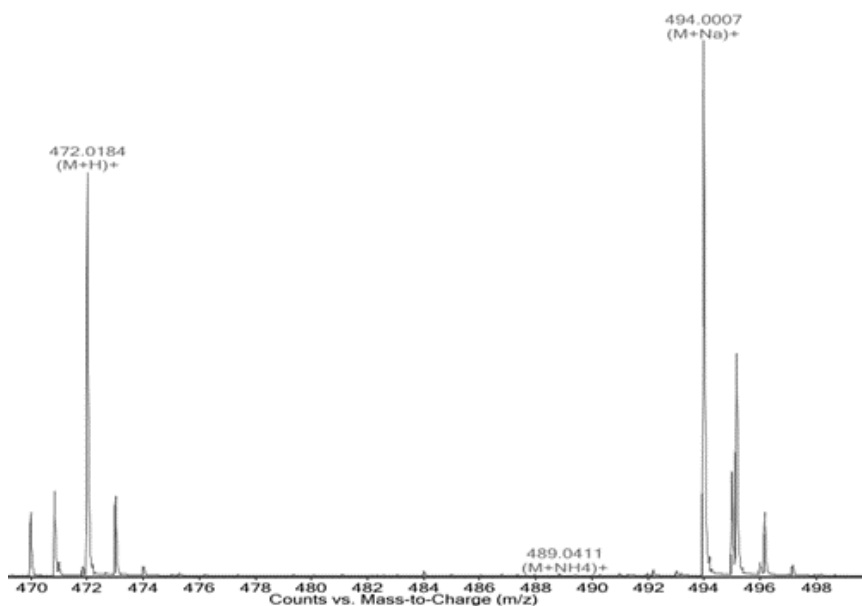


Figure 3.3.1 Cobalt complex 1-PG Hi-res mass spec.

3.2.3: Synthesis of Ruthenium Complexes.

With a history of ruthenium in use in anti-cancer trials and development, complexes with ruthenium as a metal seemed likely candidates for antimicrobial studies. Ruthenium complexes were synthesized in a similar fashion to their iridium counterparts (Figure 3.2.1). Ruthenium complexes were characterized using the same techniques as their iridium and rhodium counterparts. These analogues of the Ir/Rh piano stool analogues exhibit similar solubility and NMR properties. For spectra and other chemical properties see supplemental 1.

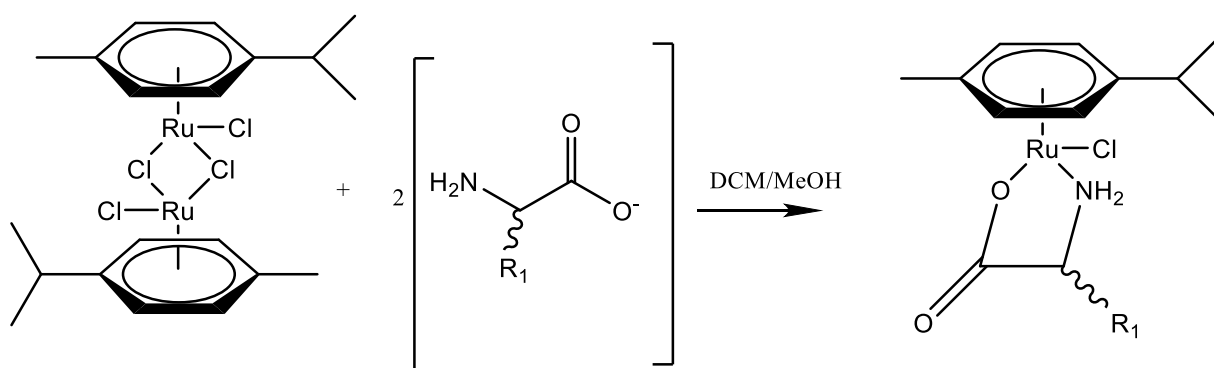


Figure 3.2.1: Synthesis for ruthenium amino-acid variants

3.3: Mycobacterial Activity

Mycobacterial strains and growth.

M. abscessus strain AAy-P-1, *M. avium* strain A5, *M. intracellulare* strain 1403^T, *M. chelonae* strain EO-P-1, *M. marinum* strain ATCC 927, *M. smegmatis* strain VT 307, and *M. bovis* BCG strain ATCC 35745 (Connaught) were used in the study (20). The strains were grown in stages from a single isolated colony in 2 mL, then 1 mL into 10 mL, and finally 50 mL of Middlebrook 7H9 (M7H9) broth (BD, Sparks, MD) containing 0.5 % glycerol and 10 % oleic acid-albumin in 500 mL nephelometry flasks and incubated with aeration (60 rpm) at 37° C or 30° C

(*M. marinum* only). Cells for measurements were used when the cultures reached mid-log phase (3-7 days).

Quality assurance.

For the work reported here, all cultures and suspensions used as inocula were uncontaminated and the colonies had the expected morphologies. All viable, uncontaminated inocula were stored up to 3 days at 4° C until used, without any differences in susceptibility to the antibiotic compounds. This was done for the measurement of minimal inhibitory concentrations (MIC) and minimal bactericidal concentrations (MBC).

MICs and MBCs of compounds dissolved in M7H9 broth medium were measured by broth microdilution in 96-well microtiter plates. A 2-fold dilution series of each compound in 50 µL of M7H9 was prepared and inoculated with 50 µL of a thousand-fold dilution of each mid-log phase mycobacterial culture (final density = 10⁵ CFU/mL). Plates were sealed with plastic film and incubated at 37° C (30° C for *M. marinum* only) and after 7 days turbidity (absorbance at 580 nm) in the wells measured and MIC defined as the lowest concentration of compound completely inhibiting turbidity. MBC was measured by spreading 10 µL of wells on M7H10 agar, allowing colony formation, and MBC was defined as the lowest concentration resulting in 99.9% lower CFU/mL compared to the inoculum only well.

Measurement of Hemolysis.

Hemolysis measurements were performed as described in Maisuria et al.⁽²¹⁾. The same procedure was followed as detailed in chapter 2.

Cytotoxicity measurements.

To determine if the complexes were specific for other microbes and not just all cell types, the complexes were screen against a series of other microorganisms as well as mammalian cells. The complexes were selected for toxicology of mammalian cells based on their activity against the previously tested mycobacterial cell lines. Only active complexes were selected. The BacTiter-Glo™ Microbial Cell Viability Assay was used to determine ATP levels produced by the cell culture over a period of 6 hrs. The protocol listed by Promega is listed in supplemental 1.

Transition metal- α -amino acid complexes.

As described previously, all 42 compounds were freely soluble in aqueous solution; the lowest solubility was that of 1-L-glycine with solubility > 3 mg/mL. Further, all the compounds were stable in the bacterial growth media. The 96-well plates were examined to identify any solubility/stability incongruities with the growth media. The compounds did not decay or form precipitates that could have caused *in vitro* concentrations to vary.

Table 3.3:
Minimal Inhibitory Concentration, MIC (mg/L) (Minimal Bactericidal Concentration, MBC, mg/L)

Compound	<i>M.smegmatis</i>	<i>M.avium</i>	<i>M.intracellulare</i>	<i>M.abscessus</i>	<i>M.marinum</i>	<i>M.bovis</i>	<i>M.chelonae</i>
1 (L-gly)	0.061	> 0.250	> 0.250	0.125	> 0.250	N/A	0.125
1 (L-pro)	0.010	0.125	0.061	0.015	> 0.250	0.015	0.015
1 (L-alanine)	0.015	> 0.250	0.061	0.031	> 0.250	0.031	0.061
1 (L-phe)	0.010	> 0.250	0.061	0.061	> 0.250	0.015	0.015
1 (phenylglycine)	0.005	> 0.250	0.015	0.031	> 0.250	0.010	0.010
1 (L-val)	0.017	> 0.250	> 0.250	0.061	> 0.250	0.031	0.031
1 (L-ser)	> 0.250	> 0.250	N/A	N/A	N/A	N/A	N/A
1 (L-gln)	0.061	> 0.250	N/A	N/A	N/A	N/A	N/A
1 (D-val)	> 0.250	> 0.250	N/A	N/A	N/A	N/A	N/A
1 (D-pro)	> 0.250	> 0.250	> 0.250	> 0.250	> 0.250	> 0.250	> 0.250

1 (L-leu)	0.032	> 0.250	0.032	0.032	> 0.250	N/A	0.032
1 (L-iso)	0.015	> 0.250	0.032	0.032	> 0.250	0.015	0.032
1 (L-hyp)	> 0.250	> 0.250	N/A	N/A	N/A	N/A	N/A
1 (L-N-methylgly)	> 0.250	> 0.250	N/A	N/A	N/A	N/A	N/A
1 (L-N-methylpro)	> 0.250	> 0.250	N/A	N/A	N/A	N/A	N/A
2 (L-gly)	0.061	> 0.250	> 0.250	0.061	> 0.250	N/A	0.125
2 (L-pro)	0.009	> 0.250	0.061	0.012	> 0.250	0.012	0.012
2 (L-ala)	0.015	> 0.250	0.061	0.031	> 0.250	0.025	0.061
2 (L-phe)	0.009	> 0.250	0.061	0.031	> 0.250	0.012	0.031
2 (L-phenylgly)	0.007	> 0.250	0.015	0.015	> 0.250	0.007	0.015
2 (L-val)	0.015	> 0.250	> 0.250	0.061	> 0.250	0.031	0.061
2 (L-ser)	> 0.250	> 0.250	> 0.250	> 0.250	> 0.250	N/A	> 0.250
2 (L-gln)	0.032	> 0.250	0.032	0.032	> 0.250	N/A	0.032
2 (D-val)	> 0.250	> 0.250	> 0.250	> 0.250	> 0.250	N/A	> 0.250
2 (D-pro)	> 0.250	> 0.250	> 0.250	> 0.250	> 0.250	N/A	> 0.250
2 (L-leu)	0.021	> 0.250	0.061	0.061	> 0.250	N/A	0.031
2 (L-iso)	0.010	> 0.250	0.061	0.031	> 0.250	N/A	0.031
2 (L-hyp)	> 0.250	> 0.250	> 0.250	> 0.250	> 0.250	N/A	> 0.250
2 (L-N-methylgly)	> 0.250	> 0.250	> 0.250	> 0.250	> 0.250	N/A	> 0.250
2 (L-N-methylpro)	> 0.250	> 0.250	> 0.250	> 0.250	> 0.250	N/A	> 0.250
3 (L-gly)	> 0.250	> 0.250	> 0.250	> 0.250	> 0.250	> 0.250	> 0.250
3 (L-phe)	> 0.250	> 0.250	> 0.250	> 0.250	> 0.250	> 0.250	> 0.250
3 (L-ala)	> 0.250	> 0.250	> 0.250	> 0.250	> 0.250	> 0.250	> 0.250
3 (L-ser)	> 0.250	> 0.250	> 0.250	> 0.250	> 0.250	> 0.250	> 0.250
3 (en)	0.125	> 0.250	0.061	0.061	> 0.251	N/A	0.061
3 (N-methyl en)	> 0.250	> 0.250	> 0.250	> 0.250	> 0.250	> 0.250	> 0.250
3 (N,N-methyl en)	> 0.250	> 0.250	> 0.250	> 0.250	> 0.250	> 0.250	> 0.250
3 (EMB)	0.061	> 0.250	> 0.250	0.061	> 0.250	N/A	0.061
4 (L-gly)	0.125	0.061	> 0.250	0.061	N/A	N/A	0.125
4 (L-phenylgly)	0.061	0.032	> 0.250	0.031	N/A	N/A	0.031
4(L-val)	0.125	0.125	> 0.250	> 0.250	N/A	N/A	0.061
4 (L-ala)	> 0.250	0.125	> 0.250	> 0.250	N/A	N/A	0.061
5-(L-PG)	0.010	0.125	0.061	0.015	> 0.250	0.015	0.015
5 (L-pro)	0.010	> 0.250	0.061	0.061	> 0.250	0.015	0.015

Table 3.3: MIC of Ir, Rh, Ru, and Co amino acid complexes. MIC (mg/L) (Minimal Bactericidal Concentration, MBC, mg/L)

Anti-mycobacterial activity of transition metal-amino acid complexes.

The MICs for all 42 α -amino acid-transition metal coordinated compounds and ethambutol were measured against each mycobacterial strain and the results listed in Table 3.3. Generally hydrophobic α -amino acids were more active than hydrophilic (e.g., L-phenylalanine, L-phenylglycine, and L-proline complexes, Table 3.3). Further, transition metal compounds complexed with D-amino acids were substantially less antimycobacterial than complexes of the corresponding L-amino acids (e.g., Ir and Rh-L-proline versus Ir-D-proline complexes against *M. smegmatis*, Table 3.3). In contrast to the cyclopentadienyl ring complexes, neither the *p*-cymene with ruthenium, nor cyclooctadiene (COD) complexes with rhodium (Class 4) had anti-mycobacterial activity, even when containing hydrophobic amino acids such as phenylalanine or phenylglycine, respectively. A number of compounds, namely 1 (L-pro), 1 (L-phe), 1 and 2 (L-val), and 1, 2, and 4 (L-phengly) were uniformly active against the rapidly growing mycobacteria (Table 3.3). Further, the data show the relative resistance of *M. avium* and the relative susceptibility of *M. intracellulare* to the compounds (Table 3.3). That difference requires further exploration with more isolates of both species and other members of the *M. avium* complex (MAC). Ethambutol (EMB) susceptibility was measured independently and exhibited anti-mycobacterial activity against *M. smegmatis* (i.e., ≥ 0.061 mg/mL, Table 3.3). As the molecular weights of the transition metals are quite different (i.e., Ir = 192.2, Rh = 102.9, and Ru 101.1) the MICs for the most active compounds are listed in Table 2 in micromolar concentrations (μ M). Bactericidal concentrations (MBCs) were essentially equal to the MICs for all the compounds (Table 3.3), indicating that all were bactericidal.

Hemolytic and cytotoxic activities of transition metal-amino acid complexes.

The concentrations required for 10% hemolysis of sheep red blood cells and 10% cytotoxicity of African Green Monkey (Vero) cells of the most active anti-mycobacterial transition metal- α -amino acid complexes were greater than the highest concentration tested (250 μ g/mL).

Although discrete endpoints were not reached, the cytotoxic and hemolytic concentrations are substantially higher (10-fold) than the MIC/MBC values.

Figures 3.4.1 and 3.4.2 show the levels of ATP produced over 6 hours. These levels are compared to a control, where there was no complex administered. Figure 3.4.1 shows similar ATP levels as the control until a concentration of 250 $\mu\text{g}/\text{mL}$ or greater. While being able to produce ATP and spend energy, the human embryonic kidney (HEK) cells were able to carry out all necessary cellular processes.

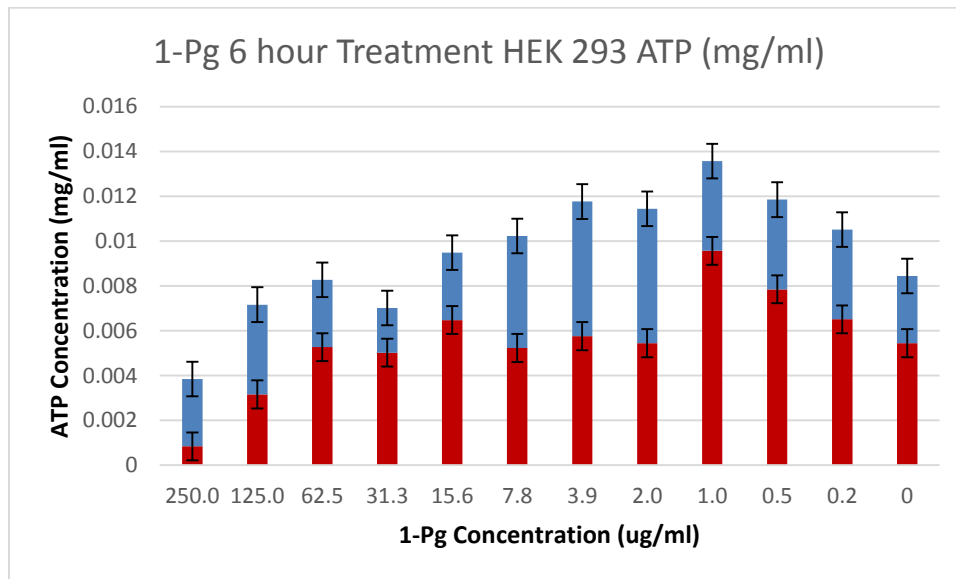


Figure 3.4.1: Human Embryonic Kidney cells (HEK) tested against 1-PG for cytotoxicity

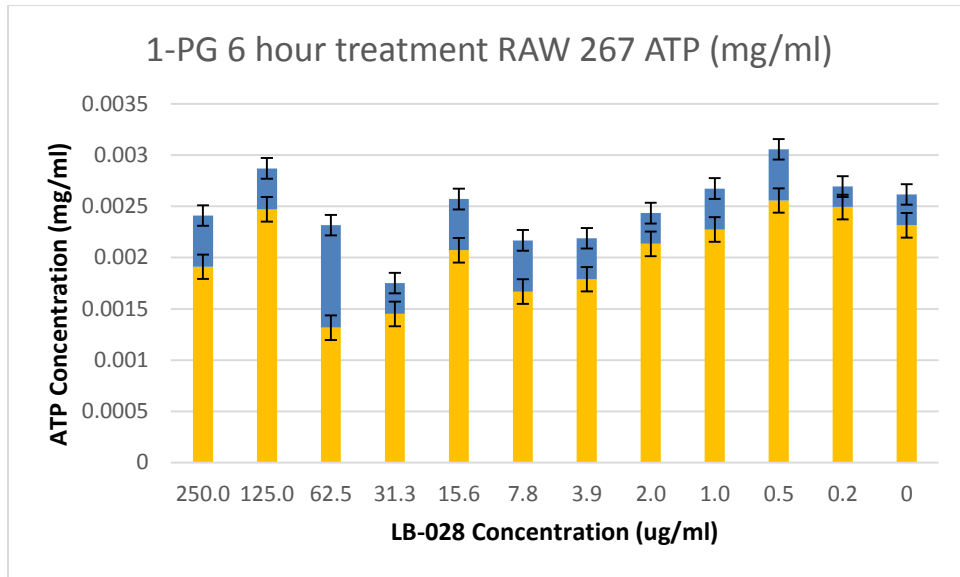


Figure 3.4.2: Murine Macrophages (RAW) were measured for ATP levels in $\mu\text{g/mL}$. Cellular ATP levels were nominal up until 125 $\mu\text{g/mL}$.

Time-kill measurements.

For the following time kill studies the *M. smegmatis* strains were acquired from **American Type Culture Collection (ATCC)**. These are laboratory tested and typed strains to ensure their purity. Survival of *M. smegmatis* when exposed to 8 mg **1-PG** (i.e., MIC/MBC) after 1, 2, 3, and 6 h exposure at 37° C were measured in two independent experiments (Figure 1). **1-PG** killed *M. smegmatis* with greater than 99% of the colonies being lysed (Figure 3.5).

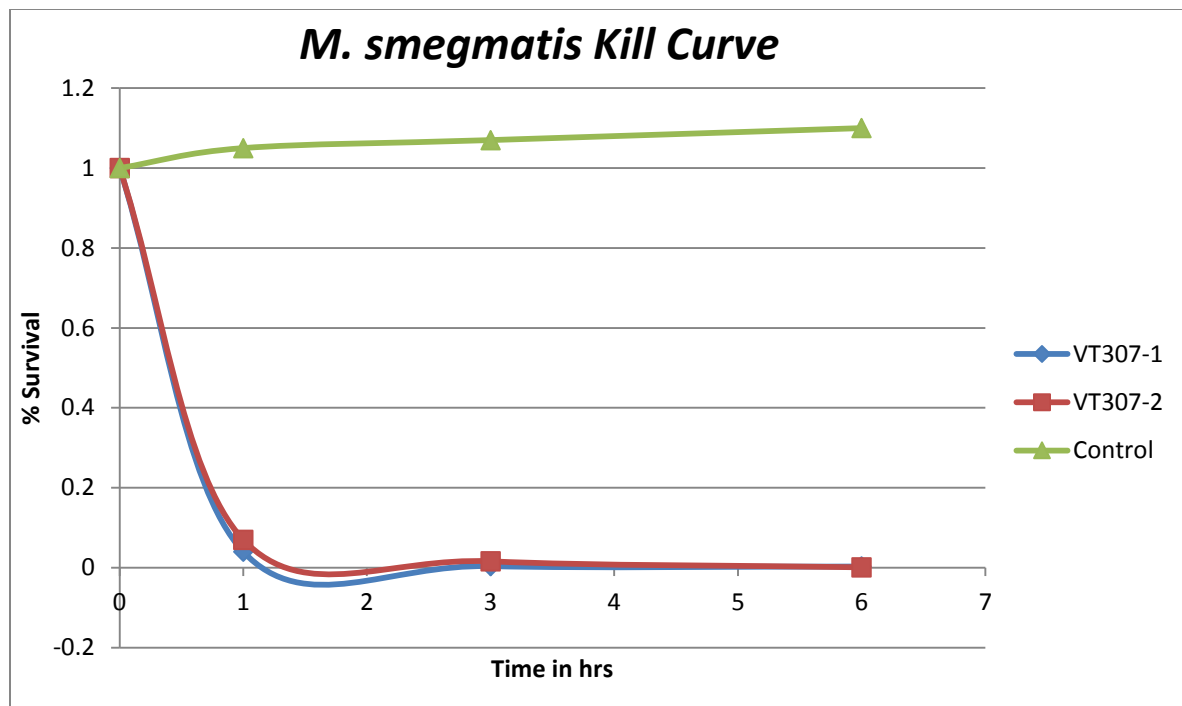


Figure 3.5: Time kill measurements over 6 hrs. Percent survival of each trial of VT307 (*M. smegmatis*) is listed.

3.3.2 Discussion

Effects of molecular weight

Transition metal- α -amino acid complexes with a different metal center had different MIC values for the same ligand set. It was expected that the effect of differences in the atomic weight of each of the metal centers would be reflected in different MIC (mg/L) values, but MICs would be similar, if not identical, when calculated on the basis of molar concentration. Iridium (192.9 atomic mass units, AMU) and rhodium (102.9 AMU) with the same α -amino acid ligand yielded similar

MICs when expressed in mg/L Table 3.3. From this it can be theorized that the metal centers serve similar roles in the anti-mycobacterial activity.

Organometallic ligand variation

The cyclopentadienyl ring appears to be essential for anti-mycobacterial activity as all the cyclooctadiene (COD) derivatives complexed with rhodium (4) lacked any substantial anti-mycobacterial activity regardless of the L- α -amino acid (Table 3.3). The data do not provide definitive evidence as to whether the presence of a metal-center-coordinated halogen is required for anti-mycobacterial activity (Table 3.3). Our theory of a possible halogen effect is that in the absence of a halogen on the metal center there is no potential for the compound to open a coordination site between the metal and cellular constituents (e.g., protein, DNA or RNA).

Hydrophobic vs. hydrophilic α -amino acids

Mycobacterial susceptibility showed specificity for certain types of amino acid ligands; namely hydrophobic, bulky L- α -amino acids (Table 3.3). For example, broad, strong anti-mycobacterial activity was demonstrated by the transition metal complexes containing L-phenylglycine linked to cyclopentadienyl rings with either iridium or rhodium (Table 3.3). Further, complexes containing a hydrophilic, polar amino acid, such as in L-serine or L-aspartic acid lacked anti-mycobacterial activity. Finally, the anti-mycobacterial activity of Ir- and Rh-complexes with L-proline was absent in complexes with D-proline (Table 3.3). Clearly, the major factor governing anti-mycobacterial activity is the nature of the side chain linked to the transition metal and cyclopentadienyl ring.

Transition metal- α -L-amino acid complexes as anti-mycobacterial agents

Demonstration of broad spectrum anti-mycobacterial activity of the transition metal- α -amino acid complexes in the absence of hemolytic and cytotoxic activity suggests that these

compounds offer promise for their use in treating mycobacterial disease. The results are particularly encouraging as a number of transition metal- α -amino acid complexes exhibited strong bactericidal activity against *M. abscessus*, one of the more difficult to treat species of *Mycobacterium*²³. Further, activity against *M. bovis* BCG suggests the possibility of activity against *Mycobacterium tuberculosis*. Finally, we are encouraged by the results and plan to continue the structure-activity analysis to identify the key elements responsible for anti-mycobacterial activity and initiate studies designed to elucidate the mechanism responsible for the anti-mycobacterial activity of these transition metal- α -L-amino acid complexes.

References

- (1) Marras TK, Daley CL. 2002. Epidemiology of human pulmonary infection with nontuberculous mycobacteria. *Clin. Chest Med.* **23**:553-567.
- (2) Marras TK, Chedore P, Ying AM, Jamieson F. 2007. Isolation prevalence of pulmonary non-tuberculous mycobacteria in Ontario, 1997-2003. *Thorax* **62**:661-666.
- (3) Billinger ME, Olivier KN, Viboud C, de Oca RM, Steiner C, Holland SM, Prevots DR. 2009. Nontuberculous mycobacteria-associated lung disease in hospitalized persons, United States, 1998-2005. *Emerg. Infect. Dis.* **15**:1562-1569.
- (4) Cassiday PM, Hedberg K, Saulson A, McNelly E, Winthrop KL. 2009. Nontuberculous mycobacteria disease prevalence and risk factors: a changing epidemiology. *Clin. Infect. Dis.* **49**:124-129.
- (5). Thomson RM. 2010. Changing epidemiology of pulmonary nontuberculous mycobacteria infections. *Emerg. Infect. Dis.* **16**:1576-1583.
- (6) Winthrop KL, McNelly E, Kendall B, Marshall-Olson A, Morris C, Cassiday M, Saulson A, Hedberg K. 2010. Pulmonary nontuberculous mycobacterial disease prevalence and clinical features. An emerging public health disease. *Am. J. Respir. Crit. Care Med.* **182**:977-982.
- (7) Prevots DR, Shaw PA, Strickland D, Jackson LA, Raebel MA, Blosky MA, de Oca RM, Shea YR, Seitz AE, Holland SM, Olivier KN. 2010. *Am. J. Respir. Crit. Care Med.* **182**:970-976.
- (8) De Groote MA, Huitt G. 2006. Infections due to rapidly growing mycobacteria. *Clin. Infect. Dis.* **42**:1756-1763.
- (9) Sermet-Gaudelus I, Le Bourgeois M, Pierre-Audigier C, Offredo C, Guillemont D, Halley S, Akoua-Koffi C, Vincent V, Sivadon-Tardy V, Ferroni A, Berche P, Scheinmann P, Lenoir G, Gaillard J-L. 2003. *Mycobacterium abscessus* and children with cystic fibrosis. *Emerg. Infect. Dis.* **9**:1587-1591.
- (10) Olivier KN, Weber DJ, Wallace RJ Jr, Faiz AR, Lee J-H, Zhang Y, Brown-Elliott BA, Handler A, Wilson RW, Schechter MS, Edwards LJ, Chakraborti S, Knowles MR. 2003. Nontuberculous mycobacteria. I. Multicenter prevalence study in cystic fibrosis. *Am. J. Respir. Crit. Care Med.* **167**:828-834.
- (11) Iredell J, Whitby M, Blacklock Z. 1992. *Mycobacterium marinum* infection: epidemiology and presentation in Queensland 1971-1990. *Med. J. Austr.* **157**:596-598.
- (12) Aubry A, Chosidow O, Caumes E, Robert J, Cambau E. 2006. Sixty-three cases of *Mycobacterium marinum* infection. *Arch. Intern. Med.* **162**:1746-1752.
- (13) Johnson PDR, Weitch MGK, Leslie DE, Hayman JA. 1996. The emergence of *Mycobacterium ulcerans* infection near Melbourne. *J. Austr. Med. Assoc.* **164**:76-78.
- (14) Johnson PDR, Stinear T, Small PLC, Plushke G, Merritt RW, Portaels F, Huygen K, Hayman JA, Asiedu K. 2005. Buruli ulcer (*M. ulcerans* Infection): new insights, new hope for disease control. *PloS Med.* **2**:282-286.

- (15) Saubolle MA, Kiehn TE, White WH, Rudinsky MF, Armstrong D. 1996. *Mycobacterium haemophilum*: microbiology and expanding clinical and geographic spectra of disease in humans. Clin. Microbiol. Rev. **9**:435-447.
- (16) Dwyer FP, Reid IK, Shulman A Laycock GM, Dixon S. 1969. Biological actions of 1,10-phenanthroline and 2,2'-bipyridine hydrochlorides, quaternary salts, and metal chelates and related compounds. 1. Bacteriostatic action on selected Gram-positive, Gram-negative, and acid-fast bacteria. Austral. J. Exp. Biol. Med. Sci. **47**:203-218.
- (17) Ben Hadda T, Akkurt M, Filali Baba M, Daoudi M, Bennani B, Kerbal A, Chohan ZH. 2009. Anti-tubercular activity of Ruthenium (II) complexes with polypyridines. J. Enzy. Inhib. Med. Chem. **24**:457-463.
- (18) Dabrowiak JC. 2009. Metals in Medicine. J. Wiley and Sons, Ltd. New York
- (20) Falkingham JO III, Macri RV, Maisuria BB, Actis ML, Sugandhi EW, Williams AA, Snyder AV, Jackson RR, Poppe MA, Chen L, Ganesh K, Gandour RD. 2012. Antibacterial activities of dendritic amphiphiles against nontuberculous mycobacteria. Tuberculosis **92**:173-181.
- (21) Maissuria BB., Actis ML, Hardrict SN, Falkingham JO III, Cole MF, Cihlar RL, Peters SM, Macri RV, Sugandhi EW, Williams AA, Poppe MA, Esker AAR, Gandour RD. 2011. Comparing micellar, hemolytic, and antibacterial properties of di- and tricarboxyl dendritic amphiphiles. Bioorg. Med. Chem. **19**:2918-2926.
- (22) Griffith D, Aksamit T, Brown-Elliott B, Catanzaro A, Daley C, Gordin F, Holland S, Horsburgh R, Huitt G, Iademarco M, Iseman M, Olivier K, Ruoss S, von Reyn C, Wallace RJ Jr, Winthrop K. 2007. An official ATS/IDSA statement: diagnosis, treatment, and prevention of nontuberculous mycobacterial diseases. Am J Respir Crit Care Med **175**:367-416.
- (23) Lance R. Byers, Lawrence F. Dahl. Inorg. Chem., 1980, 19 (2), pp 277–284

4.1: Mechanism of Action

With any new pharmaceutical, the mode of action (MOA) is crucial in understanding how not only the drug works against an organism but how it may interact with a desired target. Uncovering this MOA may give some insight on how to tailor new antimicrobials. With the previous mentioned complexes synthesized, Ir-phenylglycine (**1-PG**) exhibited high anti-mycobacterial activity with MICs of 5 µg/mL against *Mycobacterium smegmatis*, 31 µg/mL against *Mycobacterium abscessus*, and 15 µg/mL against *Mycobacterium intracellulare*, *Mycobacterium chelonae*, and *Mycobacterium bovis* BCG ¹². As **1-PG** was shown to lack cytotoxic and hemolytic activities ¹² it was decided to proceed with the identification of the drug's target. This mechanism of action is focused on the study of **1-PG**-resistant mutants of *M. smegmatis* and the identification of at least one target of the drug, the peptidyl transferase domain of the mycobacterial 23S rRNA.

The following studies were accomplished by isolating resistant mutants and analyzing possible genetic mutations. Spontaneous mutants of *Mycobacterium smegmatis* strain mc²155 resistant to **1-PG** (iridium-L-phenylglycine complex), a strongly antimycobacterial antibiotic, were isolated. Based on the discovery that some **1-PG**-resistant mutants (**1-PG^R**) were also resistant to high concentrations of clarithromycin (≥ 250 µg/mL), but no other anti-mycobacterial antibiotics, the 23S rRNA region spanning the peptidyl transferase domain was sequenced and shown to be mutated. Mutations were localized in the peptidyl transferase domain of the 23S rRNA gene. Measurements showed that **1-PG** bound to ribosomes isolated from the parent, **1-PG**-sensitive strain, but failed to bind to ribosomes from the **1-PG^R** mutant. This is confirmed by the isolation of the bound ribosomes and iridium levels were detected by ICP.

4.2: Complexes Studied

For the development of the mutants, the most active complex against *M. smegmatis* was selected with an active MIC of 5.0 µg /mL (**1-PG**). The structure of the transition metal- α -amino acid complex **1-PG** is illustrated in Figure 4.1. **1-PG** is a cyclopentadienyl complex (Cp^*) having an α -amino acid, here phenylglycine, complexed with iridium (Ir). The synthesis of 1-PG has been described previously in Section 3.1.

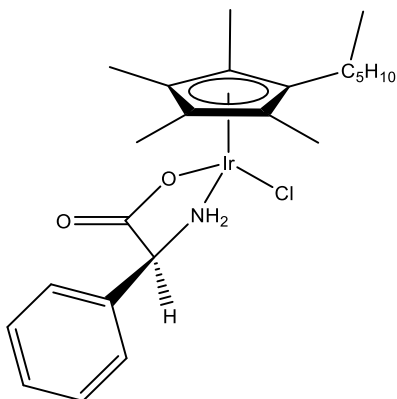


Figure 4.1: Structure of active complex 1-PG MIC >5.0 µg /mL

1-PG was also selected for its specificity for *M. smegmatis*. When the activities were compared against other microbes, **1-PG** had an MIC more than 20 times than the other native non-mutant *M. smegmatis* strains. (Table 4.2). Each trial in the study consisted of 1-PG from the same preparation sample.

Complex with varying R-group	<i>MRSA</i> MIC $\mu\text{g}/\text{mL}$	<i>E. Coli</i> MIC $\mu\text{g}/\text{mL}$	<i>C. albicans</i> MIC $\mu\text{g}/\text{mL}$	<i>M. smegmatis</i> MIC $\mu\text{g}/\text{mL}$
(1-PG)	125	125	62.5	4.0
Cp*(hexyl) (alanine)Cl	250	125	62.5	8.0
Cp*(hexyl) (glycine)Cl	250	125	62.5	32.5

Table 4.2: Table of 1-PG complex and other active transition metal complexes tested against other microbial pathogens. MIC values in $\mu\text{g}/\text{mL}$.

Antimycobacterial antibiotics.

For comparison, each of the mutant and control strains were tested against a standard panel of NTM (Non-tuberculosis mycobacteria) drugs. The antimycobacterial antibiotics, clarithromycin, ethambutol, ciprofloxacin, and were purchased from Sigma-Chemical Co. (St. Louis, MO). Each of the antibiotics used were pharmaceutical grade. For activity comparison each of the antibiotics were screened using the standard panel and screening procedure for MICs following previously described methods¹². Table 4.2.1 lists the antibiotics and their MIC for *M. smegmatis*.

Typical MIC of Known Antimicrobials	<i>M. smegmatis</i> MIC µg /mL	<i>S. aureus</i> MIC µg /mL
Ethambutol	6.0	125
Ciprofloxacin	1.0	NA
Clarithromycin	16	<2.0

Table 4.2.1: Comparison of standard NTM antibiotics for comparison to 1-PG

4.3: *Mycobacterium smegmatis* mutant isolation

M. smegmatis strain mc²155, was used in the study and its growth and preparation for susceptibility measurements are described in Falkinham et al.⁸ Cultures were grown to mid-logarithmic phase to obtain uniformity of MIC measurements. For the work reported here, all cultures and suspensions used as inocula were uncontaminated and the colonies had the expected morphologies (i.e., no colony variants). All viable, uncontaminated inocula were stored up to 3 days at 4° C until use, without any consequential differences in susceptibility to the antibiotic compounds. May it be noted that even though the 1-PG mutants were isolated, they were observed to grow slower under the same conditions as the wild type strain. This shows while these mutants exist, their ability to proliferate outside of the lab may be weakened in normal NTM hosts.

MICs and MBCs of compounds dissolved in M7H9 broth medium containing 0.5 % (vol/vol) glycerol and 10 % (vol/vol) oleic acid-albumin were measured by broth microdilution in 96-well microtitre plates⁸. The MIC values for each plate were determined using optical density of the organism's growth at 460 nm. Cultures (0.1 mL) of *M. smegmatis* strain mc²155 were spread on M7H10 agar medium containing 10 % (vol/vol) oleic acid-albumin and concentrations of **1-PG** ranging from 10-250 µg **1-PG**/mL. Plates were incubated at 37° C and single colonies picked and streaked for purification on both **1-PG**-containing and **1-PG**-free medium (to exclude **1-PG**-dependant mutants). Following isolation, the MICs of the parent and mutants were measured against **1-PG** and other antimycobacterial antibiotics as described above.

Isolation of DNA and PCR amplification of the 23S rRNA gene.

DNA was isolated from the parent and **1-PG^R** mutants and the 23S rRNA gene was amplified by PCR^(11, 15), resulting in production of 419 bp (domain V) and 1,423 bp (majority of 23S rRNA gene) amplicons.

Isolation of *M. smegmatis* ribosomes.

Ribosomes were isolated from *M. smegmatis* strain mc²155 and the **1-PG^R** mutants following the procedure of⁵. Cells were harvested from 50 mL cultures by centrifugation (5,000 x g for 20 min), supernatant medium discarded, and cells washed twice in 50 mL of Buffer A (10 mM Tris-HCl, 4 mM MgCl₂, 10 mM NH₄Cl, 100 mM KCl, pH 7.2). Washed cells were suspended in 5 mL of Buffer A, cell suspensions were cooled on ice-water, and cells lysed by sonication. DNase (RNase-free) was added to the cooled and broken cell suspensions at a final concentration of 5 units/mL and incubated on ice for 15 min. Whole cells were removed from the lysate by centrifugation (5,000 x g for 5 min) and the supernatant transferred to an ultracentrifuge tube and centrifuged at 30,000 x g for 30 min to form a pellet containing the cell walls and membranes. The

supernatant from that centrifugation was transferred to a fresh ultracentrifuge tube and ribosomes pelleted at 100,000 x g for 60 min. The pelleted ribosomes were suspended in 2 mL of Buffer A, aliquot in 0.5 mL samples, labelled and frozen at -70° C. Frozen ribosomes were thawed in a water bath of 37°C until equilibrium was achieved before performing binding studies.

1-PG-binding to ribosomes.

1-PG-binding to ribosomes was measured as described by Doucet-Populaire et al.⁴ An aliquot of each strain's, mc²155 and **1-PG^R** mutants, ribosome suspension was defrosted by placing each suspension in a water bath at 37° C and 50 µL of ribosomes was mixed with 50 µL of 1 mg **1-PG**/mL and incubated at 37° C. Immediately and at 10 min intervals up to 30 min, two 10 µL samples were withdrawn, filtered through 0.45 µm pore size filters, and washed with 5 mL of Buffer A. The filters were placed in a tube, 1 mL of 1 M HMO₃ added, and the concentration of Ir measured by ICP-OES.

ICP-OES measurements of digested ribosomes.

Each of the digested ribosome filters were diluted with Nanopure DI water to a total volume of 5 mL. Each sample was allowed to sit for 15 minutes. Following standard procedures, each sample measurement was evaluated using a Perkin Elmer 4300 DV ICP-OES selected for all iridium isotopes. Calibration was performed following procedure from PerkinElmer²⁰. Each digested ribosome sample was evaluated for overall iridium concentration. The filtrate and the filters were evaluated independently to determine what may have been bound to the ribosome and/or washed through the filter paper containing the free complex. A standard curve was constructed using samples of iridium prepared for ICP-OES by Inorganic Ventures (Christiansburg, VA).

4.4: Results and Discussion

Selection of 1-PG-resistant (1-PG^R) mutants.

Independent mutants (**7**) of *M. smegmatis* strain mc²155 resistant to 20 µg **1-PG**/mL were isolated (frequency = 3.5 x 10⁻⁷) and their susceptibility to anti-mycobacterial antibiotics measured. All seven were also resistant to clarithromycin (MIC = 2-16-fold higher than parent), but their susceptibility to other anti-mycobacterial drugs was not changed (Table 4.5).

Isolation of DNA, PCR amplification of the 23S rRNA gene, and sequence of the 23S rRNA gene.

As clarithromycin-resistant mutants have mutations in the peptidyl transferase domain (V) of the 23S rRNA gene ⁽¹⁵⁾, DNA was isolated from the parent and each mutant and the 23S rRNA gene was amplified by PCR ^(11, 15), resulting in production of 419 bp (domain V) and 1,423 bp (majority of 23S rRNA gene) amplicons. Analysis of the amplicon sequences in **two 1-PG^R/ Cla^R** mutants revealed deletion mutations within domain V (bases 2057-2058), whereas other mutations were found in the 2057-2611 bp region of the peptidyl transferase loop. We surmise that those mutations may have rendered the ***M. smegmatis*** strain resistant to **1-PG** and clarithromycin because of alterations in the conformation of that loop ⁴.

Binding of 1-PG to ribosomes.

After each ribosome sample was evaluated to determine iridium concentration using ICP-OES, the mutants were compared to the wildtype strain. Filter and filtrates of each sample were measured independently. This showed that iridium concentrations were both bound and free or allowed to pass through without being bound. Table 4.4 lists the total iridium concentration per sample including both filtrate and bound ribosomes held on the sample filter paper. Each sample was evaluated a total of 5 times and the average was recorded.

ICP-OES Ir sample	Ribosome bound (ppm)	Filtrate (ppm)
Mutant 1	0.5	1.5
Wild-type 2	1.2	0.6
Mutant 2	0.6	1.1
Wild-type 2	1.6	>0.5

Table 4.4: The total iridium concentration in the ribosome sample of both the mutant isolates and wildtype isolates.

The data (table 4.4) establishes a clear trend showing the mutant sample ribosomes bound less iridium than the wildtype by comparison was observed. The mutant ribosomes allowed for more iridium to pass through the filter paper and end in the filtrate. This data suggests that the mutant ribosomes were not binding the iridium as effectively as the wildtype. The wildtype ribosomes bind more than three times the amount of iridium in comparison to the mutants. This is significant by showing that the mutants have developed in a way to prevent binding of certain protein inhibiting antimicrobials.

Isolation and characterization of Clarithromycin-resistant mutants.

Independent Cla^R-mutants of mc²155 were also isolated, but only 4/7 were 1-PG^R, suggesting the two antibiotics do not share exactly the same range of activity. This separation of targets is consistent with observations that clarithromycin inhibits peptidyl transferase activity, ribosome assembly, and outer membrane assembly in mycobacteria. The discovery that a substantial fraction (43 %) of clarithromycin-resistant *M. smegmatis* mutants (Cla^R) were still susceptible to Ir-phenylglycine (1-PG^S) encourages us that 1-PG will prove to be a useful anti-mycobacterial drug.

Organism	Clarithromycin	1-PG	Ethambutol
Cla^R	125	8.0	2.0
Wildtype	16	8.0	2.0
1-PG^R	125	250	1.0

Table 4.5: MIC values of each of the organisms mutant and wildtype. 1-PG mutants show resistance to both clarithromycin and 1-PG.

Table 4.5 lists the different mutants observed and their potential cross resistance with different NTM drugs. As noted previously the 1-PG mutants have resistance to both clarithromycin and that of 1-PG. The clarithromycin mutants however, were still susceptible to 1-PG.

4.5 Conclusion and further work

With the development of a new type of antimicrobial drug, it is crucial to understand the mode of action (MOA). These transitional metal complexes have a unique mode of action. From the ribosome binding studies and the cross resistance towards clarithromycin isolated mutants, it can be determined that the transitional metal complexes bind to the 23s rRNA subunit. While these complexes may interact with ribosomes related to the 23s rRNA subunit like other antimicrobials (i.e. clarithromycin), they show activity against other clarithromycin resistant mutants. This suggests that the target of the 1-PG complexes may be related to this 23s subunit and yet has a different binding site on that same 23s subunit. This is also further explained by the resistance of the 1-PG mutants to clarithromycin but the lack of resistance to 1-PG in the clarithromycin mutants.

While this data narrows a specific subunit it does not determine the exact site of binding to the ribosome. Further work on going to determine the exact area or areas of binding via crystallographic determination of the 1-PG bound to the 23s subunit. This could help determine if these complexes aid in a conformational change and how that may play into the normal cellular function of the ribosome.

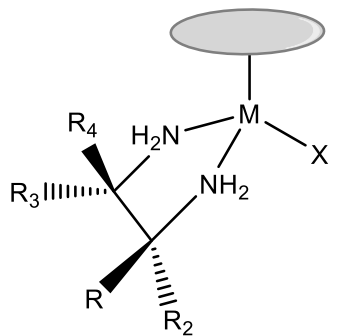
References

- (1) Billinger ME, Olivier KN, Viboud C, de Oca RM, Steiner C, Holland SM, Prevots DR. 2009. Nontuberculous mycobacteria-associated lung disease in hospitalized persons, United States, 1998-2005. *Emerg. Infect. Dis.* **15**:1562-1569.
- (2) Brennan , P.J., Nikaido, H. 1995. The envelope of mycobacteria. *Annu. Rev. Biochem.* **64**: 29-63.
- (3) Cassiday PM, Hedberg K, Saulson A, McNelly E, Winthrop KL. 2009. Nontuberculous mycobacteria disease prevalence and risk factors: a changing epidemiology. *Clin. Infect. Dis.* **49**:124-129.
- (4) De Groot MA, Huitt G. 2006. Infections due to rapidly growing mycobacteria. *Clin. Infect. Dis.* **42**:1756-17
- (5) Doucet-Populaire F, Capobianco JO, Zakula D, Jarlier V, Goldman RC. 1998. Molecular basis of clarithromycin activity against *Mycobacterium avium* and *Mycobacterium smegmatis*. *J. Antimicrob. Chemother.* **41**, 179-187.
- (6) Douthwaite, S., Aagaard, C. 1993. Erythromycin binding is reduced in ribosomes with conformational alterations in the 23S rRNA peptidyltransferase loop. *J. Mol. Biol.* **232**: 725-731.
- (7) Egelund, E.F., Fennelly, K.P., Peloquin, C.A. 2015. Medications and monitoring in nontuberculous mycobacterial infections. *Clin. Chest Med.* **36**: 55-66.
- (8) Falkinham JO III, Macri RV, Maisuria BB, Actis ML, Sughandhi EW, Williams AA, Snyder AV, Jackson RR, Poppe MA, Chen L, Ganesh K, Gandour RD. 2012. Antibacterial activities of dendritic amphiphiles against nontuberculous mycobacteria. *Tuberculosis* **92**:173-181.
- (9) Gangadharan, P.R.J. 1984. *Drug Resistance in Mycobacteria*, CRC Press, Boca Raton, Florida, USA.
- (10) Griffith D, Aksamit T, Brown-Elliott B, Catanzaro A, Daley C, Gordin F, Holland S, Horsburgh R, Huitt G, Iademarco M, Iseman M, Olivier K, Ruoss S, von Reyn C, Wallace RJ Jr, Winthrop K. 2007. An official ATS/IDSA statement: diagnosis, treatment, and prevention of nontuberculous mycobacterial diseases. *Am J Respir Crit Care Med* **175**:367-416.
- (11) Jamel, M.A., Maeda, S., Nakata, N., Kai, M., Fukuchi, K., Kashiwabara, Y. 2000. Molecular basis of clarithromycin-resistance in *Mycobacterium avium-intracellulare* complex. *Tubercle Lung Dis.* **80**: 1-4.
- (12) Karpin, G., Merola, J.S., Falkinham, J.O., III. 2013. Transition metal- α -amino acid complexes with antibiotic activity against *Mycobacterium* spp. *Antimicrob. Agents Chemother.* **57**: 3434-3436.

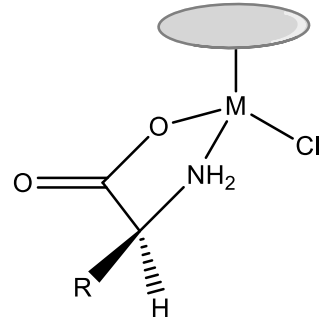
- (13). Marras TK, Chedore P, Ying AM, Jamieson F. 2007. Isolation prevalence of pulmonary non-tuberculous mycobacteria in Ontario, 1997-2003. *Thorax* **62**:661-666.
- (14) Marras TK, Daley CL. 2002. Epidemiology of human pulmonary infection with nontuberculous mycobacteria. *Clin. Chest Med.* **23**:553-567.
- (15) Meier, A., Kirschner, P., Springer, B., Steingrube, V.A., Brown, B.A., Wallace, R.J. Jr., Böttger, E. 1994. Identification of mutations in 23S rRNA gene of clarithromycin-resistant *Mycobacterium intracellulare*. *Antimicrob. Agents Chemother.* 38: 381-384.
- (16) Prevots DR, Shaw PA, Strickland D, Jackson LA, Raebel MA, Blosky MA, de Oca RM, Shea YR, Seitz AE, Holland SM, Olivier KN. 2010. Nontuberculous mycobacterial lung disease prevalence at four integrated health care delivery systems. *Am. J. Respir. Crit. Care Med.* **182**:970-976.
- (17) Ravaglione, M.C., Ditiu, L. 2013. Setting new targets in the fight against tuberculosis. *Nat. Med.* 19: 263.
- (18) Wallace, R.J. Jr. Zhang, Y., Brown-Elliott, B.A., Yakrus, M.A., Wilson, R.W., Mann, L., Couch, L., Girard, W.M., Griffith, D.E. 2002. Repeat positive cultures in *Mycobacterium intracellulare* lung disease after macrolide therapy represent new infections in patients with nodular bronchiectasis. *J. Infect. Dis.* 186: 266-273.
- (19) Winthrop KL, McNelly E, Kendall B, Marshall-Olson A, Morris C, Cassiday M, Saulson A, Hedberg K. 2010. Pulmonary nontuberculous mycobacterial disease prevalence and clinical features. An emerging public health disease. *Am. J. Respir. Crit. Care Med.* **182**:977-982.

5. Conclusions

A number of organometallic half sandwich complexes ($\text{Cp}^{*R}\text{M(L)X}$, where L is an amino-acid (aa) or an ethylenediamine (en) and (X) is either Cl or I, were synthesized. The synthesis to produce each of the complexes (Figure 5.1) was successfully utilized with several different metal centers. The synthesis of the transition metal precursor $[(\text{Cp}^{*R})_2\text{M}_2\text{X}_4]$ used was successful in serving as a general scaffold to tailor more than 50 complexes. Each of these complexes were completely characterized by ^1H NMR, ^{13}C NMR, high-res mass spectroscopy, and elemental analysis; several were examined via X-ray crystallography. Each of the fully characterized complexes were studied for their antimicrobial activity. Ruthenium complexes ($\eta^6\text{-arene})\text{Ru(L)Cl}$ were formed using the same conditions as their iridium and rhodium counterparts. Reactions with Co and Cp^{*R} ligands formed a dark black/purple complex in the form $[\text{Cp}^{*R}\text{Co(CO)I}_2]$. Reaction with the ligands (aa or en) yielded dark blue or purple products.



(1) Ethylenediamine Complex



(2) Amino-acid Complex

Figure 5.1: Basic structure of 2 class of complexes synthesized and studied for antimicrobial development

It was determined that the ethylenediamine complexes $[(\text{Cp}^*\text{R})\text{Ir}(\text{en})\text{Cl}]$ showed activity against gram positive organisms including *S. aureus* and MRSA (Figure 5.1). This activity is unique to the diamine complexes. When tested against gram negative and specific mycobacteria no visible or recordable MIC levels were observed. MIC values were as low as 4 $\mu\text{g}/\text{mL}$ for several of the $(\text{Cp}^*\text{R})\text{Ir}(\text{en})\text{Cl}$, complexes where $-\text{R}$ in the (Cp^*R) were hexyl or octyl aliphatic sidechains. It was discovered that activity of several of the ethylenediamine complexes were dependent on the the specific ethylenediamine. The diamine complexes formed with trans and cis-1,2-diaminocyclohexane showed very stark contrasting MIC values, >125 $\mu\text{g}/\text{mL}$ as compared to 4 $\mu\text{g}/\text{mL}$ respectively. X-ray crystallographic data obtained showed several significant differences in their structures. One possibility is the interaction between the metal center and the active site within the microorganism. When the metal centers of each complexes were substituted with rhodium, identical MIC results were observed. Furthermore, time kill measurement studies showed that within 6 hr. of inoculation with the active complexes, over 99% the cells were killed. Such rapid cell death suggests that the mechanism must be affecting a critical piece of the cellular machinery. Due to the cell lysis observed and the rapid cell death, it is most likely affecting a process involving the synthesis or make-up of the cell wall. The fact that these complexes were active against only gram positive bacteria, proves that even transition metal complexes can be “tailored” to be active against a specific set of microorganisms.

For the amino acid complexes, activity was seen specifically for mycobacteria. This included but was not limited to *M. smegmatis*, *M. bovis*, and *M. tuberculosis*. MIC values were as low as 4 $\mu\text{g}/\text{mL}$ for several of the $(\text{Cp}^*\text{R})\text{M}(\text{aa})\text{X}$ complexes where $-\text{R}$ in the (Cp^*R) were hexyl or octyl aliphatic sidechains. This increase in activity and hydrophobicity follows a trend similar to the ethylenediamine complexes. In all tested complexes, the D-amino acid variants lacked activity against all microorganisms that were susceptible to the L-amino acid variants. This difference is exemplified in the ring containing amino acids, specifically D and L-proline. MIC values were >125

$\mu\text{g/mL}$ for the D-proline and 8 $\mu\text{g/mL}$ for the L-proline complex. As previously stated, the 3D structure may determine whether or not the complex has an open coordination site for the iridium to interact. This opening for coordination has proven to play a critical role as to whether or not the compound shows activity. Complexes that contained a hydrophilic, polar amino acid, such as L-serine or L-aspartic acid, lacked anti-mycobacterial activity.

Based on these results a structure activity relationship was constructed. A distinctive pattern emerged. Complexes became more active against a set of microorganisms based on the length of the aliphatic sidechains in the Cp^{*-R} . As the length of the aliphatic sidechain increased the activity for a particular ligand increased. This is evident until the sidechain length is increased beyond the -R octyl group. The increased hydrophobicity of each of the complexes allows for easier cellular permeability. However, the exact amount of each complex inside the cell was not able to be calculated. These hydrophobicity trends were also shown when comparing ligand side chain length. For each ligand, increased activity is observed upon increasing the hydrophobicity of the amino acid side chain or the hydrophobicity of the ethylenediamine. This is critical data. Each piece of the half-sandwich compound functions in concert together to form an active antimicrobial agent. While each ligand modification can show different activity, there is a clear pattern to what elicits higher antimicrobial activity.

In order for these complexes to provide any therapeutic benefit safety and toxicology tests were performed. Increasing the hydrophobic side chain on both the ligands and cyclopentadienyl ring showed increased red blood cell lysis. While there was lysis of red blood cells, it was at concentrations 10X higher than that of the MICs. This is within an acceptable ratio for a possible drug candidate. It was determined that cellular function and ATP levels were uninhibited when compared to a control at concentrations of $>250 \mu\text{g/mL}$. These levels were 75X higher than the MIC values tested for the same complexes. The ethylenediamine complex (Cp^*)Ir (cis-1,2-diaminocyclohexane)Cl was tested for toxicity in mice. No detrimental side effects were observed

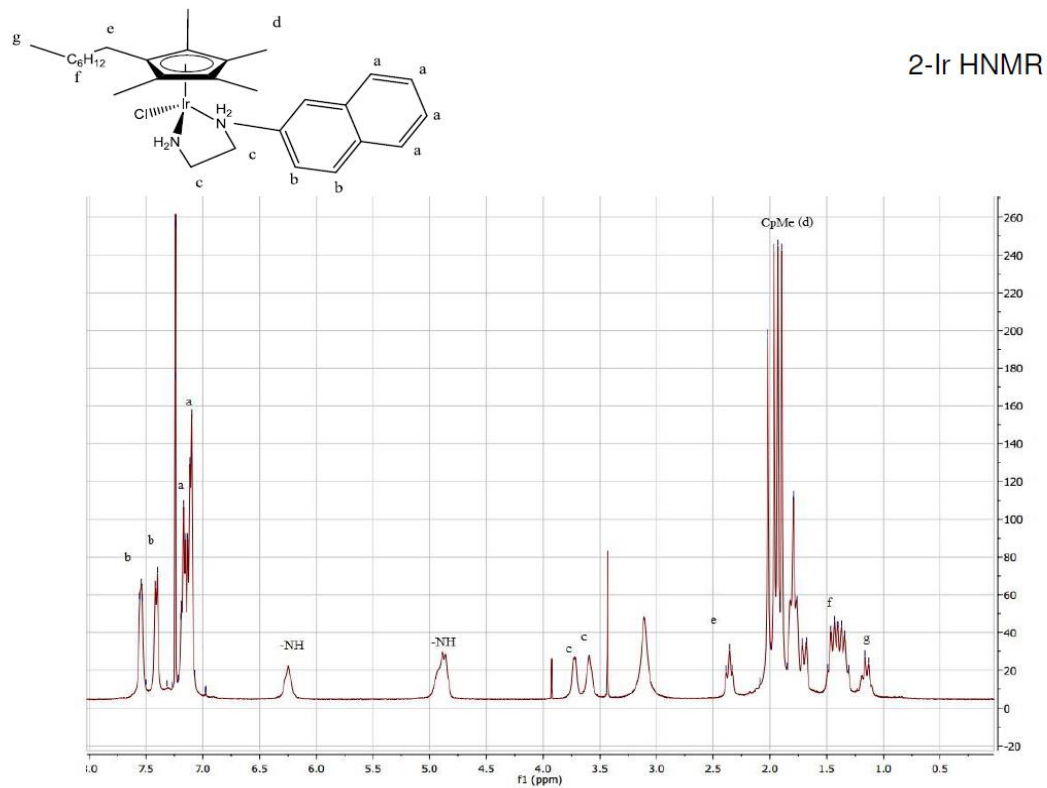
after 14 days at an IV dosage of 5 µg/kg. It was also determined that the blood and organs had little no residual iridium. Most of the iridium was seen in the urine collected after 14 days. The safety studies show that these drug candidates can be metabolized and are excreted. This further proves as a preliminary study that these complexes could lead to viable drug candidates.

The mechanism of action (MOA) was studied by the isolation of mutants resistant to the most active complexes. These mutants had MIC values greater than >62.5 µg/mL as compared to the 4 µg/mL of the wildtype. Mutants of a gram positive bacteria were unable to be isolated. It was determined that these mutants had a drug cross resistance with clarithromycin. These mutants were both resistant to the amino acid complexes as well as clarithromycin. This lead to the discovery of a genetic mutation in the 23s ribosome domain that gives rise to clarithromycin resistance. More specifically the peptidyl transferase domain of the mycobacterial 23S rRNA. Mutants revealed deletion mutations within domain V (bases 2057-2058), whereas other mutations were found in the 2057-2611 bp region of the peptidyl transferase loop. While these region is similar to that of the MOA of clarithromycin it does not act in the same way. Since clarithromycin resistant mutants were still susceptible to the transitional metal complexes, this may suggest a new way to combat microbes resistant to currently used antimicrobials.

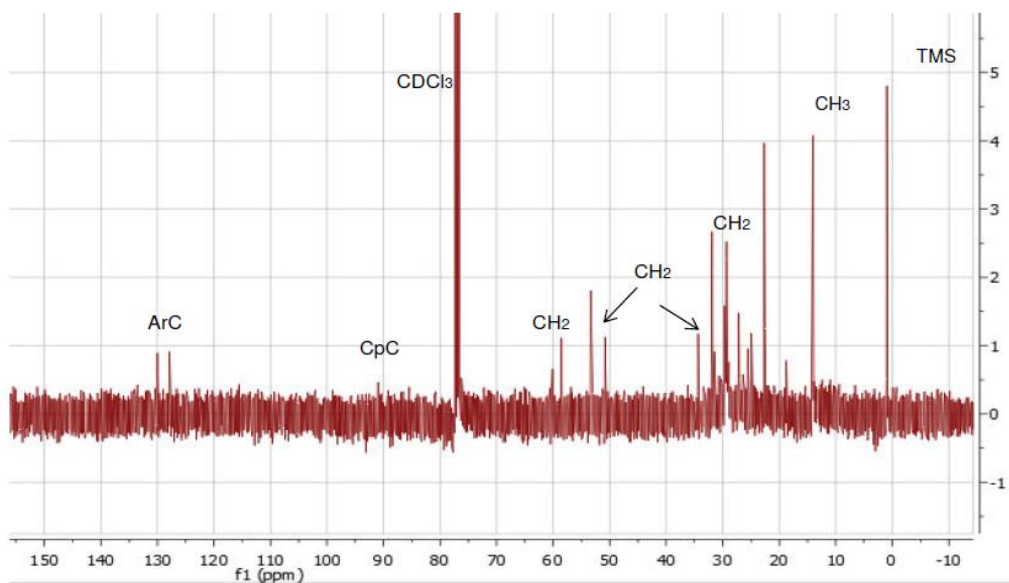
Previously, transition metal complexes have been only examined as anti-cancer pharmaceuticals. Many have discounted transition metals simply because of label as a broad biocide, damaging to all organisms. This has stifled the research in this area. This body of work shows that transition metal complexes can have a future as possible non-traditional antibiotics. The data shows that transition metal complexes can be designed, modified and tailored to create antimicrobial agents. Furthermore, this shows that not all transition metal complexes are toxic to mammalian cells. With so little advancements made in the field of antimicrobials over the past 15 years, it is time to start looking at this relatively unexplored field. These easily tailored modular complexes could lead to a new line of antimicrobials. With the rise in resistant microbes and

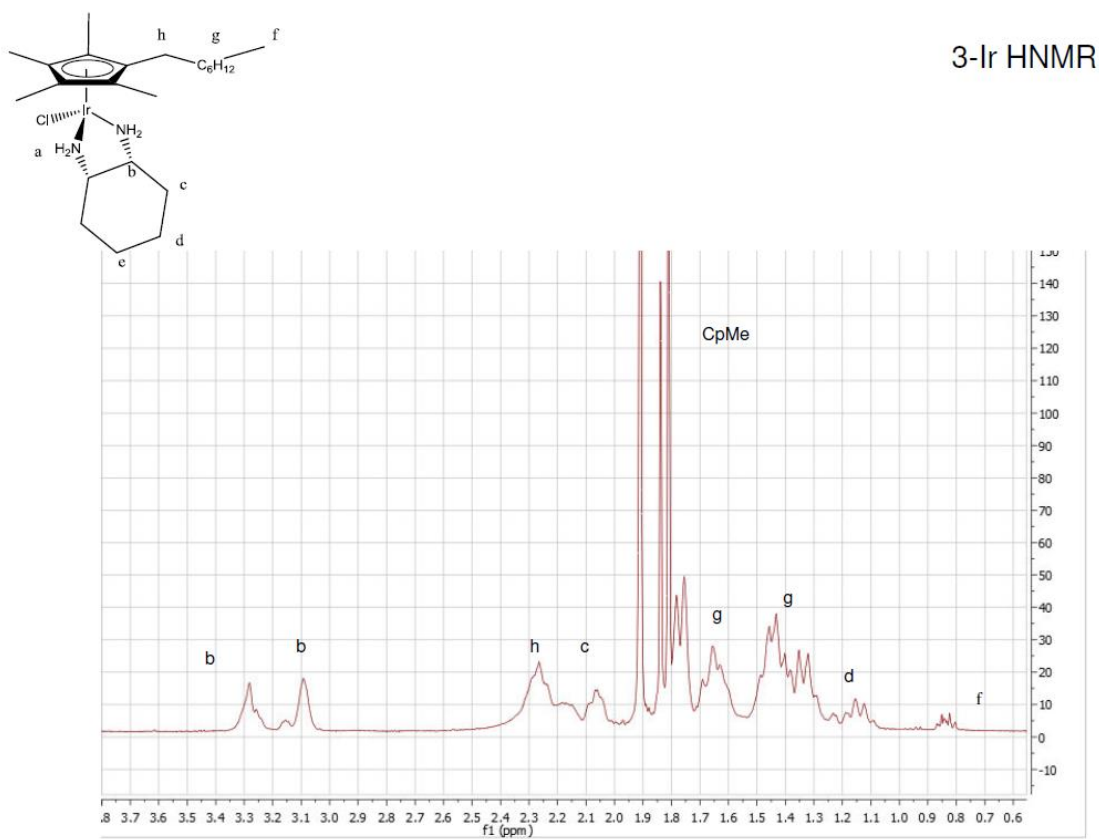
decreasing availability of treatments, these transition metal complexes could provide hope for preventing the next microbiological pandemic.

SUPPLEMENTAL - 1

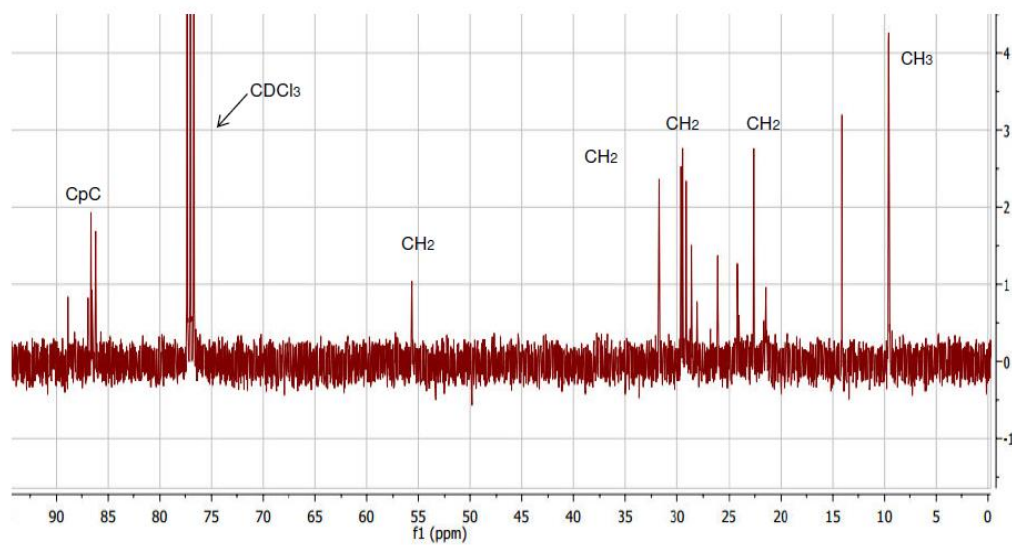


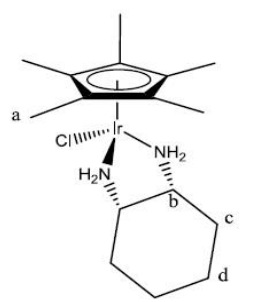
2-Ir CNMR



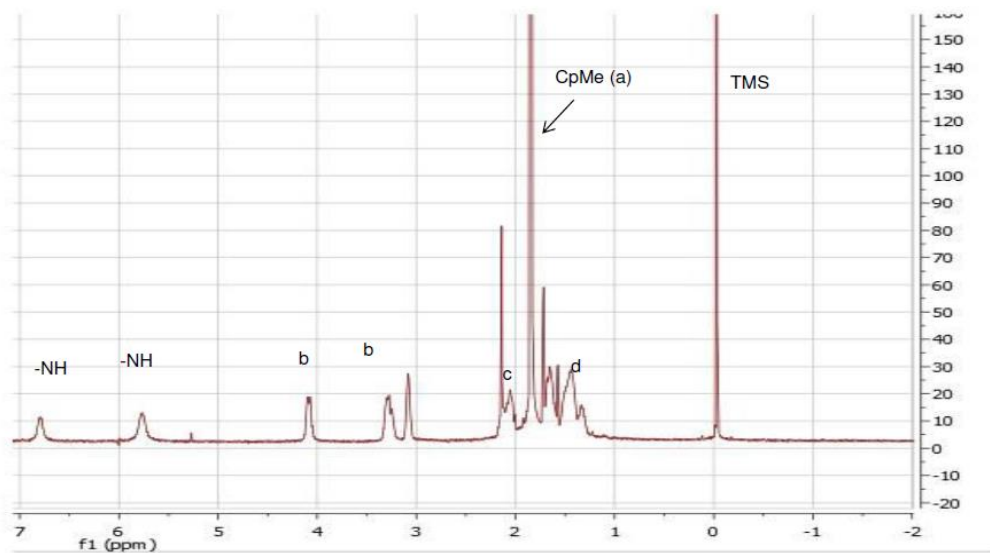


3-Ir CNMR

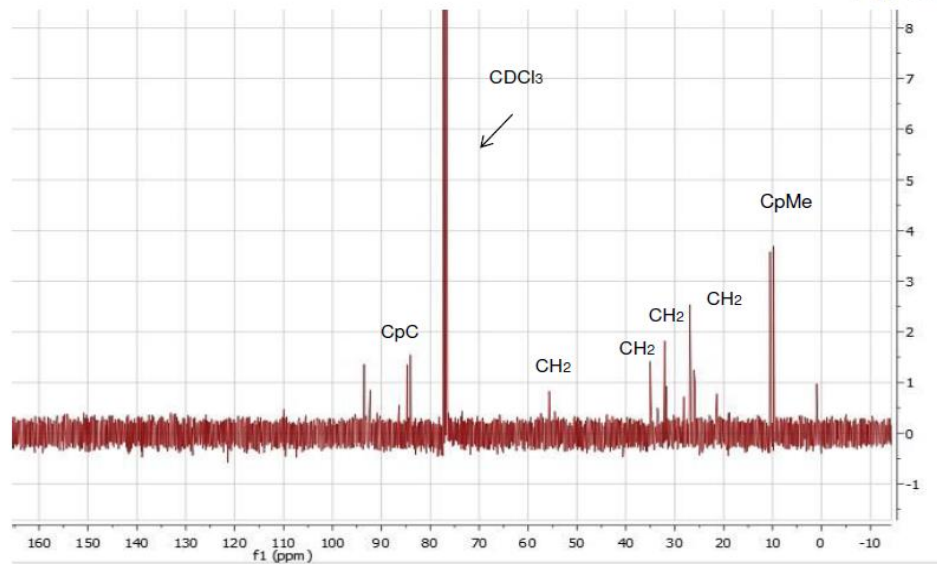




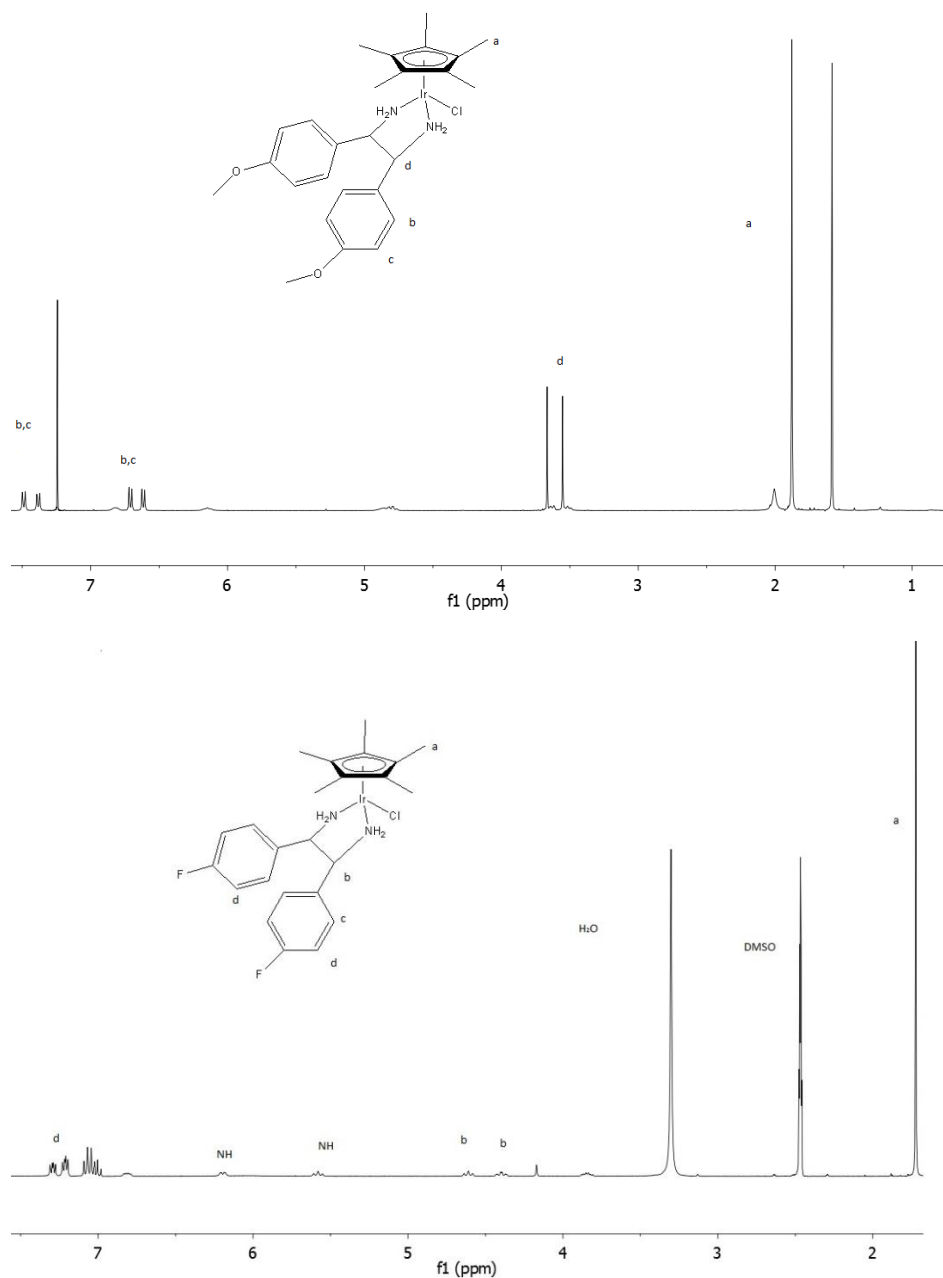
7-Ir HNMR

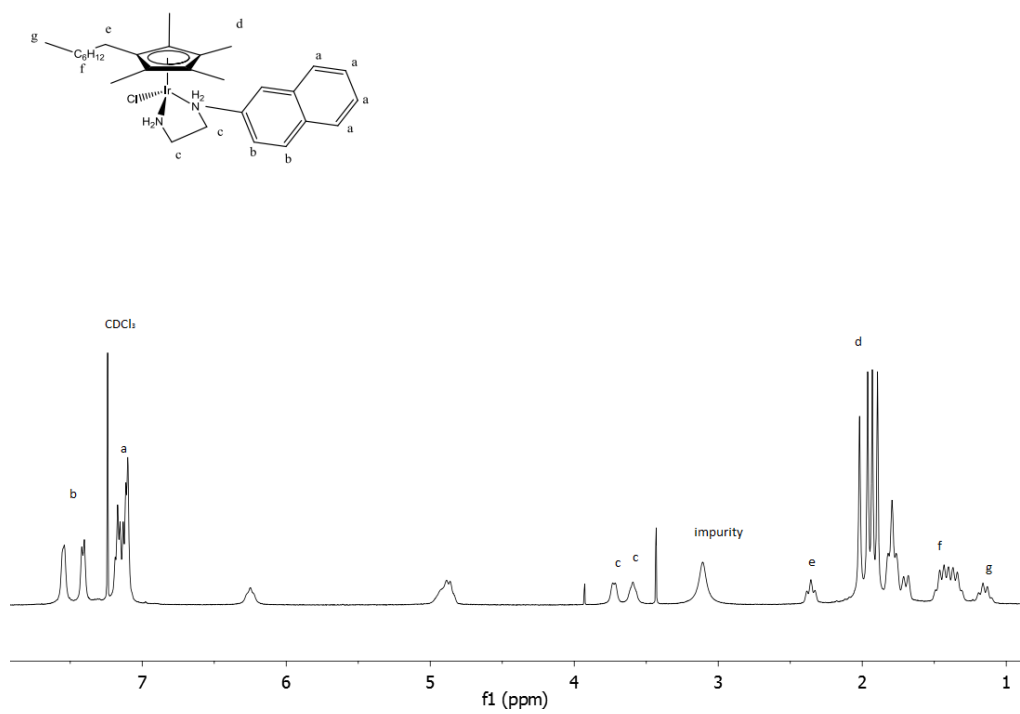
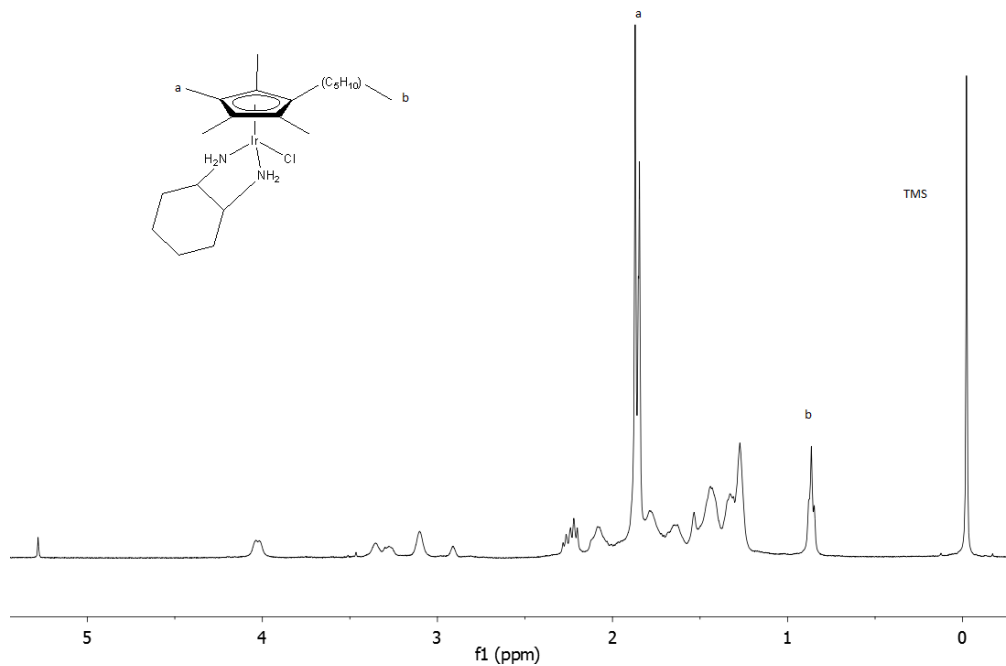


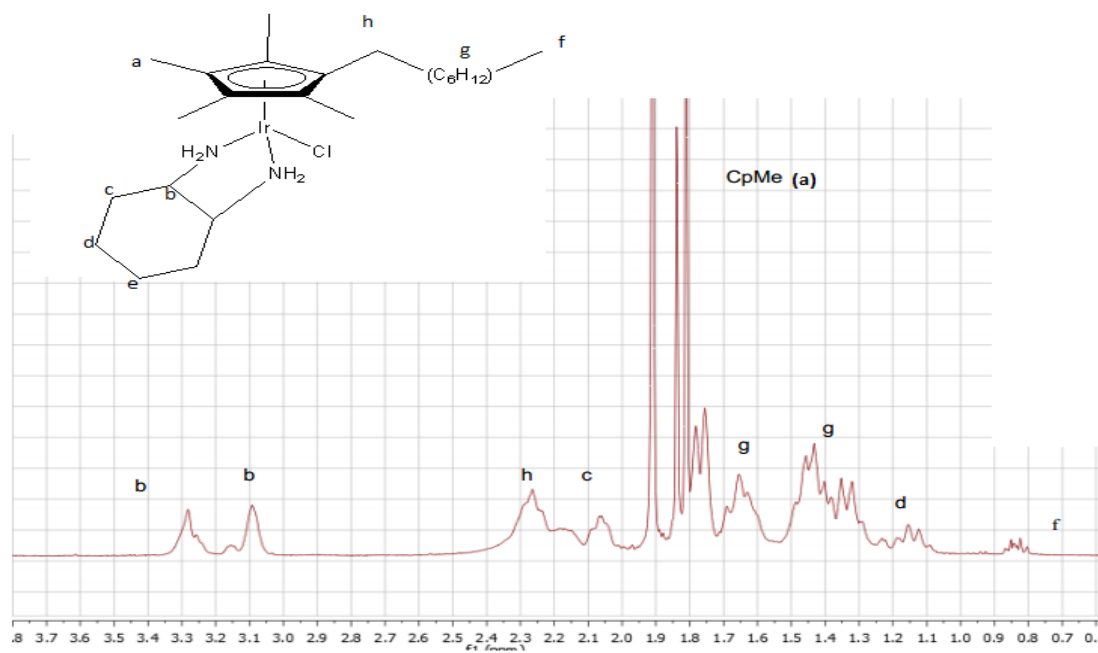
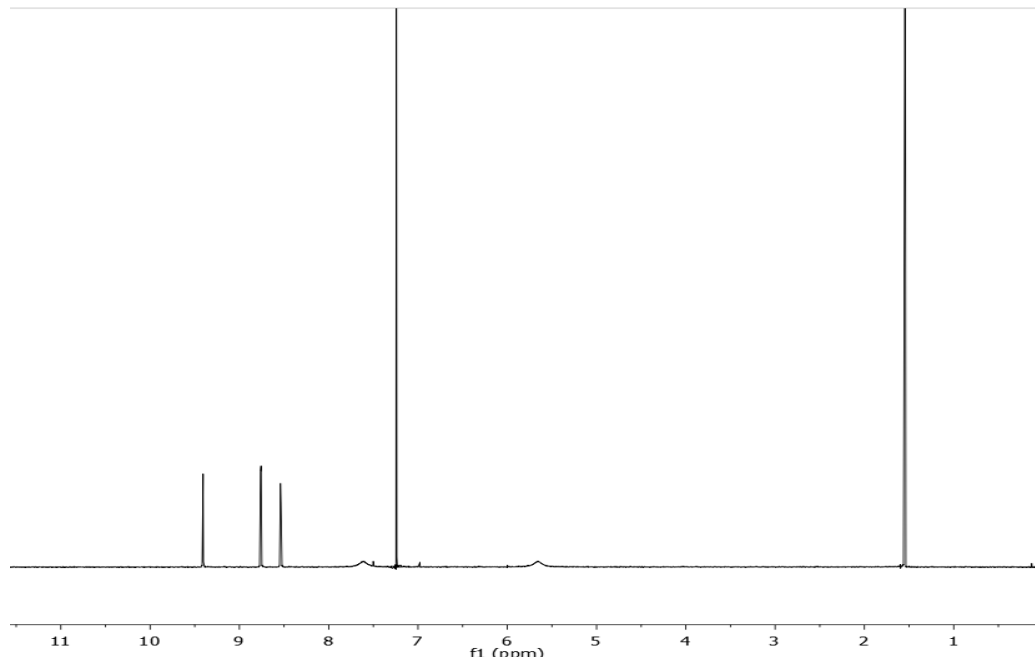
7-Ir CNMR



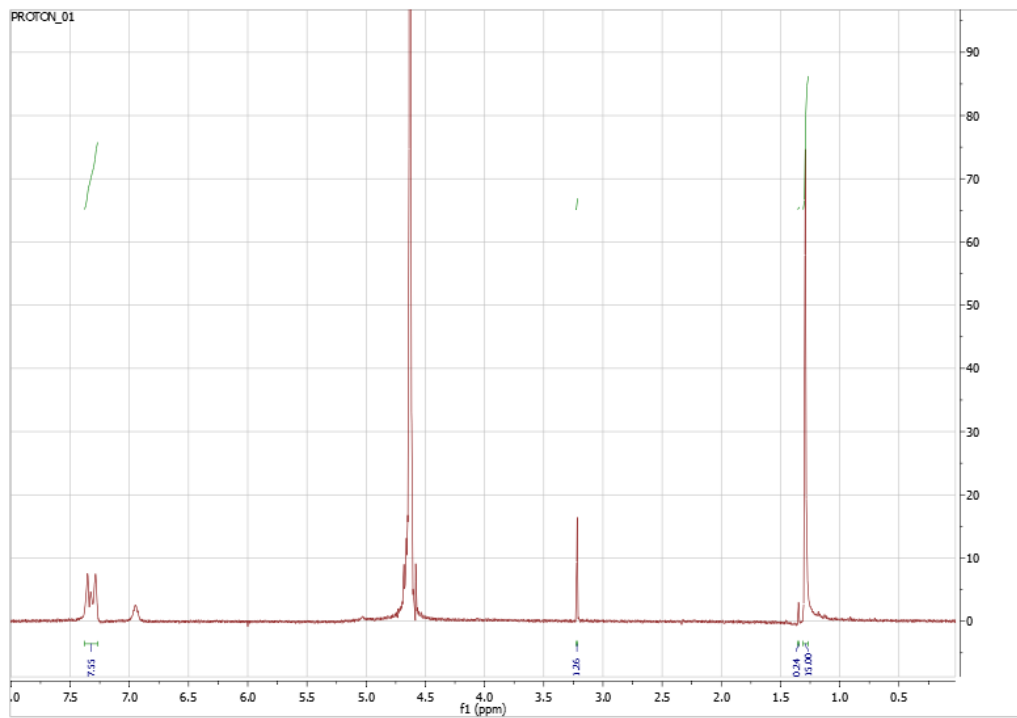
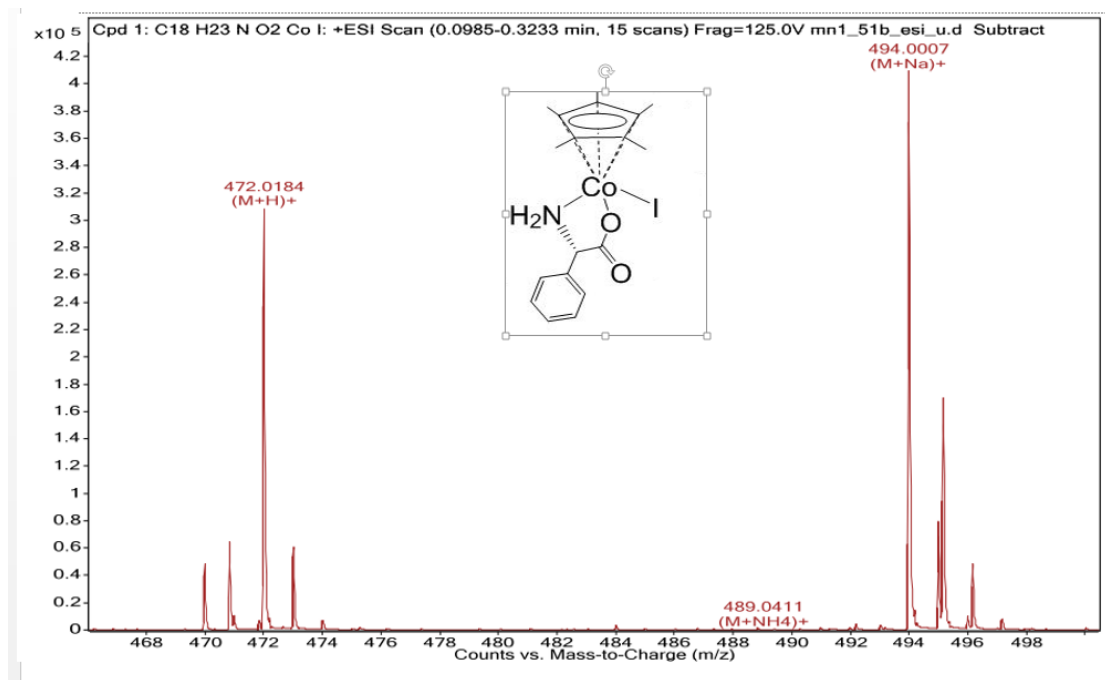
14- Ir HNMR



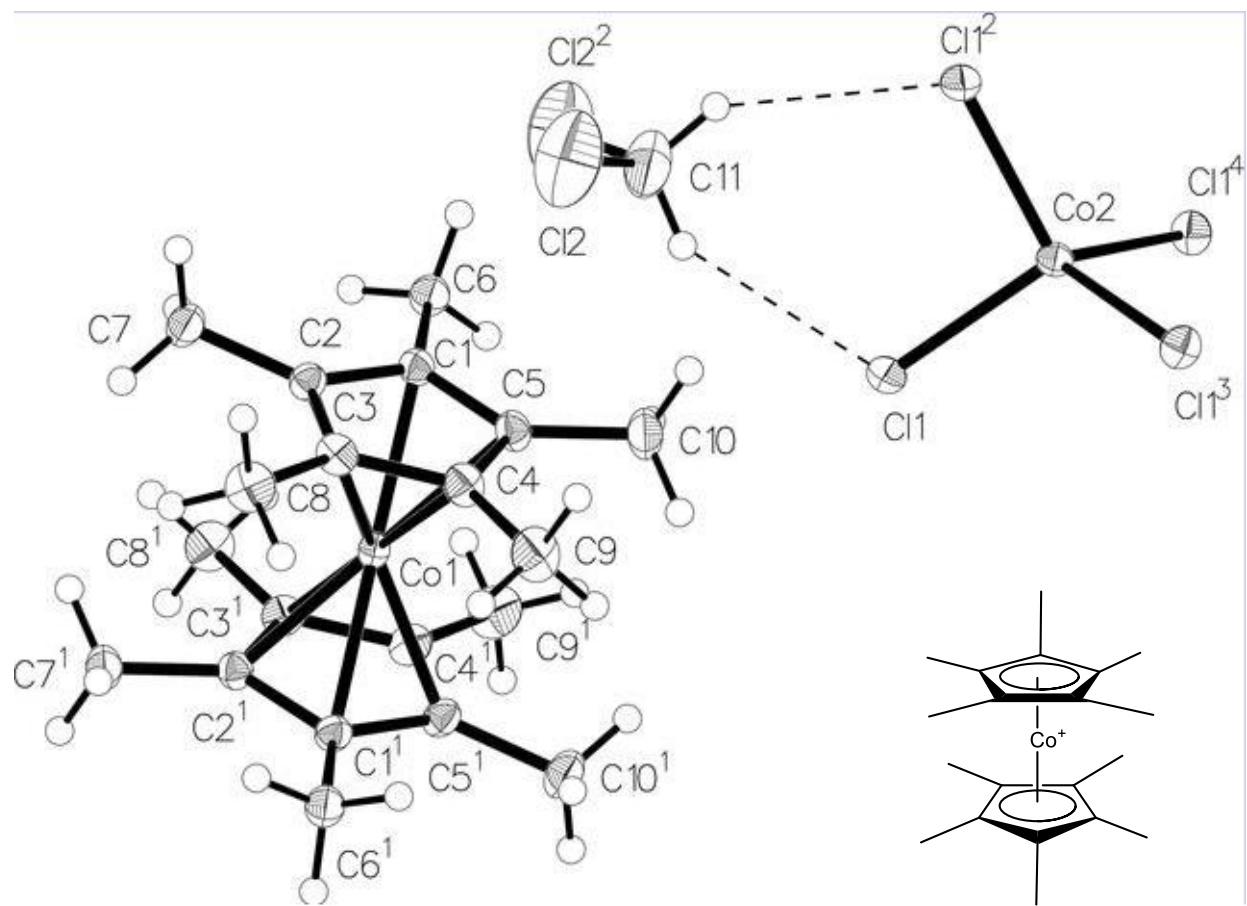




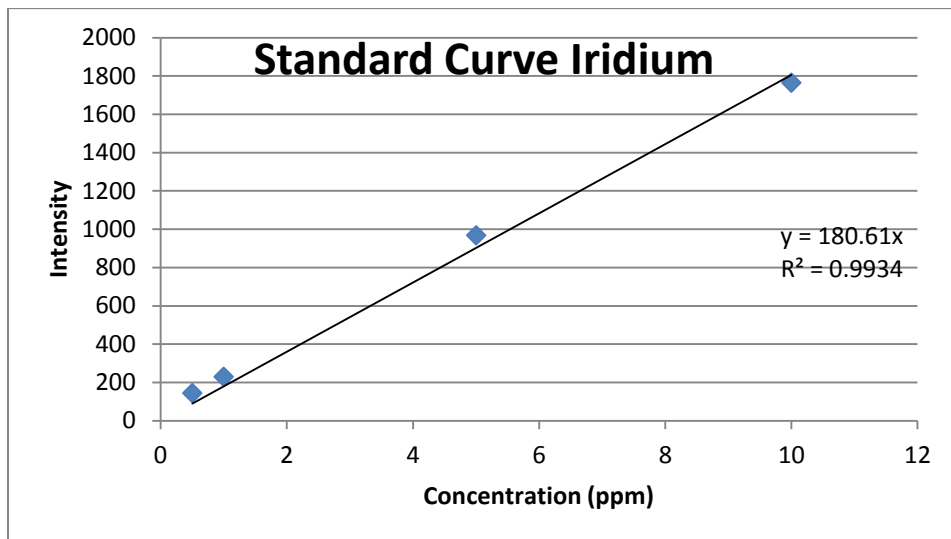
10-Co HNMR



Decamethylcobaltacinium



Mouse Iridium Calibration Data -ICP-OES



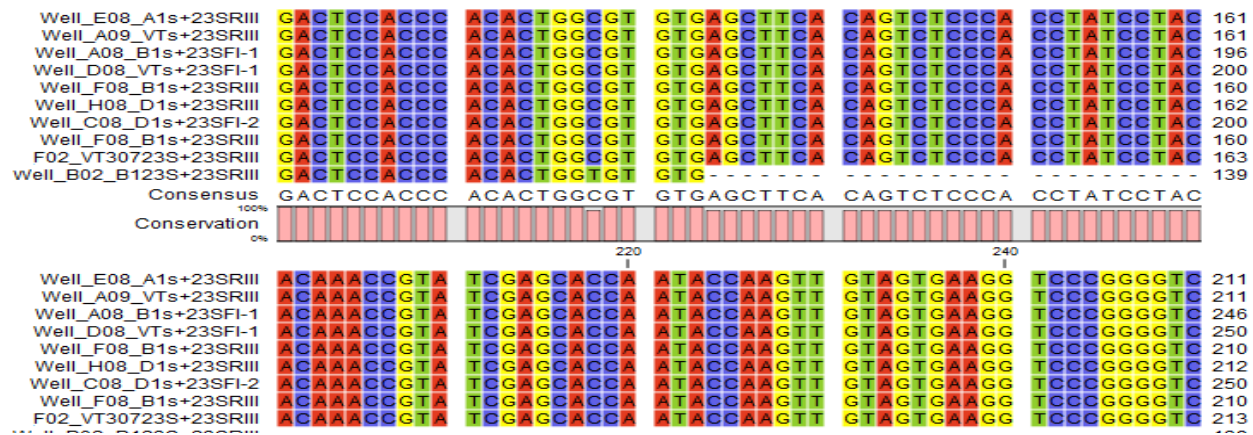
Mouse Samples					
Blood	DAY 1		Day 4		Day 14
	ppm		ppm		ppm
	1.12		0.12		0.00
	2.75		0.25		0.00
	1.65		0.17		0.00
	2.01		0.25		0.00

Concentration of iridium in blood for each 14 day mouse studied

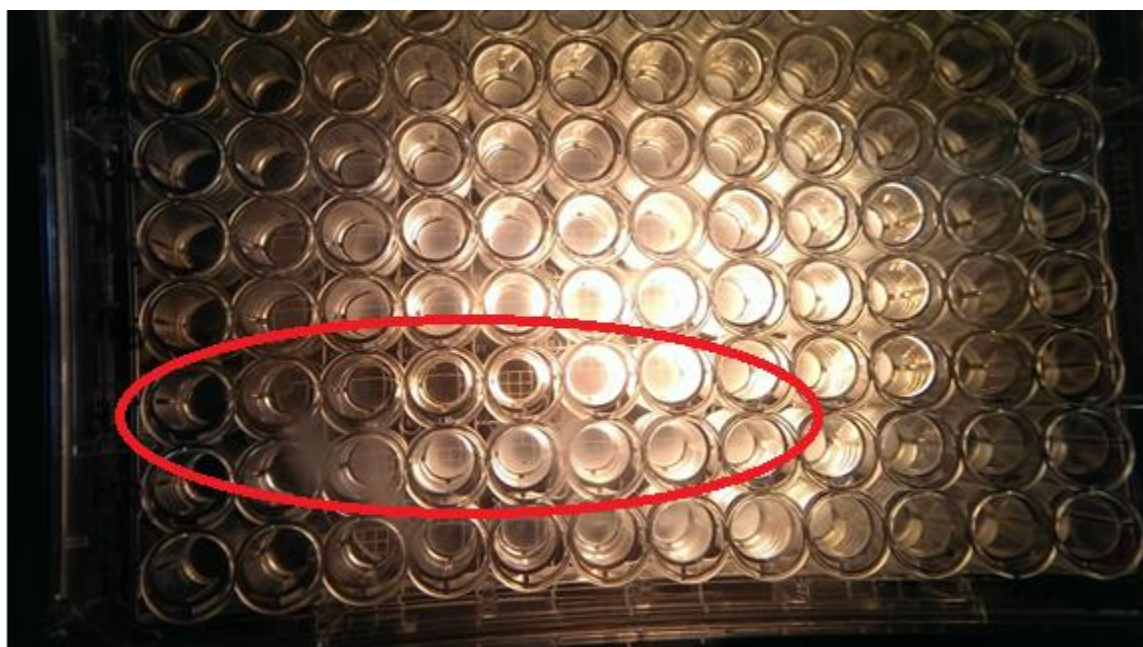
Urine (avg)	DAY14 ONLY
	ppm
	0.198
	0.221
	0.220
	0.219
	0.255
	0.219
	0.185
	0.185

Iridium concentration excreted at the end of each 14 day mouse studied

DNA Profile of Mutants in Mechanism of Action study



Revealed mutations within domain V (bases 2057-2058), whereas other mutations were found in the 2057-2611 bp region of the peptidyl transferase loop



Mutant growth after exposure to 1-PG for 48hrs